1961

A Study of the Structure of Turbulent Shear Flow in Pipes.

William Alfred Brookshire
Louisiana State University and Agricultural & Mechanical College

A STUDY OF THE STRUCTURE OF TURBULENT SHEAR FLOW IN PIPES

A Dissertation

Submitted to the Graduate Faculty of the
Louisiana State University and
Agricultural and Mechanical College
in partial fulfillment of the
requirements for the degree of
Doctor of Philosophy

in

The Department of Chemical Engineering

by
William Alfred Brookshire
B.S., University of Houston, 1957
M.S., Louisiana State University, 1959
January, 1961

ACKNOWLEDGEMENTS

Many people have given their assistance to this research. Dr. Adrian Johnson and Mr. Larry Morton did much of the computer work. Mr. L. M. Carpenter assisted in setting up the apparatus. Mr. Elmo P. Bergeron took many of the photographs and Miss Helen Chisholm superbly typed this dissertation. The assistance of these people is sincerely appreciated.

Dr. D. U. von Rosenberg's guidance and assistance in directing this work is sincerely appreciated. A special thanks is extended to Professor W. E. Owens, of the Department of Electrical Engineering, who gave very unselfishly of his time to the solution of many of the instrumentation problems in this research. The author is indebted to his wife, Cynthia Gaida Brookshire, who not only tolerated him but assisted in the preparation of this dissertation. The financial assistance of the Humble Division of Humble Oil and Refining Company is gratefully acknowledged.

TABLE OF CONTENTS

LIST OF TABLES

LIST OF FIGURES

ABSTRACT

The present status of knowledge of turbulent shear flow in pipes is inadequate for the formulation of a general theory. It is felt that more experimental data and the subsequent interpretation of these data will be necessary before a workable theory can be formulated. It is to this end that this research was conducted.

The experimental studies were carried out in a 40 foot length of schedule 40 aluminum pipe which was preceded by a large calming box. The turbulence quantities and mean velocity were measured with a constant temperature hot wire anemometer.

The choice of a pipe as a test section is an excellent one as it yields turbulence that is homogeneous in two directions. This homogeneity greatly simplifies the Reynolds equations for turbulent pipe flow. It is shown by the Reynolds equations and the boundary conditions that there is a definite tendency toward isotropy at the pipe center, i.e., $\overline{uv} = \overline{uw} = \overline{vw}$ and $w' = v'$. The only condition lacking for isotropy is $u' = v'$ and the data of Laufer[13] show that this condition was satisfied in his test equipment.

In this research mean velocity and axial intensity of turbulence were measured at twelve different Reynolds numbers varying between 4,800 and 201,000. At each Reynolds number measurements were made at twenty-seven points distributed almost logarithmically with respect to distance from the wall. Axial dissipation length was measured at the same points as mean velocity and axial intensity; however, the minimum Reynolds number in the dissipation length studies was 81,800. Azimuthal intensity and correlation between the azimuthal and axial fluctuating velocity were measured at eight Reynolds numbers varying between 39,800 and 201,000. These measurements were made only in the turbulent core.

The axial and azimuthal intensity of turbulence are a minimum at the pipe center and, in the turbulent core, increase almost linearly as the pipe wall is approached. The axial intensity reached a maximum very near the wall at a dimensionless distance, Y^+, of about 15. At Reynolds number of 4,800 and a distance from the wall of 0.0025 inches no turbulence was detectable. This is, to the knowledge of the author, the only experimental evidence of a true laminar sublayer in turbulent flow.

Oscillograms of the axial fluctuating velocity, very near the wall, showed velocity spikes (sharp increases in velocity) similar to those observed by von Rosenberg[25] in parallel flat jets.

The axial dissipation length measurements were a maximum near the pipe center and decreased to a minimum near the pipe wall. These measured dissipation lengths were nearly independent of Reynolds number except in the region near the wall where dissipation length decreased with increasing Reynolds number.

The mean velocity data correlated well with the logarithmic velocity distribution for $Y^+ > 30$ and with $U^+ = Y^+$ for $Y^+ < 6$. A second equation, derived by Pai[18], was compared to the mean velocity data. This equation gave excellent agreement in the turbulent core and for $Y^+ < 4$, but showed deviations up to 20% in the outer edge of the transition region. Pai's equation has the virtue of satisfying the Reynolds equations which the logarithmic velocity profile does not.

The axial intensity of turbulence written in dimensionless form was found to be a function only of Y^+ for $Y^+ < 7$ and for $Re > 20{,}000$, this result may be extended to $Y^+ \sim 40$. In the turbulent core u'/U^* and w'/U^* appear to be primarily a function of radial position and only slightly a function of Reynolds number.

CHAPTER I

INTRODUCTION

At present, the knowledge of turbulent shear flow is inadequate for the formulation of a general theory that is sound and complete. It is the feeling of most researchers in this field that more experimental work, and the subsequent interpretation of the results, will be necessary before a workable theory can be formulated. It is to this end that the present research was undertaken, namely, to take experimental data on turbulent shear flow in pipes and to ascertain, as far as possible, the relationships between the experimental variables.

The reason for the choice of the pipe as a test section was twofold: (1) Steady state incompressible pipe flow affords a turbulence that is homogeneous in two directions. The relevant equations are thus greatly simplified by the absence of many of the terms present in other types of flow. (2) Turbulent pipe flow is of great importance to the chemical engineer; and a general theory, or even a better understanding of the functional relationships, would be of considerable value to him. For the chemical engineer the value would not be limited to momentum transport but would definitely be extended

to heat and mass transfer as well. In fact, a workable theory of momentum transport is, in the author's opinion, a prerequisite for a rational mechanistic approach to heat and mass transfer in turbulent shear flow.

The research of Laufer[13] stands out as the most complete, if not the only, experimental work that has been done on the turbulent variables in pipe flow. At well chosen positions along the radius of the pipe he measured mean velocity, intensity, double, triple and quadruple correlation coefficients, and many of the terms in the turbulent energy equation. The measurements were taken on air at Reynolds numbers (based on center line velocities) of 50,000 and 500,000. He also made several measurements of the spectrum of turbulence. Throughout this paper Laufer's work will be referred to frequently and the author's data and conclusions compared, where possible, to his.

CHAPTER II

THEORY

1. Definition of Turbulent Flow

There are two types of flow situations that occur, namely laminar and turbulent. The first is considered by researchers in the field of fluid mechanics to be any motion which is capable of description as periodic motion or which has a somewhat regular eddy pattern[20]. Turbulent flow is thus a flow which is random in nature, restricted, in general, only by the conservation laws and the containing boundaries. Hinze has set forth the definition: "Turbulent fluid motion is an irregular condition of flow in which the various quantities show a random variation in time and space coordinates, so that statistically distinct average values can be discerned."[7]

In general, it may be said that the fluctuating velocities of turbulent flow are a result of, or a measure of, the size, shape, and intensity of motion of small particles of fluid, moving somewhat as an entity, called eddies. Of course, the size of these eddies varies with the particular flow conditions but it is possible, at least qualitatively, to ascertain what determines the size limits. The upper limit in eddy size is

usually determined by, and is of the order of magnitude of, the dimensions of the containing apparatus. The lower limit is determined primarily by the viscosity; i.e., as the eddy becomes smaller the velocity gradient in the eddy becomes larger, and thus the viscous shear (the motion within the smaller eddies is laminar) becomes larger. This increase in viscous shear counteracts the eddying motion, thus limiting the size of the eddy. Some more quantitative figures on minimum eddy size will be given later in this paper.

2. Comparison of Turbulent Motion to Molecular Motion

The random motion in turbulent flow is often compared with the random motion of molecules in the kinetic theory of gases. However, the comparison is not a particularly good one and most theories based on this comparison have had very limited success. Townsend points out that the analogy between turbulent flow and the kinetic theory of gases is imperfect in two important points.

> "The motion of a gas molecule is only affecting the motion of, at most, one other molecule and mixing on the macroscopic scale takes place freely. Secondly, the turbulent motion requires a continuous supply of energy to maintain it, which is obtained from the working of the mean flow against the turbulent stresses. The turbulent motion so depends for its kinetic energy on one of the quantities that it diffuses, the momentum of the mean flow, and the diffusing processes cannot be considered as small pertubations of an already existing motion as in the kinetic theory of gases. The necessary connection between the diffusion of momentum and the supply of energy to the turbulent motion is a fundamental

characteristic of turbulent shear flow."[24]

A second question that often arises is whether the diameter of the eddies approaches the mean free path of the molecules as the mean velocity and mean velocity gradient increases. If this were the case the motion would be molecular in the smallest eddies. However, this is not the case as pointed out by Hinze[7]. For velocities of less than 300 ft/sec the minimum eddy diameter is of the order of 1 mm which is much greater than the 10^{-4} mm mean free path of gases under atmospheric conditions. Therefore, for the moderate velocities (less than 100 ft/sec) used in this paper the turbulent motion will definitely not extend to the molecular scale.

3. Definition of Turbulence Quantities

In turbulent flow it is customary to represent the instantaneous velocity as the sum of an average and fluctuating velocity in the direction under consideration. For the x direction:

$$U = \overline{U} + u \qquad \text{(II-1)}$$

where

U = instantaneous velocity in x direction

$\overline{U}$ = average velocity in x direction

u = fluctuating component of the velocity in the x direction

The average velocity is defined mathematically by:

$$\bar{U} = \frac{1}{\Delta t}\int_{o}^{\Delta t} U dt \qquad \text{(II-2)}$$

where

t = time

Δt = time interval over which average is taken

It is obvious that the average of the fluctuating velocity is zero, i.e.,

$$\bar{u} = \frac{1}{\Delta t}\int_{o}^{\Delta t} u dt = 0 \qquad \text{(II-3)}$$

Since in turbulence research it is the fluctuating component of the velocity that is of interest it will be necessary to define an average value of the fluctuating velocity that is non zero. Probably the first non zero average of the fluctuating velocity that would come to mind would be the average of the absolute value $\overline{|u|}$; however, this quantity has seen very little use. This fact is primarily because the root mean square of the velocity $(\overline{u^2})^{\frac{1}{2}}$ is much easier to measure with conventional turbulence measuring equipment and because $\overline{u^2}$ occurs quite naturally in many of the equations governing turbulent flow. The root mean square of the fluctuating velocity is also known as the intensity of turbulence and may be defined mathematically as:

$$u' = (\overline{u^2})^{\frac{1}{2}} = \left(\frac{1}{\Delta t}\int_{o}^{\Delta t} u^2 dt\right)^{\frac{1}{2}} \qquad \text{(II-4)}$$

Similar definitions may be made for the intensities in the other coordinate directions.

It should be pointed out that the average defined above (II-2, II-3, and II-4) are all taken with respect to time; however, there are other types of averages that can be discerned for turbulent flow; namely, space average, space-time average, and statistical or ensemble average. From the viewpoint of the statistical theory of turbulence it is the ensemble average that should be used, but it is generally not possible to measure the ensemble average experimentally. Consider, for example, if we should wish to measure the average value of the velocity in a pipe at a given time. This would require that the averaging process be made in an infinite number of identical pipes in which the physical conditions are the same, with the component of the velocity being measured at the same time in all the pipes[20]. This is of course experimentally impossible.

The impossibility of taking ensemble averages has led to the extensive use of the time average and the necessity of a proof of the equality of the time average and statistical average. Such a proof (which would be an ergodic theorem for turbulence similar to the ergodic theorem for statistical mechanics and which gives sufficient conditions for the equality of the statistical average and the time average) has yet to be formulated and is one of the outstanding shortcomings in the

statistical theory of turbulence. In this paper, as is customary in the research in this field, the time average and statistical average will be assumed equal.

4. Isotropic and Homogeneous Turbulence

Throughout this paper isotropic turbulence and homogeneous turbulence will be referred to frequently; therefore, it is felt that a definition and brief description of these special flow cases is in order. Isotropic turbulence is defined as that condition under which the time smoothed value of any function of the velocity components and of their space derivatives at a particular point, defined with respect to a given set of axes, is unaltered if the axes are rotated or reflected in any plane through the origin[1]. Thus, all the intensities are equal.

$$u' = v' = w'$$

It can also be shown[7] that the correlation between the fluctuating components of the velocity are zero, i.e.,

$$\overline{uv} = \overline{uw} = \overline{vw} = 0$$

Homogeneous turbulence is defined as turbulence in which the time smoothed quantities are independent of position; i.e.,

$$u'_{x_1} = u'_{x_2} = u'_{x_3} \quad \cdots$$

It should also be pointed out that it is possible to have turbulence that is homogeneous along only one or two of the coordinate axes, as, for example, pipe flow which is homogeneous in the x direction and the θ direction.

5. Navier-Stokes, Continuity, and Reynolds Equations

A momentum balance around a differential fluid element with the assumptions that the flow is incompressible, isothermal, Newtonian, and that the influence of external fields is negligible results in the following equations:

$$\frac{\partial V}{\partial t} + V\frac{\partial V}{\partial r} + \frac{W}{r}\frac{\partial V}{\partial \theta} + U\frac{\partial V}{\partial x} - \frac{W^2}{r} = -\frac{1}{\rho}\frac{\partial P}{\partial r} + \frac{\mu}{\rho}\nabla^2 V - \frac{\mu}{\rho r^2}\left[V + 2\frac{\partial W}{\partial \theta}\right] \qquad \text{(II-5a)}$$

$$\frac{\partial W}{\partial t} + V\frac{\partial W}{\partial r} + \frac{W}{r}\frac{\partial W}{\partial \theta} + U\frac{\partial W}{\partial r} + \frac{VW}{r} = -\frac{1}{r\rho}\frac{\partial P}{\partial \theta} + \frac{\mu}{\rho}\nabla^2 W - \frac{\mu}{\rho r^2}\left[W - 2\frac{\partial V}{\partial \theta}\right] \qquad \text{(II-5b)}$$

$$\frac{\partial U}{\partial t} + V\frac{\partial U}{\partial r} + \frac{W}{r}\frac{\partial U}{\partial \theta} + U\frac{\partial U}{\partial x} = -\frac{1}{\rho}\frac{\partial P}{\partial x} + \frac{\mu}{\rho}\nabla^2 U \qquad \text{(II-5c)}$$

where

U = velocity in the axial direction

V = velocity in the radial direction

W = velocity in the aximuthal direction

x, r, θ = axial, radial, and azimuthal coordinates

μ = viscosity

ρ = density

t = time

$$\nabla^2 = \frac{\partial}{\partial x^2} + \frac{\partial^2}{\partial r^2} + \frac{1}{r}\frac{\partial}{\partial r} + \frac{1}{r^2}\frac{\partial^2}{\partial \theta}$$

These equations, as are most of the equations in this paper, are expressed in cylindrical coordinates, which, it will be seen in section (6) will lead to many simplifications for the axially symmetrical pipe flow. The derivation of the Navier-Stokes equations, as the above equations are often called, can be found in many of the advanced books on fluid mechanics[1,4,12,21].

Another equation that is basic in fluid mechanics is the continuity equation or the equation for the conservation of mass. For an incompressible steady state flow it may be written as

$$\frac{\partial U}{\partial x} + \frac{1}{r}\frac{\partial rV}{\partial r} + \frac{1}{r}\frac{\partial W}{\partial \theta} = 0 \qquad \text{(II-6)}$$

This equation is also derived in the standard texts on fluid mechanics[1,4,12,21].

In an effort to formulate a set of equations for turbulent flow Osborne Reynolds assumed that the instantaneous fluid velocity satisfies the Navier-Stokes equations for a viscous fluid and that the instantaneous velocity may be separated into a mean and fluctuating velocity as given in equation (II-1). Substituting the instantaneous velocity, as the sum of a mean and fluctuating velocities, into the Navier-Stokes

equations and averaging by a special set of rules known as the Reynolds rule of averages, Reynolds obtained a new set of equations known as the Reynolds equations[1,4,12,21]. The Reynolds rules of averages have been summarized by Pai[20] and have the following four properties.

$$\overline{f + g} = \bar{f} + \bar{g}$$

$$\overline{cf} = c\bar{f}$$

$$\overline{\bar{f}g} = \bar{f}\bar{g}$$

$$\overline{\lim f_n} = \lim \bar{f}_n$$

where

f,g = functions

c = constant

f_n = sequence of a function

and the bar refers to the average value.

Pai[20] also points out that if we define the mean value of a function f by the statistical average (see section 3) the four Reynolds rules are obviously satisfied and concludes that the systematic use of random functions in the theory of turbulence is desirable.

The substitution of the instantaneous velocities, in the form (II-1), into the Navier-Stokes equations (II-5) yield after applying the Reynolds rule of average to both sides of the equations:

$$\bar{U}\frac{\partial\bar{V}}{\partial x}+\bar{V}\frac{\partial\bar{V}}{\partial r}+\frac{\bar{W}}{r}\frac{\partial\bar{V}}{\partial\theta}-\frac{\overline{W^2}}{r}=$$

$$-\frac{1}{\rho}\frac{\partial\bar{P}}{\partial r}+\frac{\mu}{\rho}\nabla^2\bar{V}-\frac{\mu}{r^2\rho}\left[\bar{V}+\frac{2\partial\bar{W}}{\partial\theta}\right]$$

$$-\left[\frac{\partial}{\partial x}\overline{uv}+\frac{1\partial}{r\partial r}\overline{rv^2}+\frac{1}{r}\frac{\partial}{\partial\theta}\overline{vw}-\frac{\overline{w^2}}{r}\right] \qquad \text{(II-7a)}$$

$$\bar{U}\frac{\partial\bar{W}}{\partial x}+\bar{V}\frac{\partial\bar{W}}{\partial r}+\frac{\bar{W}}{r}\frac{\partial\bar{W}}{\partial\theta}+\frac{\bar{V}\bar{W}}{r}=-\frac{1}{\rho r}\frac{\partial\bar{P}}{\partial\theta}$$

$$+\frac{\mu}{\rho}\nabla^2\bar{W}-\frac{2\mu}{\rho r^2}\left[\bar{W}-2\frac{\partial\bar{W}}{\partial\theta}\right]$$

$$-\left[\frac{\partial}{\partial x}\overline{uw}+\frac{\partial}{\partial r}\overline{vw}+\frac{1}{r}\frac{\partial}{\partial\theta}\overline{w^2}+\frac{2\overline{vw}}{r}\right] \qquad \text{(II-7b)}$$

$$\bar{U}\frac{\partial\bar{U}}{\partial x}+\bar{V}\frac{\partial\bar{U}}{\partial r}+\frac{\bar{W}}{r}\frac{\partial\bar{U}}{\partial\theta}=-\frac{1}{\rho}\frac{\partial\bar{P}}{\partial x}+\frac{\mu}{\rho}\nabla^2\bar{U}$$

$$-\left[\frac{\partial\overline{u^2}}{\partial x}+\frac{1}{r}\frac{\partial r\overline{uv}}{\partial r}+\frac{1}{r}\frac{\partial}{\partial\theta}\overline{uw}\right] \qquad \text{(II-7c)}$$

It should be noted that the Reynolds equations (II-7) differ from the Navier-Stokes equations for steady laminar flow only by the addition of the last bracketed term in each of the equations. These terms contain the fluctuating velocities and are responsible for the high turbulent shear rate and correspondingly high energy loss in turbulent flow. The terms such as

$$\rho\overline{uw},\ \rho\overline{uv},\ \rho\overline{v^2},\ \rho\overline{vw},\ \text{etc.}$$

are turbulent stresses or eddy stresses and are commonly called Reynolds stresses after Osborne Reynolds.

A similar substitution of instantaneous velocity, as the

sum of an average and fluctuating velocity, into the continuity equation for incompressible, steady state flow yields:

$$\frac{\partial \bar{U}}{\partial x} + \frac{1}{r}\frac{\partial r\bar{V}}{\partial r} + \frac{1}{r}\frac{\partial \bar{W}}{\partial \theta} = 0 \qquad \text{(II-8)}$$

More detailed derivations of the Reynolds equations and turbulent continuity equation may be found in Townsend[24] and Rouse[21].

6. Reynolds Equations for Pipe Flow

One of the primary reasons for the choice of the pipe as a test section was that the Reynolds equations reduce to a simple form for axially symmetrical flow. As pointed out in section (4) pipe flow is homogeneous in the axial and azimuthal directions, i.e.,

$$\frac{\partial}{\partial \theta} = 0 \qquad \text{(II-9)}$$

$$\frac{\partial}{\partial x} = 0 \text{ for all but the total pressure} \qquad \text{(II-10)}$$

When (II-9) and (II-10) are applied to the Reynolds equations with the restriction that the average velocities in the radial and azimuthal directions are zero, the following equations are obtained:

$$0 = -\frac{1}{\rho}\frac{\partial \bar{P}}{\partial r} - \frac{1}{r}\frac{\partial r\overline{v^2}}{\partial r} + \frac{\overline{w^2}}{r} \qquad \text{(II-11a)}$$

$$0 = -\frac{\partial \overline{vw}}{\partial r} - \frac{2\overline{vw}}{r} \qquad \text{(II-11b)}$$

$$0 = -\frac{1}{\rho}\frac{\partial \bar{P}}{\partial x} + \frac{\mu}{\rho}\frac{\partial^2 \bar{U}}{\partial r^2} + \frac{\mu}{\rho r}\frac{\partial \bar{U}}{\partial r} - \frac{1}{r}\frac{\partial \overline{ruv}}{\partial r} \qquad \text{(II-11c)}$$

Because the velocity field is homogeneous in the axial and azimuthal directions the partial derivatives of velocities with respect to r become total derivatives. Equations (II-11) thus become upon some rearrangement:

$$\frac{1}{\rho}\frac{\partial \bar{P}}{\partial r} = -\frac{1}{r}\frac{dr\ \overline{v^2}}{dr} + \frac{\overline{w^2}}{r} \qquad \text{(II-12a)}$$

$$0 = \frac{d\overline{vw}}{dr} + \frac{2\overline{vw}}{r} \qquad \text{(II-12b)}$$

$$\frac{1}{\rho}\frac{\partial \bar{P}}{\partial x} = -\frac{1}{r}\frac{\partial}{\partial r}\left[r\left(\overline{uv} - \frac{\mu}{\rho}\frac{d\bar{U}}{dr}\right)\right] \qquad \text{(II-12c)}$$

Integrating equation (II-12b) between $r = r_a$ and $r = r$

$$\ln \frac{\overline{vw}}{\overline{vw}_a} = 2 \ln \frac{r_a}{r} \qquad \text{(II-13)}$$

or

$$\frac{\overline{vw}}{\overline{vw}_a} = (r_a/r)^2$$

further

$$\overline{vw}\ r^2 = \overline{vw_a}\ r_a^2 = C$$

At the center of the pipe $r = 0$ and $\overline{vw}$ is finite which forces C to be zero. Therefore, $\overline{vw}$ must be zero everywhere except the pipe center and if $\overline{vw}$ is a continuous function of r (which most of the variables in fluid mechanics are) $\overline{vw}$ is also zero at the pipe center. The Reynolds equations have now been reduced to (II-12a) and (II-12c) for pipe flow.

Differentiating equation (II-12a) with respect to x and again noting that because of the homogeneity the velocity components are independent of x, one obtains:

$$\frac{\partial}{\partial x}\left(\frac{\partial \bar{P}}{\partial r}\right) = 0 = \frac{\partial}{\partial r}\left(\frac{\partial \bar{P}}{\partial x}\right) \quad \text{or}$$

$$\frac{\partial \bar{P}}{\partial x} \neq \phi\ (r) \tag{II-14}$$

$$\frac{\partial \bar{P}}{\partial r} \neq \phi\ (r) \tag{II-15}$$

Differentiating equation (II-12c) with respect to x and again applying the condition of homogeneity one now obtains

$$\frac{\partial}{\partial x}\frac{\partial \bar{P}}{\partial x} = 0 \quad \text{or}$$

$$\left(\frac{\partial \bar{P}}{\partial x}\right) = \text{constant} \neq \phi\ (x) \tag{II-16}$$

Integration of equation (II-12c) while noting that $\left(\frac{\partial \bar{P}}{\partial x}\right)$ is a constant yields

$$\frac{r^2}{2\rho}\left(\frac{\partial \bar{P}}{\partial x}\right) = -\ r\left(\overline{uv} - \frac{\mu}{\rho}\frac{d\bar{U}}{dr}\right) + A \tag{II-17}$$

Using the boundary conditions at the center of the pipe

$$r = 0$$

$$\overline{uv} = \text{finite}$$

$$\frac{d\bar{U}}{dr} = 0$$

$$\frac{\partial \bar{P}}{\partial x} = \text{finite}$$

one obtains for the constant of integration

$$A = 0$$

By balancing the pressure drop against the shear forces on a differential length of pipe one obtains

$$\frac{\partial \overline{P}}{\partial x} = - \frac{2\tau}{r} \qquad \text{(II-18)}$$

or at the wall of the pipe

$$\frac{\partial \overline{P}}{\partial x} = - \frac{2\tau_o}{r_o} \qquad \text{(II-19)}$$

Now defining a friction velocity U* as

$$U^* = \left(\frac{\tau_o}{\rho} \right)^{\frac{1}{2}} \qquad \text{(II-20)}$$

one obtains from (II-19) and (II-20)

$$\frac{\partial \overline{P}}{\partial x} = - \frac{2\rho}{r_o} U^{*2} \qquad \text{(II-21)}$$

where

U^* = friction velocity

r_o = radius of pipe

τ = shear stress

τ_o = shear stress at the wall

Substituting (II-21) into (II-17) yields

$$\overline{uv} = \frac{\mu}{\rho} \frac{d\overline{U}}{dr} + \frac{r}{r_o} U^{*2} \qquad \text{(II-22)}$$

Rearrangement of equation (II-12a) and integration

$$\frac{1}{\rho} \int \left(\frac{\partial \overline{P}}{\partial r} \right) dr = - \int d\overline{v^2} + \int \frac{\overline{w^2} - \overline{v^2}}{r} dr \qquad \text{(II-23)}$$

Performing the indicated integration between the limits r_o and r and noting at $r = r_o$, $\overline{v^2} = 0$ one obtains

$$\frac{\overline{P}_{r,x} - \overline{P}_{r_o,x}}{\rho} = - \overline{v^2} + \int_{r_o}^{r} \frac{\overline{w^2} - \overline{v^2}}{r} dr \qquad \text{(II-24)}$$

$\overline{P}_{r,x}$ = average pressure at r,x

$\overline{P}_{r_o,x}$ = average pressure at r_o,x

Integration of equation (II-21) yields

$$\frac{\overline{P}_{r,x} - \overline{P}_{r,x_o}}{\rho} = - \frac{2\, U^{*2}\, x}{r_o} \qquad \text{(II-25)}$$

$\overline{P}_{r,x_o}$ = average pressure at r,x_o

x_o = arbitrary origin for x

But, since $\left(\frac{\partial \overline{P}}{\partial x} \right)$ is not a function of r, (II-25) may be written

$$\frac{\overline{P}_{r_o,x} - \overline{P}_{r_o,x_o}}{\rho} = - \frac{2\, U^{*2}\, x}{r_o} \qquad \text{(II-26)}$$

Adding (II-26) to (II-24) yields

$$\frac{\overline{P}_{r,x} - \overline{P}_{r_o,x_o}}{\rho} = - \overline{v^2} + \int_{r_o}^{r} \frac{\overline{w^2} - \overline{v^2}}{r}\, dr - \frac{2\, U^{*2}\, x}{r_o} \qquad \text{(II-27)}$$

From equation (II-22) we see that at r = 0, $\overline{vu} = 0$ and also $\overline{uv} = \overline{uw} = 0$ (because at the center the azimuthal and radial directions are the same). Also at r = 0, $\overline{v^2}$ must equal $\overline{w^2}$, otherwise, the integral in equation (II-27) would be infinite.

At this point it would be appropriate to summarize the Reynolds equations and boundary conditions for pipe flow and to make some comments about them.

Reynolds equations (integrated form)

$$\overline{v^2} + \int^{r} \frac{\overline{v^2} - \overline{w^2}}{r}\, dr = - \frac{\overline{P}_{r,x} - \overline{P}_{r_o,x_o}}{\rho} - \frac{2x}{r_o}\, U^{*2} \qquad \text{(II-27)}$$

$$\overline{uv} = \frac{\mu}{\rho} \frac{d\overline{U}}{dr} + \frac{r}{r_o}\, U^{*2} \qquad \text{(II-22)}$$

Boundary conditions

$$\text{at} \quad r = 0$$

$$\overline{v^2} = \overline{w^2}$$

$$\overline{uv} = \overline{uw} = \overline{vw} = 0$$

$$\frac{d\bar{U}}{dr} = 0$$

$$\text{at} \quad r = r_o$$

$$\overline{v^2} = \overline{w^2} = \overline{u^2} = \overline{uv} = \overline{vw} = \overline{uw} = 0$$

$$\frac{d\bar{U}}{dr} = -\frac{\tau_o}{\mu} \qquad \text{(II-28)}$$

General

$$\frac{\tau}{\tau_o} = \frac{r}{r_o}$$

$$\tau = -\frac{r}{2}\frac{\partial \bar{P}}{\partial x}$$

$$\frac{\partial \bar{P}}{\partial x} = -\frac{2\rho}{r_o} U^{*2}$$

Conclusions:

1. Pressure decreases linearly with distance as in laminar flow.

2. From the experimental data of Laufer[13] $\overline{w^2} > \overline{v^2}$, therefore, from equation (II-24) the pressure at the center of the pipe must always be less than or equal to the pressure at the wall (for x = constant). It should be pointed out that Pai[18], in his derivation of these equations, concluded that the pressure at the center of the pipe would be greater than, or equal to, the pressure at the wall. This conclusion is in direct contrast to the author's conclusion.

3. There is definitely a tendency toward isotropy at the pipe center since all the conditions except $\overline{u^2} = \overline{v^2}$ are met there.

4. The boundary condition and Reynolds equations afford an excellent means of checking experimental data, and in Laufer's[13] work they checked his data very well.

7. Pai's Mean Velocity Distribution[18]

Most of the semiempirical equations that are used for mean velocity distribution in pipes apply to only one region of the pipe, e.g., viscous sublayer*, transition region, fully developed turbulent core. Therefore, in order to obtain a reasonable agreement with experimental data it usually becomes necessary to apply different equations in different regions of the pipe. This dilemma led Pai[18] to consider the possibility of finding one equation that would satisfy the Reynolds equations and the boundary conditions and would give good agreement with experimental data. A derivation of the equation Pai formulated follows.

Pai assumed that a solution to equation (II-22) could be written in the form

$$\frac{\overline{U}}{\overline{U}_m} = 1 + a\eta^2 + b\eta^{2n} \qquad \text{(II-29)}$$

* In this paper the viscous sublayer refers to the region near the wall where the influence of viscosity is very great and laminar sublayer refers to the layer that is in true laminar flow.

where

$n > 2$

$\eta = r/r_o$

$\bar{U}_m$ = maximum velocity, i.e., at center.

In order to satisfy the boundary conditions at $\eta = 1$, $\bar{U} = 0$, $\frac{d\bar{U}}{dr} = -\frac{\tau_o}{\mu}$ and equation (II-22) the constants become

$$a = \frac{s - n}{n - 1} \tag{II-30}$$

$$b = \frac{1 - s}{n - 1} \tag{II-31}$$

where

$$s = \frac{\tau_o}{\mu\left(\frac{2\bar{U}_m}{r_o}\right)} = \frac{\tau_o}{\tau_1} \tag{II-32}$$

It should be noted that s is the ratio of the shearing stress on the wall for turbulent flow to the corresponding shearing stress on the wall for the laminar flow with the same maximum velocity. Equation (II-29) may thus be written

$$\frac{\bar{U}}{\bar{U}_m} = 1 + \frac{s - n}{n - 1}\eta^2 + \frac{1 - s}{n - 1}\eta^{2n} \tag{II-33}$$

According to (II-31) for laminar flow s is equal to 1 and, therefore, equation (II-33) becomes (upon insertion of s = 1) simply the parabolic velocity profile of laminar flow. It should be remarked that although equation (II-33) is a solution to the Reynolds equation (II-22) it is not a unique solution. This is because the number of unknowns in the Reynolds equation is more than the number of equations[18].

Differentiation of equation (II-33) with respect to η and substitution of the result into (II-22) gives an expression for the correlation coefficient $\overline{uv}$.

$$\frac{\overline{uv}}{U^{*2}} = \frac{n\ (s - 1)}{s\ (n - 1)}\ \eta \left[1 - \eta^{2(n-1)}\right] \qquad \text{(II-34)}$$

The constants n and s are a function of the Reynolds number; thus, it would be desirable to have an explicit relationship for them as a function of the Reynolds number. The derivation follows.

Recalling that

$$s = \frac{\tau_o r_o}{2\ \bar{U}_m} \qquad \text{(II-32)}$$

and

$$\tau_o = \frac{-r_o}{2}\ \frac{d\bar{P}}{dx} \qquad \text{(II-19)}$$

and the Moody[23] definition of friction factor

$$\frac{d\bar{P}}{dx} = \frac{f\overline{U_A^2}\ \rho}{4\ r_o} \qquad \text{(II-35)}$$

combining equations (II-32), (II-19) and (II-35) yields

$$s = \frac{f\rho\overline{U_A^2}\ r_o}{16\ \bar{U}_m}$$

or

$$s = \frac{f}{32}\ Re\ \frac{\bar{U}_A}{\bar{U}_m} \qquad \text{(II-36)}$$

where

$$Re = \frac{2r_o\bar{U}_A\ \rho}{\mu}$$

$\bar{U}_A$ = average velocity

In order to evaluate n it will be necessary to integrate the velocity distribution over the pipe cross section to determine the average velocity. Performing that integration

$$\bar{U}_A = 2 \int_o^1 \bar{U}\, \eta\, d\, \eta \qquad \text{(II-37)}$$

or

$$\frac{\bar{U}_A}{2\bar{U}_m} = \int_o^1 \left[1 + \frac{s - n}{n - 1}\, \eta^2 + \frac{1 - s}{n - 1}\, \eta^{2n}\right] \eta\, d\, \eta \qquad \text{(II-38)}$$

continuing

$$\frac{\bar{U}_A}{\bar{U}_m} = 1 + \frac{1}{2}\frac{s - n}{n - 1} + \frac{1 - s}{(n - 1)(n + 1)} \qquad \text{(II-39)}$$

After some algebraic manipulation

$$\frac{\bar{U}_A}{\bar{U}_m} = \frac{s + n}{2(n + 1)} \qquad \text{(II-40)}$$

Substituting the value for s (II-36) into (II-40) and solving for n

$$n = \frac{\frac{f}{64}\, Re - 1}{1 - \frac{\bar{U}_m}{2\bar{U}_A}} \qquad \text{(II-41)}$$

Thus by using equation (II-41) and (II-36) to calculate s and n, for a given Reynolds number, and then using the calculated s and n in equation (II-33) it is possible to calculate the velocity distribution. It should again be pointed out that velocity distribution thus obtained would be a solution to the Reynolds equations but not a unique solution, thus

the value of equation (II-33) will be determined by how well it fits the experimental data.

8. "Law of the Wall," Logarithmic Velocity, Distribution, and Deissler Equation for Mean Velocity Distribution

Townsend[24] has shown from the turbulent energy equation that for moderately high Reynolds numbers most of the turbulent energy production takes place within a region, next to the wall, over which the shear stress is essentially constant. This finding, couples with his analysis that the layer next to the wall is in energy equilibrium, led him to propose that the motion in this region is statistically determined if τ, d and μ (which are sufficient to specify the boundary conditions) are known. Here, d is defined as the thickness of the layer where most of the turbulent energy production takes place. From his analysis Townsend concluded that

$$\frac{\bar{U}}{U^*} = g\left(\frac{U^* y \rho}{\mu}, \frac{y}{d}\right) \qquad \text{(II-42)}$$

where

$$y = r_o - r$$

and that, if y is large enough to include substantially all the energy production but not so large as to be outside the constant stress layer, then

$$\frac{\bar{U}}{U^*} = f\left(\frac{U^* y \rho}{\mu}\right) \qquad \text{(II-43)}$$

It should be noted that close to the wall where the Reynolds stresses are negligible it is generally assumed that f reduces to

$$\frac{\bar{U}}{U^*} = \frac{U^* y \rho}{\mu} \qquad \text{(II-44)}$$

This relationship is equivalent to an assumption that $\frac{d\bar{U}}{dy}$ is constant and equal to the value at the wall. In equations (II-42) and (II-43) it is the mean velocity that is considered; however, Townsend's analysis, and equations (II-42) and (II-43), should be equally valid for the fluctuating velocities. This change would be accomplished by replacing the mean velocity in equations (II-42) and (II-43) by the appropriate fluctuating velocity and by inserting U* to the appropriate power to make the left hand side of the equations dimensionless.

Townsend[24] further pointed out that in the turbulent core, where the Reynolds stresses are much larger than viscosity effects, the flow is largely independent of viscosity and that the principle of Reynolds numbers simularity may be applied to the turbulent core. He thus proposed

$$\bar{U} = U_t + U^o \, f(r/r_o) \qquad \text{(II-45)}$$

where

U^o = characteristic velocity

U_t = an arbitrary velocity

Letting $U^o = U^*$ and $U_t = \bar{U}_m$ equation (II-45) becomes

$$\bar{U} = \bar{U}_m + U^* \, f(r/r_o) \qquad \text{(II-46)}$$

In order for both equations (II-43) and (II-44) to hold in the region where the constant stress layer and turbulent core

overlaps Townsend showed that equation (II-43) must be of the form

$$\frac{\bar{U}}{U^*} = \frac{1}{K} \log \left(\frac{U^* y \rho}{\mu} \right) + A \qquad \text{(II-47)}$$

where K and A are universal constants (Townsend lists A = .41 and K = 5.85). This is the familiar logarithmic velocity profile which has been derived in many different ways; e.g., using Prandtl's mixing length hypothesis and Taylor's vorticity transfer hypothesis.

Deissler[5] has also done considerable work on mean velocity profiles, and he found a semi-empirical equation that gives a good fit in the vicinity of the wall. His equation for velocity requires the evaluation of an iterated integral. The equation appears below:

$$U^+ = \int_0^{y^+} \frac{dy^+}{1 + m^2 U^+ y^+ (1 - e^{-m^2 u^+ y^+})} \qquad \text{(II-48)}$$

where

$U^+ = \bar{U}/U^*$

$y^+ = \frac{U^* \rho y}{\mu}$

m = constant determined from experimental data = 0.124

Deissler claims a good fit for $y^+ < 26$. For the turbulent core he also recommends the logarithmic velocity distribution (II-47) and he lists the values of A and B to be .36 and 3.8 respectively.

9. Correlation Coefficients and Dissipation Length

The turbulence at a fixed point in a flow field is, in general, not independent of the motion of the flow elsewhere; it is especially affected by the motion at nearby points. It would thus be desirable to have some measure of how the flow at one point is influenced by, or correlated with, the flow at other points in the fluid. To this end, G. I. Taylor proposed the spatial correlation coefficients R_{ij} of which there are nine, namely,

$$(R_{ij})_{AB} = \frac{\overline{(u_i)_A \, (u_j)_B}}{u'_{iA} \, u'_{jB}} \qquad \text{(II-49)}$$

where

$(R_{ij})_{AB}$ = correlation coefficient between the fluctuating velocities i and j at points A and B, respectively

u_{iA} = fluctuating velocity in direction i at point A

u_{jB} = fluctuating velocity in direction j at point B

u'_{iA} = intensity of turbulence in direction i at point A

u'_{iB} = intensity of turbulence in direction j at point B

Some remarks concerning the spatial correlation coefficient are in order:

(1) $(R_{ij})_{AB} \leq 1$ This can be shown by a simple application of the Schwarz inequality[21].

(2) As A approaches B or the separation between the points of measurement decreases, the coefficient

approaches the point correlation coefficients $(u_i u_j)_A$ which occur in the Reynolds equations.

(3) When measuring the spatial correlation coefficient between u_i at A and u_i at B, R_{ij} will approach unity as A approaches B.

(4) As the distance between A and B increases $(R_{ij})_{AB}$ should approach zero more or less smoothly.

In this paper only one of the nine spatial correlation coefficients will be investigated; namely, the correlation coefficient between the fluctuating velocities in the axial direction with A and B taken in the axial direction. This coefficient is commonly called $f(\psi)$.

$$f(\psi) = \frac{\overline{u(x)\ u(x+\psi)}}{u'(x)\ u'(x+\psi)} \qquad \text{(II-50)}$$

where

ψ = distance along the x axis between the velocities to be correlated

For pipe flow the field is homogeneous in the x direction and $u'(x)$ is equal to $u'(x+\psi)$. Thus equation (II-50) becomes

$$f(\psi) = \frac{\overline{u(x)\ u(x+\psi)}}{u'^2} \qquad \text{(II-51)}$$

$f(\psi)$ can be expanded in a Taylor's series as follows

$$f(\psi) = 1 + \psi\left(\frac{\partial f}{\partial \psi}\right) + \frac{\psi^2}{2!}\left(\frac{\partial^2 f}{\partial \psi^2}\right)_{\psi=0} + \frac{\psi^3}{3!}\left(\frac{\partial^3 f}{\partial \psi^3}\right)_{\psi=0} + \ldots\ldots \qquad \text{(II-52)}$$

It can be shown[7] by applying the principle of homogeneity that

$$\left[\frac{\partial^{n+m} f}{\partial\psi^{n+m}}\right]_{\psi=0} = \frac{1}{u_1^2}\left[\overline{\frac{\partial^n u}{\partial\psi^n}\frac{\partial^m u}{\partial\psi^m}}\right]_{\psi=0} = 0 \qquad \text{(II-53)}$$

and

$$\left[\frac{\partial^{2n} f}{\partial\psi^{2n}}\right]_{\psi=0} = \frac{1}{u'^2}\left[\overline{u\frac{\partial^{2n} u}{\partial\psi^{2n}}}\right]_{\psi=0} = (-1)^n \frac{1}{u'^2}\overline{\left[\frac{\partial^n u}{\partial x_2^n}\right]^2} \qquad \text{(II-54)}$$

Combination of (II-53), (II-54) and (II-52) yields

$$f(\psi) = 1 - \frac{\psi^2}{2!}\frac{1}{u'^2}\left[\frac{\partial u}{\partial\psi}\right]^2_{\psi=0} + \frac{\psi^4}{4!}\frac{1}{u'^2}\left[\frac{\partial^2 u}{\partial\psi^2}\right]^2_{\psi=0} - \ldots. \qquad \text{(II-55)}$$

By truncating the series at the second term and defining

$$\frac{1}{\lambda^2} = \frac{1}{u'^2}\left[\frac{\partial u}{\partial\psi}\right]^2_{\psi=0} \qquad \text{(II-55)}$$

where

λ = longitudinal dissipation length

one obtains

$$f(\psi) = 1 - \frac{\psi^2}{2\lambda^2} \qquad \text{(II-56)}$$

The Parameter λ is the radius of curvature of the f vs ψ curve at $\psi = 0$.. Physically, λ is usually regarded as a measure of (though not equal to) the diameters of the smallest eddies, which are primarily responsible for the dissipation of energy by molecular viscosity[21]. The proof of equation (II-56) has been rather sketchy, because, in complete detail, it is very long. However, the complete proof of equation (II-56), along with an excellent discussion of correlation coefficients in general, can be found in Hinze[7].

10. Hot Wire Anemometry

In turbulence research one technique has emerged above all others as giving reliable and relatively easily attainable measurements of the fluctuating velocities; this technique is hot wire anemometry. The reason the plurality of the measurements have been taken with a hot wire anemometer is obvious when an analysis is made of the requirements that must be met by an instrument for measuring the turbulence quantities.

Hinze[7] has listed the requirements of a turbulence measuring instrument and his analysis is summarized below:

(1) The detecting element must be small thus making as little as possible disturbance in the flow field.

(2) The size of the sensing element should be smaller than the smallest eddies.

(3) The response of the sensing element must be rapid so as to be able to measure turbulence frequencies up to 5000 cycles per second.

(4) The sensing element must be sensitive to the small fluctuations in turbulent flow, i.e., a few per cent of the mean velocity.

(5) The instrument must be stable.

(6) The measuring instrument must be rigid enough not to be affected by wind tunnel vibrations, etc., as they would be recorded as turbulence by the recording apparatus.

Of course, the hot wire anemometer does not satisfy all of these requirements in every detail, but it has far outstripped other detectors.

Basically, the hot wire anemometer consists of a short length (~0.03 inches) of a small diameter wire (~0.0001 inches) placed in the air stream and heated to about 200°C by electric current. The rate of heat transfer from the wire is a function of the velocity over the wire; thus, as the velocity changes the rate of heat loss changes and if the wire is kept at a constant temperature (heat content of the wire constant) the power input to the wire must change. This change in input to the wire is by virtue of a change in current through the wire; the current is monitered and thus translated by the recording instrument into a reading that can be further translated, with suitable calibration, into the desired turbulence quantity.

Since the sensing element of the hot wire anemometer is simply a long thin cylinder, it would be expected that the heat transfer laws for the two would be the same. This is the case. Assuming that the fluid is an incompressible gas and that the effects of natural convection and radiation are negligible, the heat transfer coefficient for the wire is given by[7]

$$Nu = \frac{hd}{k} = 0.42\ Pr^{0.2} + 0.57\ Pr^{0.33}\ Re^{0.50} \qquad \text{(II-57)}$$

where

$Pr = \frac{C_p \mu}{k}$ = Prandtl number

$(Re)_w = \frac{\rho \vec{U}_e d}{\mu}$ = Reynolds number of the wire

$(Nu)_w = \frac{hd}{k}$ = Nusselt number of the wire

C_p = heat capacity of the gas

d = diameter of the wire

k = thermal conductivity of the gas

h = heat transfer coefficient for the wire

ρ = density of the gas

$\vec{U}_e$ = vector velocity perpendicular to wire

In the preceding equation all of the gas physical properties are evaluated at the "film temperature," i.e., the average of the temperature of the wire and the bulk gas. The equation is valid when[7]:

(1) $0.01 < (Re)_w < 10{,}000$

After some calculation it can be shown that this gives a velocity range

$.1 < U < 10^5$ ft/sec

which is sufficiently wide for the velocities that will be considered.

(2) Natural convection may be neglected for the range

$Re > 0.5$ if

$$(Gr)_w \, Pr = \frac{g C_p \rho^2 \beta d^3 \Delta T}{\mu k} < 10^{-4}$$

where

g = acceleration due to gravity

β = coefficient of expansion of gas

T = temperature

ΔT = difference in temperature between the wire and gas

$(Gr)_w = \frac{g\rho^2 d^3 \beta \Delta T}{\mu^2}$ = Grashof Number of wire

For air and a wire 0.002 inches in diameter

$(Gr)_w Pr \sim 10^{-6}$ which is acceptable.

(3) Thermal radiation is considered negligible if the temperature of the wire is less than 300°C. For our experiments the wire is approximately 200°C which is acceptable.

The heat loss per unit time from the wire is

$$h \pi dS(T_w - T_g) \qquad \text{(II-58)}$$

where

T_w = wire temperature

T_g = gas temperature

S = length of wire

Upon using the value of h calculated from equation (II-57) equation (II-58) becomes

$$\pi kS(T_w - T_g)\ 0.42\ (Pr)^{0.20} + 0.57\ (Pr)^{0.33}\ (Re)_w^{0.50} \qquad \text{(II-59)}$$

Since for constant temperature operation the heat loss due to

forced convection is equal to the heat input by electrical means (i^2R) or

$$i^2R = \pi k S (T_w - T_g) \left[0.42(Pr)^{0.2} + 0.57(Pr)^{0.33}(Re)_w^{0.50} \right] \quad \text{(II-60)}$$

The temperature dependence of the resistance of the wire may be represented by

$$R_w = R_o \left[1 + \gamma(T_w - T_o) \right] \quad \text{(II-61)}$$

where

R_w = resistance of the wire

R_o = resistance at an arbitrary reference temperature, say 0°C

γ = temperature coefficient of electrical resistivity of the wire

By representing R_g by a similar relationship $(T_w - T_g)$ may be expressed as

$$T_w - T_g = \frac{R_w - R_g}{\gamma R_o} \quad \text{(II-62)}$$

where

R_g = resistance the wire would have at T_g

Thus, equation (II-61) may be written as

$$\frac{i^2 R_w}{R_w - R_g} = \frac{\pi k S}{\gamma R_o} \left[0.42(Pr)^{0.2} + 0.57(Pr)^{0.33}(Re)_w^{0.50} \right] \quad \text{(II-63)}$$

or

$$\frac{i^2 R_w}{R_w - R_g} = K_1 + K_2 \sqrt{U_e} \quad \text{(II-64)}$$

where

$$K_1 = \frac{\pi k S \; 0.42(Pr)^{0.2}}{\gamma \; R_o}$$

$$K_2 = \frac{\pi k S \; 0.57(Pr)^{0.33}}{\gamma \; R_o} \frac{\rho d^{0.5}}{\mu}$$

Equation (II-64) is called King's equation and shows the functional relationship between the electrical signal and the velocity; namely, the square of the current through the wire is proportional to the square root of the velocity. The constants K_1 and K_2 are generally determined experimentally. The general equation (II-63) has been derived as it is useful for estimating the effects of gas and wire properties on the constants.

11. Directional Sensitivity of the Hot Wire

In the equations for heat loss from a heated wire it is seen that the loss is proportional to $\vec{U}_e$; i.e., the effective vector velocity or the vector velocity perpendicular to the wire. Thus, a wire is sensitive to various components of the velocity according to the orientation of wire with respect to the velocity vector. This result makes it possible, by changing the orientation of the wire and using two or more wires, to measure various fluctuating components of the velocity and the correlations between them.

Referring to Figure (1a) it is seen that adding w to $\overline{U} + u$ has no effect on the magnitude of the velocity vector

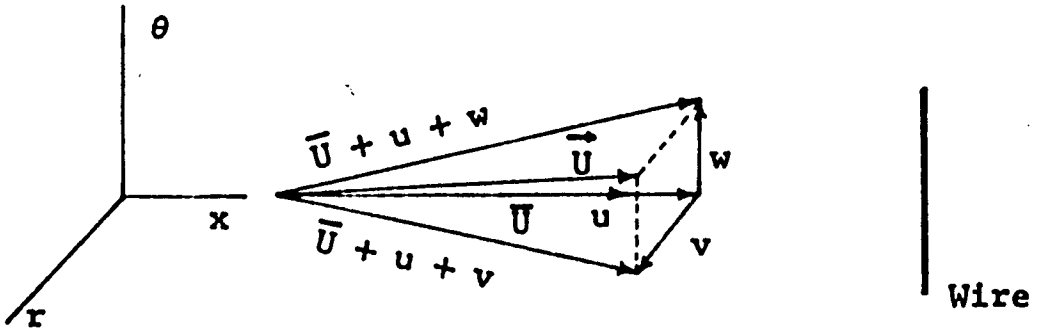

FIGURE (1a)

RESOLUTION OF THE VELOCITY VECTOR INTO ITS COMPONENTS

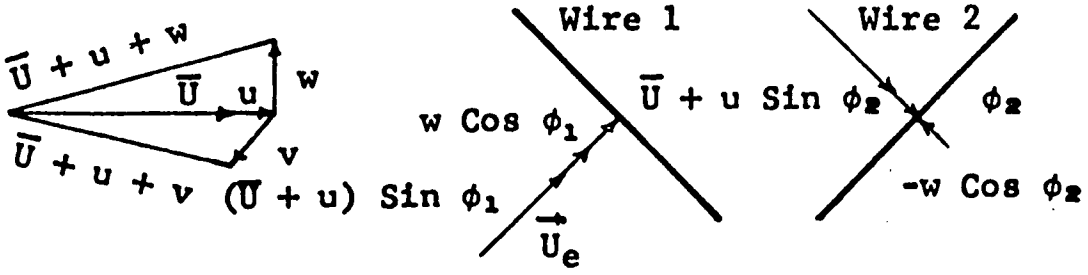

FIGURE (1b)

CROSS WIRE MEASUREMENTS

perpendicular to the wire; thus, it may be said that the wire is insensitive to w. By adding v to $\bar{U} + u$ only very little change is made in the effective velocity vector. The above qualitative conclusions may be shown mathematically by considering the components that make up $\vec{U}_e$. Since w is parallel to the wire it offers no contribution to $\vec{U}_e$; thus, since $\bar{U} + u$ and v are perpendicular to the wire, we may write

$$(\vec{U}_e)^2 = (\bar{U} + u)^2 + v^2 \qquad \text{(II-65)}$$

or

$$(\vec{U}_e)^2 = \bar{U}^2 + 2u\bar{U} + u^2 + v^2$$

but since

$$\bar{U}^2 >> 2u\bar{U} >> v^2$$

it is possible to neglect v^2 and equation (II-65) becomes

$$\vec{U}_e = \bar{U} + u \qquad \text{(II-66)}$$

Thus, it is certainly permissible to neglect v^2 and w^2 with respect to $\bar{U} + u$ and we may say, that a wire perpendicular to the mean flow is insensitive to the fluctuations in the radial and azimuthal directions.

Now consider the case when the wire is not perpendicular to the mean flow, as shown in Figure (1b). From the figure it would be sensitive to all three velocity vectors and this is the case. However, it is considerably more sensitive to the two components $\bar{U} + u$ and w, that are in the plane of the wire, than it is to v, which is not in the plane of the wire;

FIGURE (2)

SCHEMATIC OF SERVO CONTROL AMPLIFIER

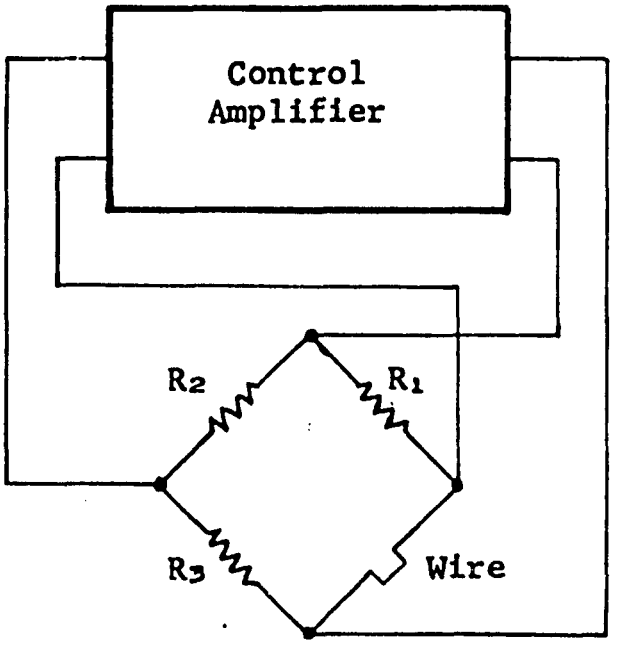

e.g., see equation (II-65) and (II-66) where $(\bar{U} + u)$ are in the plane of the wire and v is not. Thus, neglecting v and considering the velocity vectors as shown in Figure (1b) the following semi-quantitative analysis may be made of the heat transfer rate of the wires:

(1) The component of the vector $(\bar{U} + u)$ perpendicular to wire 1 is $(\bar{U} + u)$ Sin ϕ_1, and that of w is w Cos ϕ_1.

(2) The component of the vector $(\bar{U} + u)$ perpendicular to wire 2 is $(\bar{U} + u)$ Sin ϕ_2, and that of w is -w Cos ϕ_2.

(3) If the electrical signals from the two wires are added w cos ϕ_1 and -w cos ϕ_2 will cancel when $\phi_1 = \phi_2 = \pi/4$. The signal is thus proportional to $(\bar{U} + u)$.

(4) When the electrical signals are subtracted, the $(\bar{U} + u)$ Sin ϕ_1 would be opposite in sign to $(\bar{U} + u)$ Sin ϕ_2. The resultant signal would be proportional to w.

We can conclude that by arrangement of the wires, as shown in Figure (1b), and by proper manipulation of the electrical signals it is possible to obtain a measure of the aximuthal fluctuating velocity, w. By rotating the axis 90° about the x axis a similar measurement may be made of v.

A more extensive analysis of the directional sensitivity of the hot wire is given in the appendix.

CHAPTER III

APPARATUS

1. Design and Details of the Test Equipment

The aim of this research was to measure fully developed turbulent shear flow in a 5 inch pipe, at velocities from the transition velocity up to 100 ft/sec. It was with this criterion in mind that the test equipment was designed. Photographs and drawings of the equipment are shown in Figures (3), (4), and (5).

Two blowers were used to supply air to the test section, a 1 hp centrifugal blower, for high velocities and a 1/20 hp centrifugal blower for low velocities. The blowers are attached through rubber sleeves (vibration eliminators) to a calming box, Figure (4). The calming box consists of a circular section 3 feet in diameter and 4 feet long attached to a conical section which tapers at a 25 degree angle to the 5 inch diameter of the pipe. In the calming box, to prevent circulation and straighten the flow, is a honeycomb fabricated from 10 inch lengths of vent pipe stacked parallel to the axis of the box and soldered in place. Following the honeycomb are two screens for breaking up any large, slowly

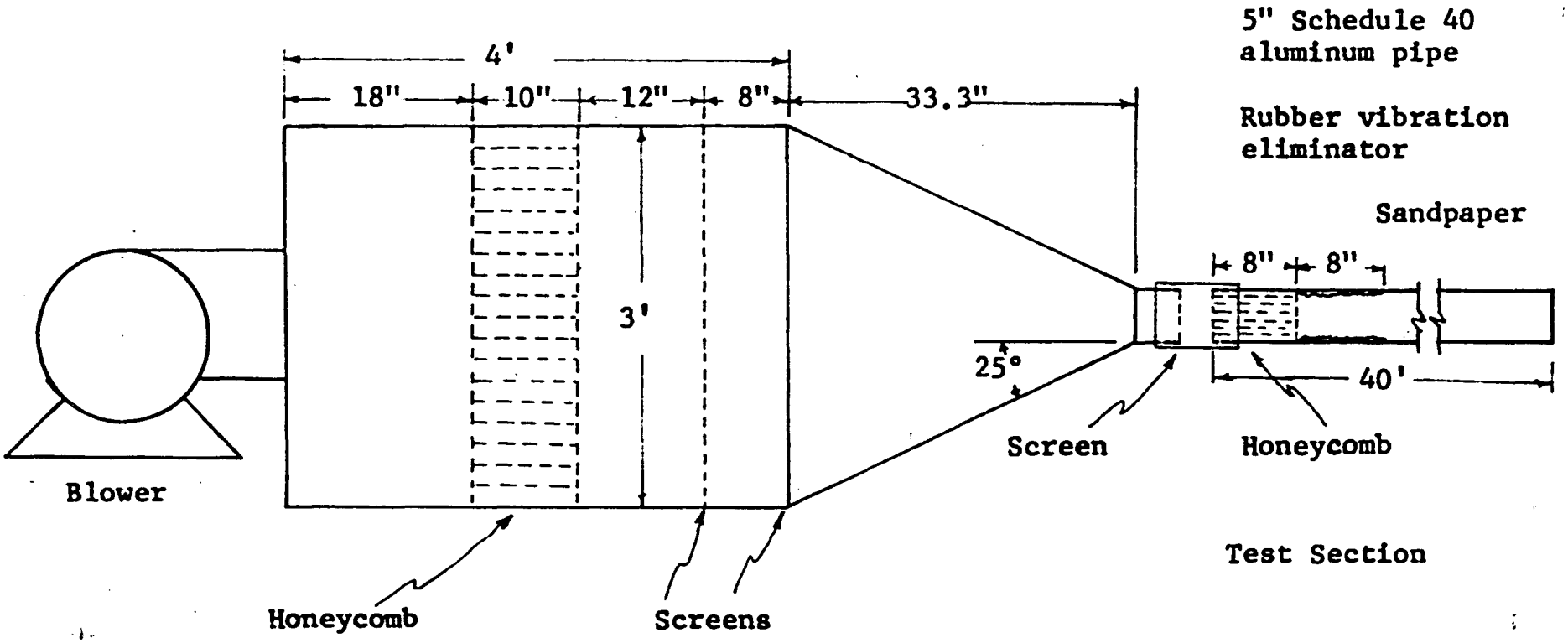

Calming Box

FIGURE (3)

TEST EQUIPMENT

FIGURE (4a)

BLOWERS AND FLOW CONTROLLING VANE

FIGURE (4b)

BLOWERS, CALMING AND TEST SECTION

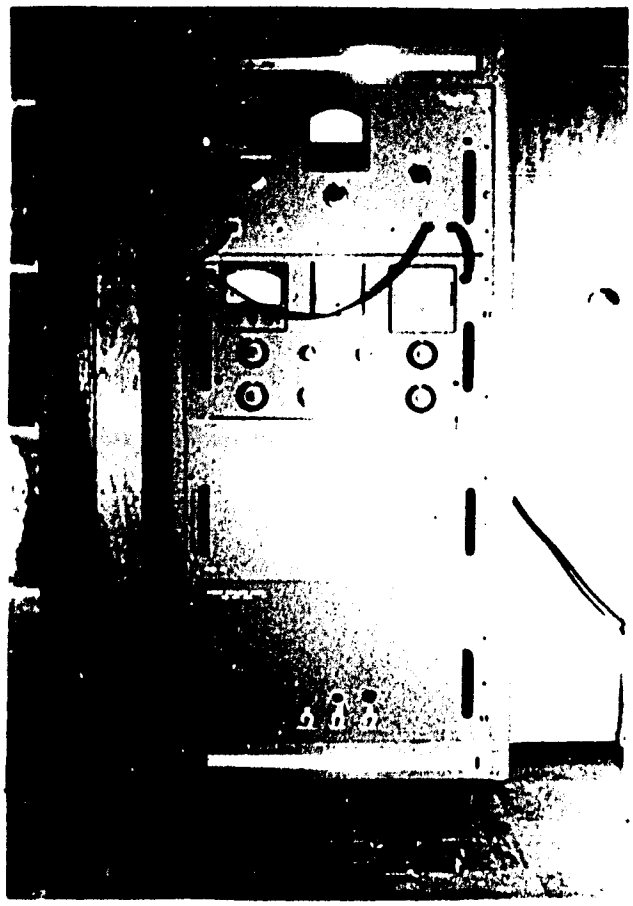

FIGURE (5a)

MODEL IIHR TYPE 3A
TWIN CHANNEL
HOT WIRE ANEMOMETER

FIGURE (5b)

PITOT TUBE AND ADJUSTABLE
DRAFT GAGE

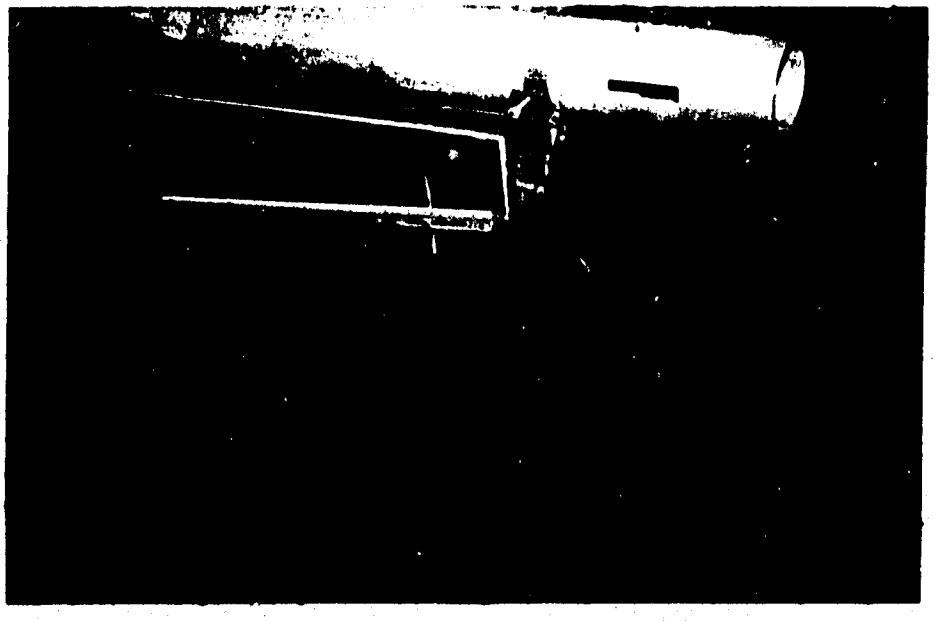

decaying eddies which might be formed by the blowers. The screens were made of ordinary household screen wire.

The calming box is attached through a second rubber sleeve (vibration eliminator) to the 40 foot test section of 5 inch schedule 40 aluminum pipe. A third screen and a honeycomb, fabricated out of 8 inch lengths of 7/8 inch condenser tubing, were placed at the entrance to the test section. Following the honeycomb an 8 inch length of very coarse sandpaper was glued to the wall. This served to induce boundary layer formation.

The 40 foot test section of pipe consisted of two 20 foot lengths connected by a precision machined coupling. The pipes and other equipment were mounted, through rubber vibration eliminators, on heavy steel cradles.

The criterion by which the test section must be judged is whether or not the turbulence is fully developed at the measuring point. Hinze[7] recommends that a minimum of 40 pipe diameters be used to assure that turbulence is fully developed. In this research the measuring point is 96 diameters from the entrance and the sandpaper, etc. should further guarantee that the turbulence will be fully developed at the measuring point. In order to verify that the turbulence was fully developed at the measuring point. In order to verify that the turbulence was fully developed at the point of measurement velocity and intensity traverses were made at center line velocities of 20 and 100 ft/sec under four different conditions:

(1) Measuring point normal with screen and honeycomb, at the pipe entrance, in place.

(2) Measuring point rotated 90° counterclockwise with screen and honeycomb in place.

(3) Measuring point normal with screen and honeycomb removed.

(4) Measuring point rotated 90° counterclockwise with screen and honeycomb removed.

When the four runs for each velocity were compared they agreed within experimental error. Therefore the conclusion is made that the turbulence, at the measuring point, is independent of the history of the fluid and must be fully developed.

2. Hot Wire Anemometer

The Hot Wire Anemometer used in this research was the model I I H R Type 3A Linear Constant-Temperature Hot Wire Anemometer System obtained from the Hubbard Instrument Company, 4 West Park Road, Iowa City, Iowa. A photograph of the instrument is shown in Figure (5a).

The chassis housing the electronic components of the anemometer consists of four separate sections. They are from bottom to top:

(1) Dual Power Supply--This is used to supply +250 volt D.C. and -140 volt D.C. to the R.M.S. Analyzer

and amplifiers. The power supplies employ specially designed regulators so that the total hum and noise in the 250 volt source is kept very low (50 microvolts).

(2) Fan--The fan is used to blow warm air around the electronic components and thus shorten warm up time and eliminate drift due to change in operating temperature of the components.

(3) Two Channel Control Amplifiers and Linearizing Stage--Two completely separate servo-type control amplifiers are housed in this section; each contains a linearizing circuit for translating the fourth-root relationship between current and velocity into a proportionality. This is done by varying the operating temperature of the wire (varying R in Figure (5a), a variable resistor located on the panel of the instrument) so that the bridge characteristic is the inverse of the relationship between signal current and control voltage. The servo-type amplifiers are used to maintain the wires at essentially constant temperature and in so doing generate a current. The average value of this current ($\bar{I}$) is measured on the D.C. panel meter located on the front of each amplifier.

(4) R.M.S. Analyzer--The fluctuating signals from either of the two channels can be combined in the R.M.S. Analyzer in the following ways:

(a) Either signal can be metered separately.
(b) The signals can be added and then metered.
(c) The signal from channel 2 can be subtracted from the channel 1 signal and then metered.

The metering instrument is an RMS reading thermocouple type milliammeter mounted on the panel of the RMS Analyzer. There is also a facility for differentiating any of the signals (a), (b), or (c) and then metering it. A scopejack is provided on the front panel so that it is possible to view on an auxiliary oscilloscope, the fluctuating signal that is metered by the RMS Analyzer.

The operation of the Type 3A anemometer can be described as follows. Refer to the servo control loop in Figure (2). As the velocity past the wire changes (increases, for example) the rate of heat transfer from the wire will increase, thus tending to cool the wire and lower the resistance. This error signal (generated by the unbalance in the Wheatstone bridge) causes the control amplifier to act accordingly; in this case increases the current and thus heat the wire back up to the desired resistance and put the bridge back in balance, thus maintaining the wire at constant temperature. For the purposes of this research the response of the control amplifier can be considered instantaneous.

As the velocity over the wire changes it causes the current through the wire to change and the voltage drop across the bridge changes. This voltage drop across the bridge, which bears the usual fourth root relationship to the velocity, is applied to the linearizing circuit which contains a tube in which the relationship between signal current and control voltage is the inverse of the bridge characteristic for a wire of the recommended size when operated at the correct temperature[9]. It is this current that is metered on the D.C. Panel Meter (which with calibration gives the mean velocity) and is fed through a blocking capacitor to the RMS Analyzer, which in turn will give readings which bear a known relationship to the fluctuating velocities.

Photographs of the probes and traversing mechanism used in this research are given in Figures (6), (7), and (8). In Figure (6) is the single wire with its traversing mechanism. Notice that the back of the probe tube is hinged onto the piece of tubing that carries the hot wire leads to the instrument and bears on the probe tube a bit further up toward the tip. This allows one, by screwing the micrometer in and out, to traverse the entire pipe radius. With suitable calibration of micrometer reading versus pipe radius, it is possible to determine the pipe position to about $\pm$ 0.0005 inches. The probe wires used in this research were 0.00014 inches in

FIGURE (6)

PROBE WITH MOUNT AND TRAVERSING MECHANISM

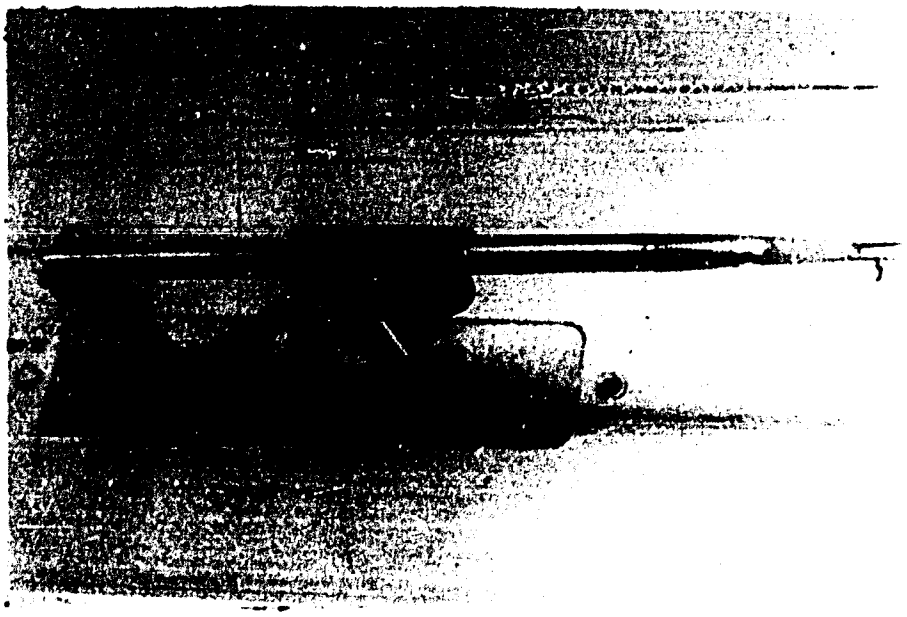

FIGURE (7a)

PROBE MOUNTED IN PIPE (INSIDE VIEW)

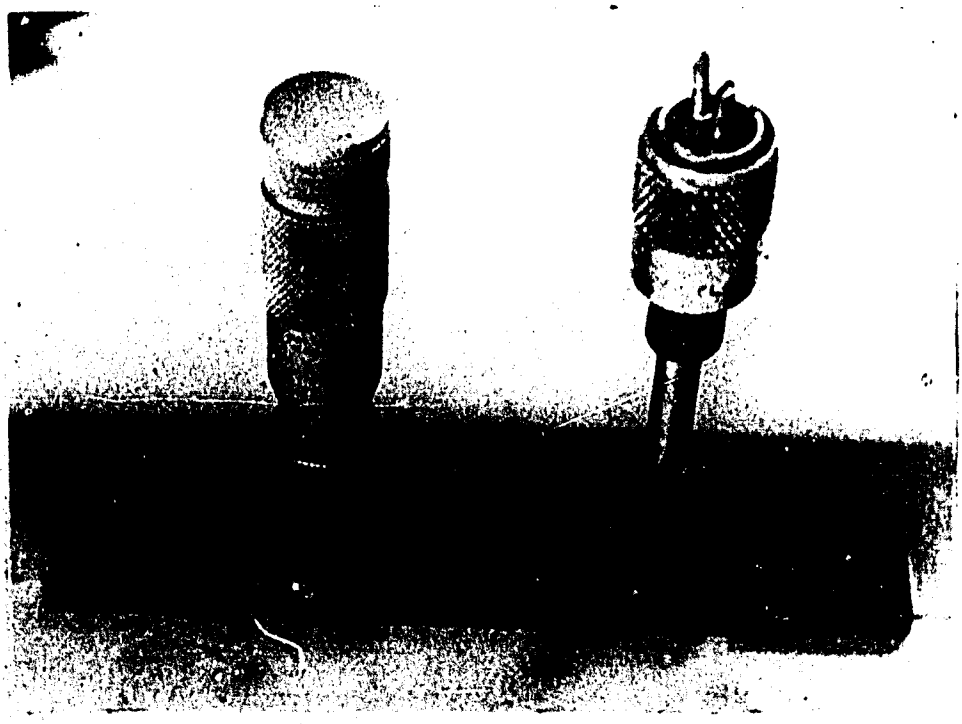

FIGURE (7b)

PROBE MOUNTED IN PIPE (OUTSIDE VIEW)

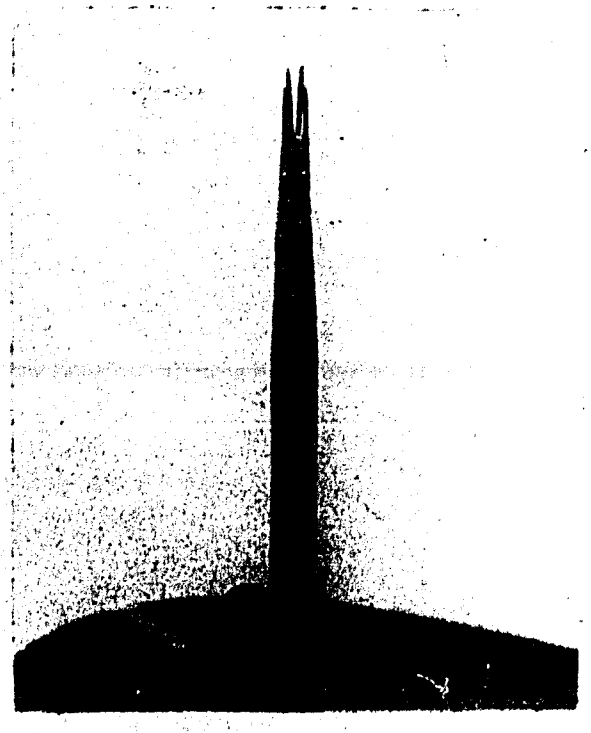

FIGURE (8a)

PROBE TIP (CROSS WIRE)

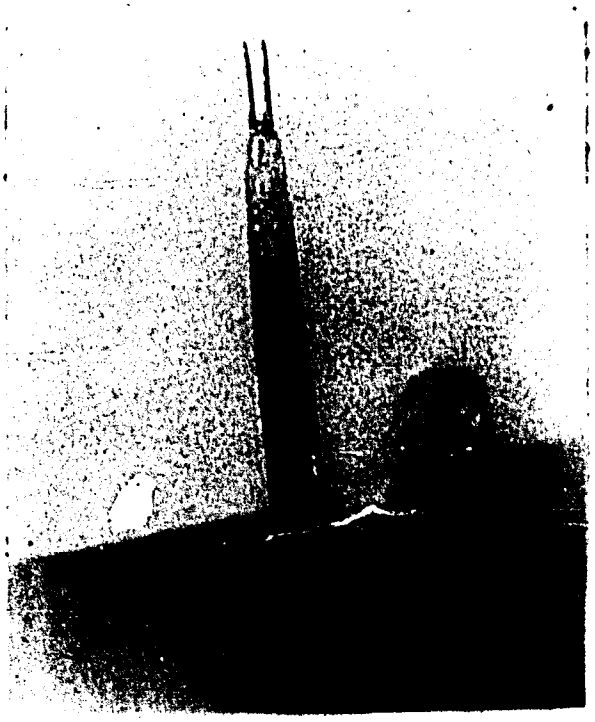

FIGURE (8b)

PROBE TIP (SINGLE WIRE)

diameter tungsten which were obtained from the Sigmund Cohn Corporation, Mount Vernon, New York. Inasmuch as tungsten cannot be soldered it was necessary to plate the wire with copper before it could be soldered across the probe tips. After the wires were soldered across the tips of the probe the copper was etched to the desired length with nitric acid, thus leaving the tungsten wire exposed to the air stream.

3. Auxiliary Equipment

In the semi-quantitative photographic studies of the axial fluctuating velocity a Hewlett-Packard Model 130B Oscilloscope was used to monitor the signals and to produce the trace for the photographs. The specfications of the scope were as follows:

(1) Band Width of Output Amplifiers - D.C. to 300 K.C.
(2) Internal Calibration - $\pm$ 2%
(3) Input Impedence - 2 megohm

The camera used in the photographic studies was a Dumont Type 297 Oscillograph Record Camera. The film used was Polaroid Type 47, 3000 speed.

For the primary standard in the velocity calibration a Type M-168 pitot tube, obtained from the Meriam Instrument Company, was used. A custom fabricated draft gage, which could be inclined to 0.1 inch per foot was used as the pressure differential indicator for the pitot tube. Varsol (ρ = 0.7680 gm/ml @ 80°F) was used as the manometer fluid.

CHAPTER IV

EXPERIMENTAL STUDIES

1. General on the Measurement of Turbulence

In turbulent pipe flow, or any boundary flow, it is in the region next to the wall where the turbulence quantities change the most. This phenomenon is a result of changing from a region of small velocity gradient, which resembles free turbulent flow with negligible viscous effects, to a region of extreme velocity gradient, where viscosity effects are starting to play an important role and then, finally to the region immediately adjacent to the wall where the viscous effects control the flow. Thus, it would seem logical to concentrate the larger number of experimental measurements in the wall region so as to be able to define the derivative of the relationships in this region. This was the case in this research.

In order to better define the distances from the wall at which the turbulence quantities varies the most, a trial set of data was taken. With these data as a guide experimental points along the pipe radius were taken so as to best define the relationships among the variables. To this end 27

experimental points were chosen along the radius of the pipe, with 16 being taken in the 0.5 inch next to the wall (the radius of the pipe was 2.524 inches).

From an experimental standpoint it is indeed unfortunate that the region next to the wall is of so much interest. There are very many difficulties that are encountered in making hot wire measurements next to the wall. Some of these are:

1. It is difficult to ascertain when the wire is at $r = r_o$. It is not possible to allow the wire to touch the wall as this would result in a broken wire. In this research the position of the wall was determined by extrapolating the velocity distribution data to $\overline{U} = 0$.
2. Very close to the wall the heat transfer from the wire to the wall causes the mean velocity measurements to be high, and could cause the calibration constant, used in calculating turbulence quantities, to be in error.
3. Near the wall the intensity of turbulence reaches a maximum thus causing both the intensity and mean velocity meters to fluctuate a great deal; there are resultant errors in these readings. These fluctuations are particularly noticeable in the low velocity runs; for example, in the run at Re = 4,800 one $\overline{I}$ reading (proportional to mean velocity) was 0.77 and fluctuated between 0.62 and 0.90.

4. The wires for the cross wire probe must of necessity be separated by sufficient distance to prevent electrical contact, and from the fabrication standpoint it was not possible to separate the wires by less than about 0.030 inches; in the region next to the wall the mean velocity and some of the turbulence quantities may vary 30 per cent in 0.030 inches; thus, readings taken with a cross wire instrument, in the vicinity of the wall, would have little or no meaning.

From the foregoing statements it should be obvious that hot wire data in the vicinity of the wall should be used with discretion.

2. Mean Velocity Measurements

Mean velocity profiles were measured at center line velocities of 100, 90, 80, 70, 60, 50, 40, 30, 20, 10, 5.03, and 2.53 ft/sec. At each velocity a total of 27 measurements starting at a distance of 0.0025 inches from the wall and distributed approximately logarithmetically (with respect to distance from the wall) were taken. The results are given in Figures (9) through (14) and in Tables I through XII.

As pointed out above the measurements close to the wall were a bit high due to the heat transfer from the wire to the wall. This effect, of course, becomes more severe as the velocity decreases, because the heat transfer from the wire to the gas by forced convection decreases, and the heat transfer

FIGURE (9)

MEAN VELOCITY PROFILE IN THE TURBULENT CORE
(HIGH VELOCITY)

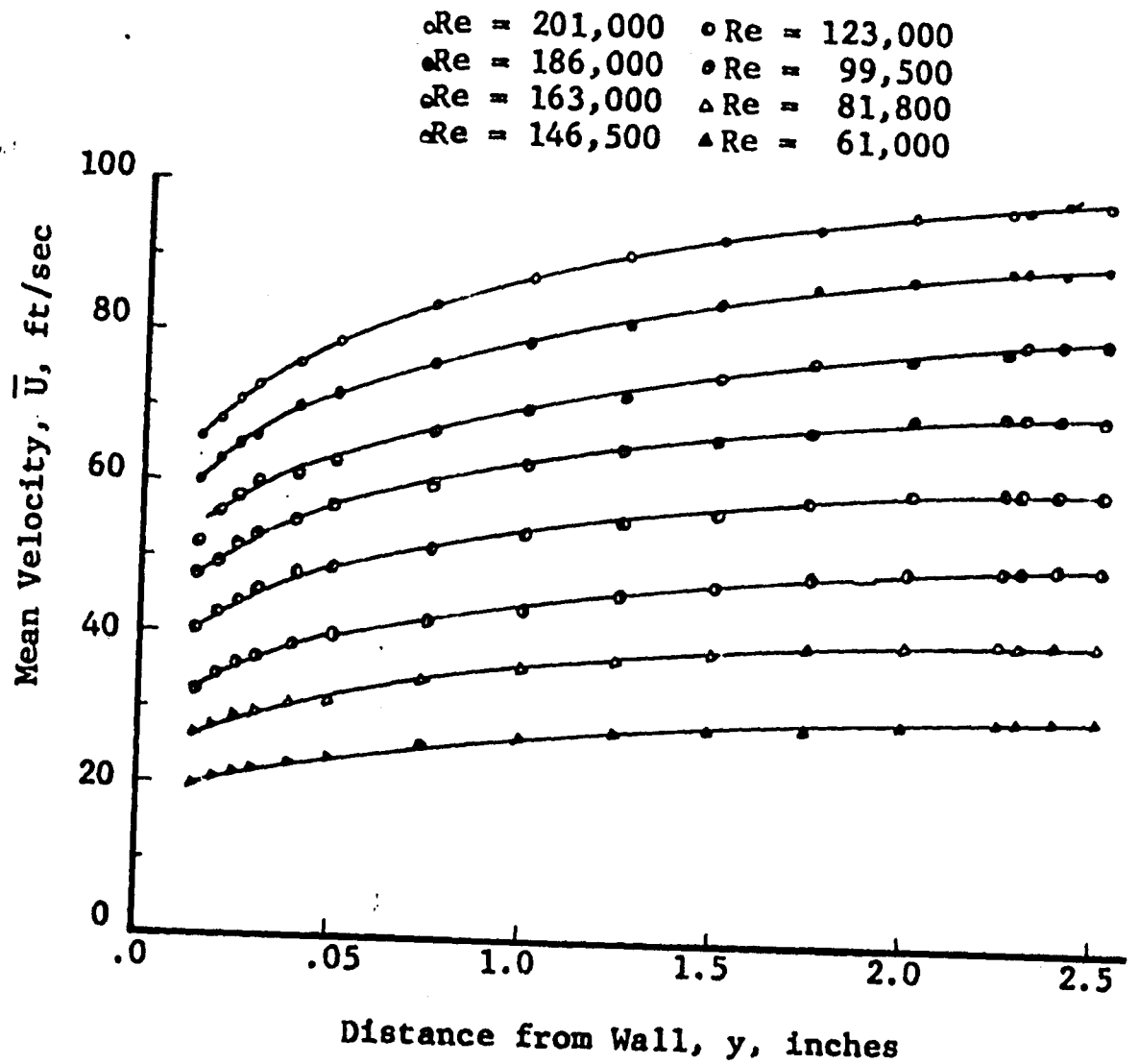

FIGURE (10)

MEAN VELOCITY PROFILE IN THE TURBULENT CORE
(MODERATE VELOCITY)

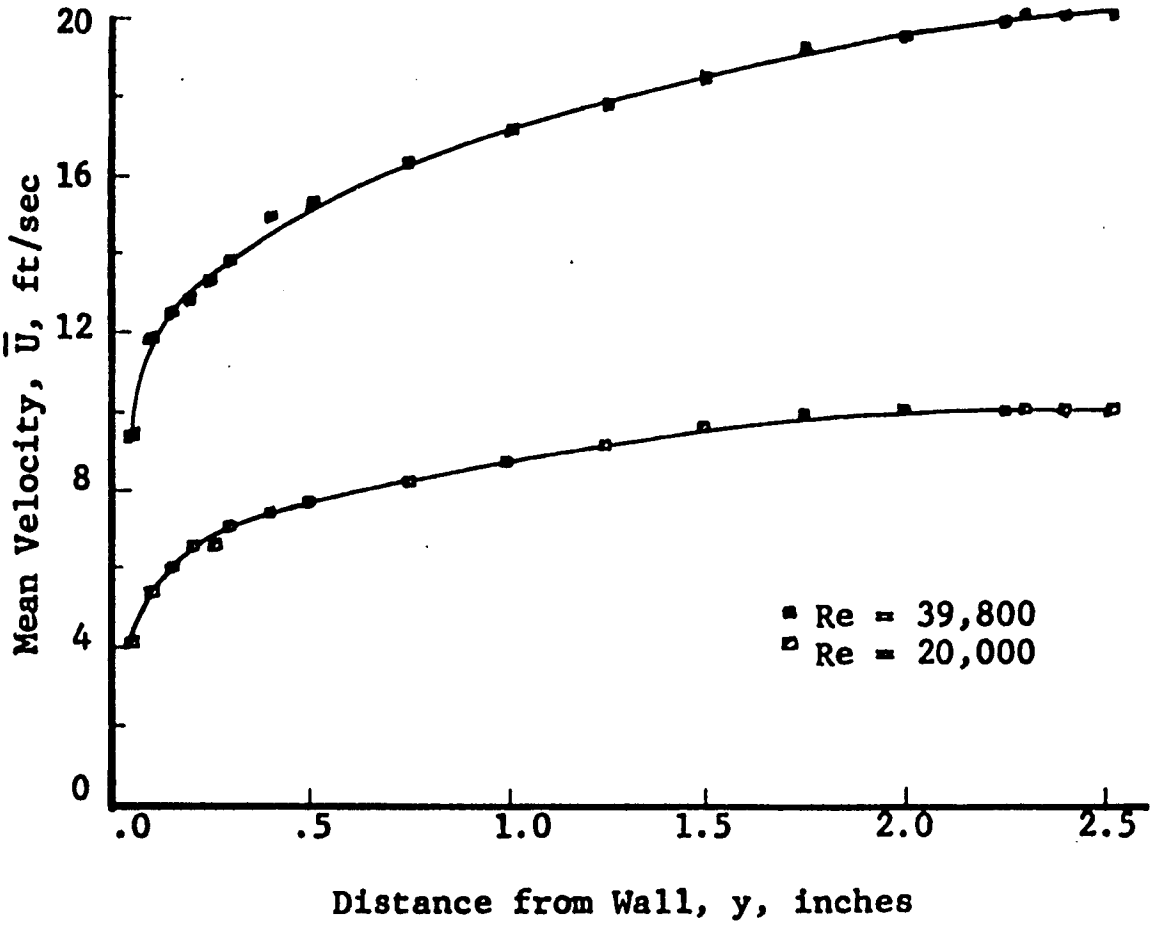

FIGURE (11)

MEAN VELOCITY PROFILE IN THE TURBULENT CORE
(LOW VELOCITY)

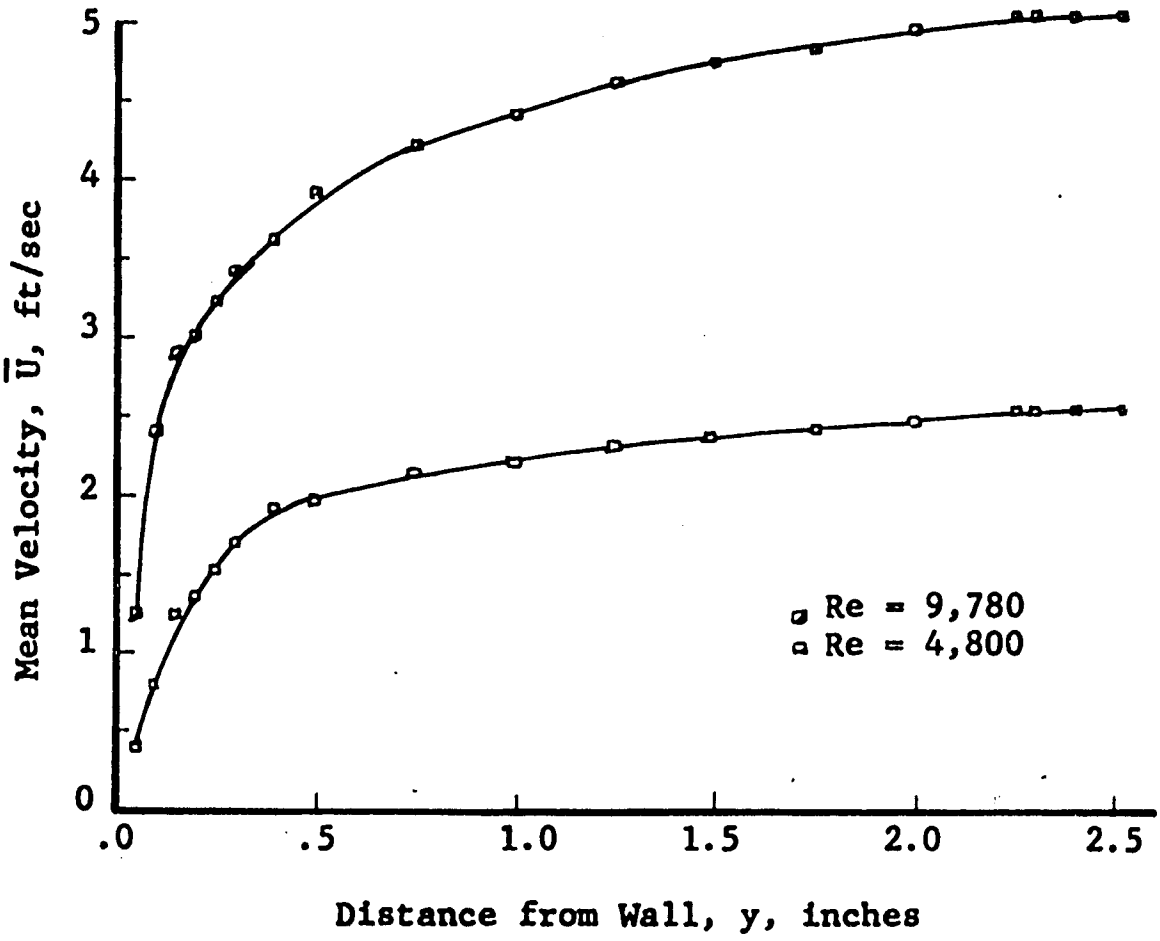

FIGURE (12)

MEAN VELOCITY PROFILE IN THE WALL REGION
(HIGH VELOCITY)

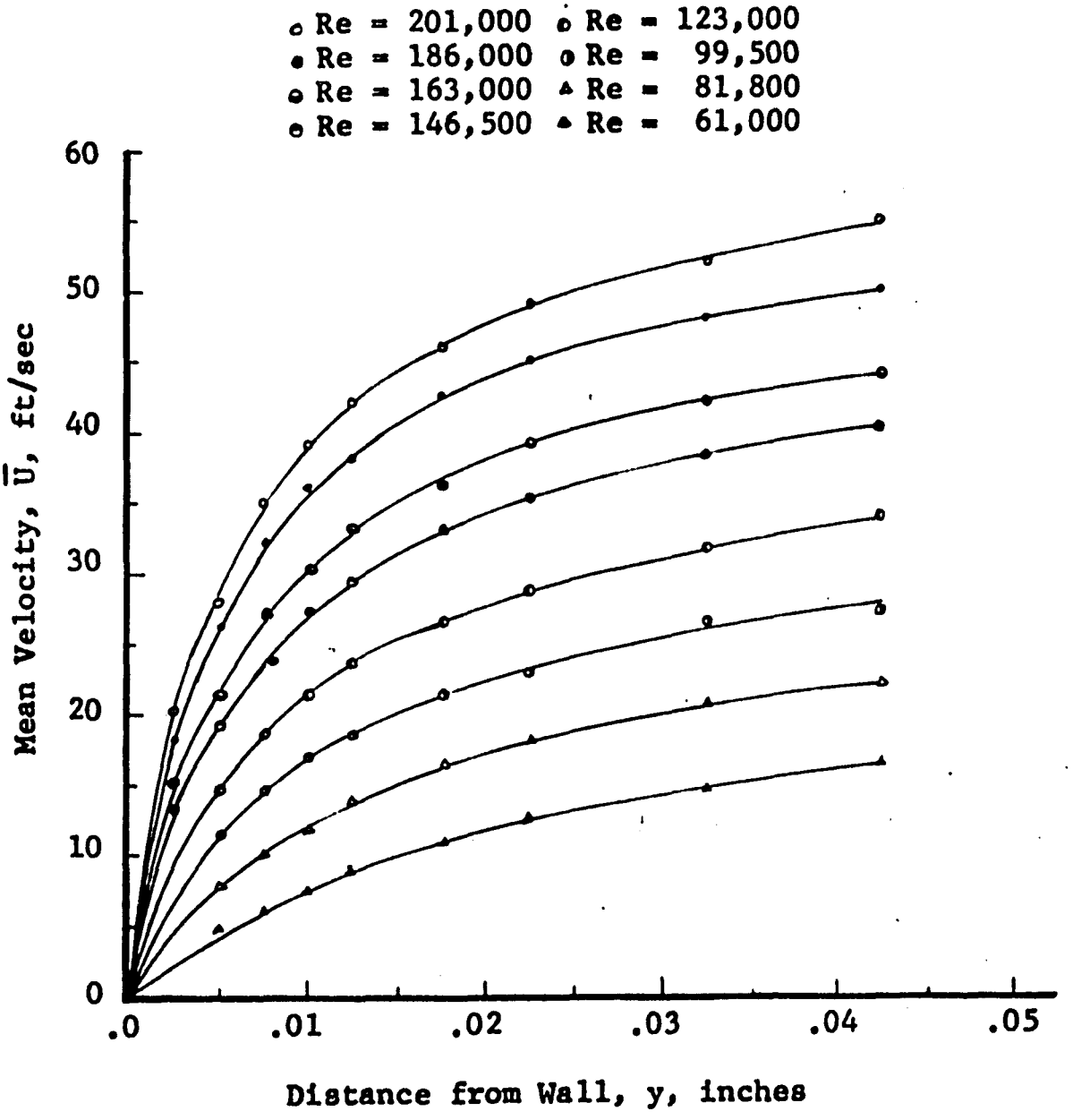

FIGURE (13)

MEAN VELOCITY PROFILE IN THE WALL REGION
(MODERATE VELOCITY)

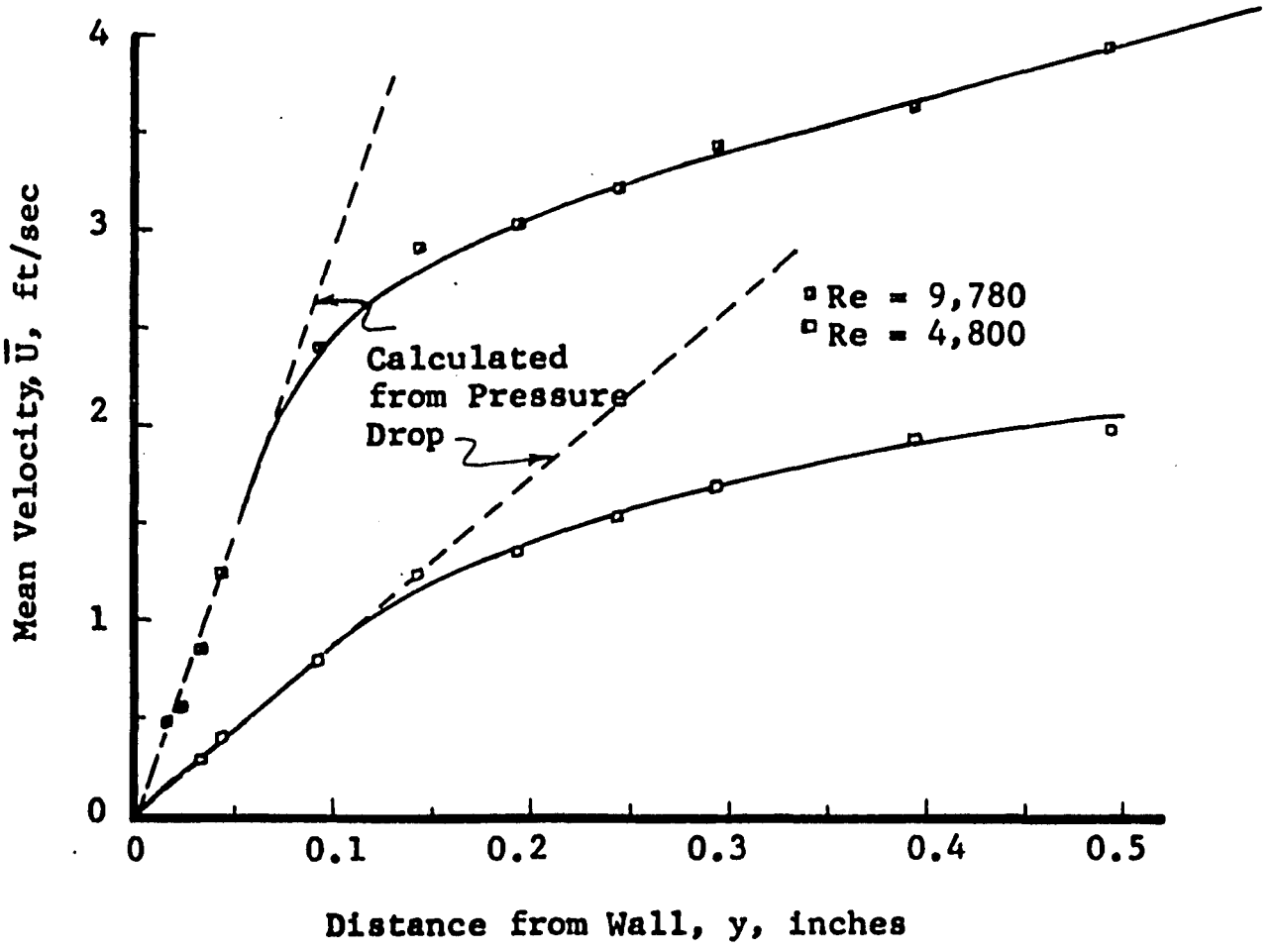

FIGURE (14)

MEAN VELOCITY PROFILE IN THE WALL REGION
(Low Velocity)

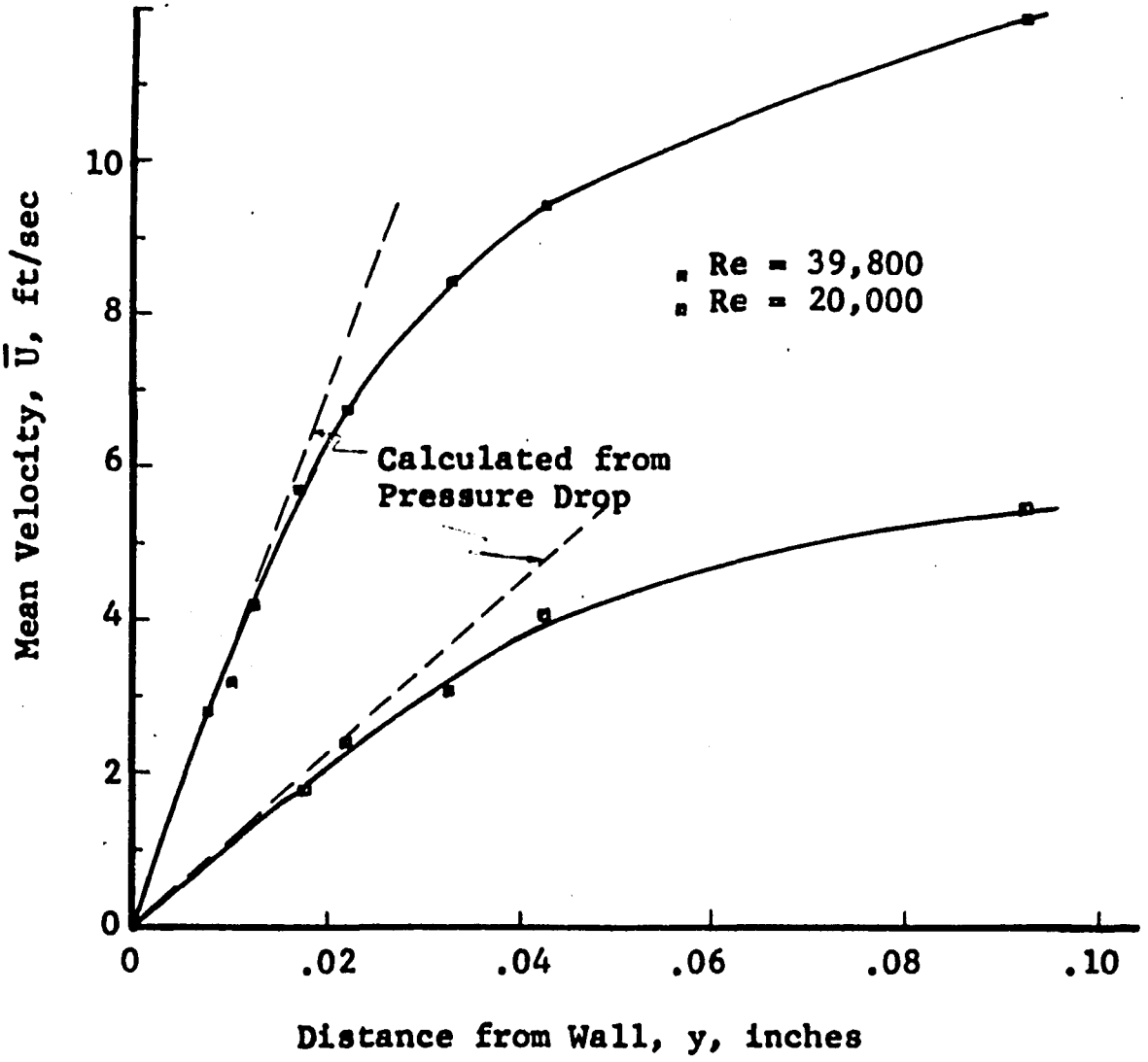

to the wall assumes a larger percentage of the total heat loss from the core. It is therefore necessary to have some criterion for discarding the measurements, near the wall, when they appear to be too high. The procedure adopted was that when the measured mean velocity was higher than that given by $U^+ = Y^+$ (i.e., $\frac{d\overline{U}}{dy}$ = constant = $\frac{\tau_o}{\mu}$), it was usually disregarded.

The general curvature of the mean velocity data is as would be expected; i.e., the velocity gradients are everywhere small except near the wall, and, as Reynolds number is increases, the velocity distributions become flatter. This result can, of course, be explained by the fact that as the Reynolds number increases the ratio of eddy viscosity to absolute viscosity increases and thus absolute viscosity plays a smaller part in controlling the flow mechanism.

3. Intensity of Turbulence Measurements

The intensity of turbulence was measured at the same points and velocities as given above for mean velocity. The results of these measurements are given in Figures (15) through (21) and in Tables I through XII.

In Figure (15) it is seen that the intensity of turbulence increases fairly linearly from the center of the pipe to the wall over about 90 per cent of the pipe radius. Then as the wall is approached more closely the intensity starts to increase rapidly reaching a maximum close to the wall and then decreases to zero at or near the wall.

FIGURE (15)

INTENSITY OF TURBULENCE IN THE TURBULENT CORE
(HIGH VELOCITY)

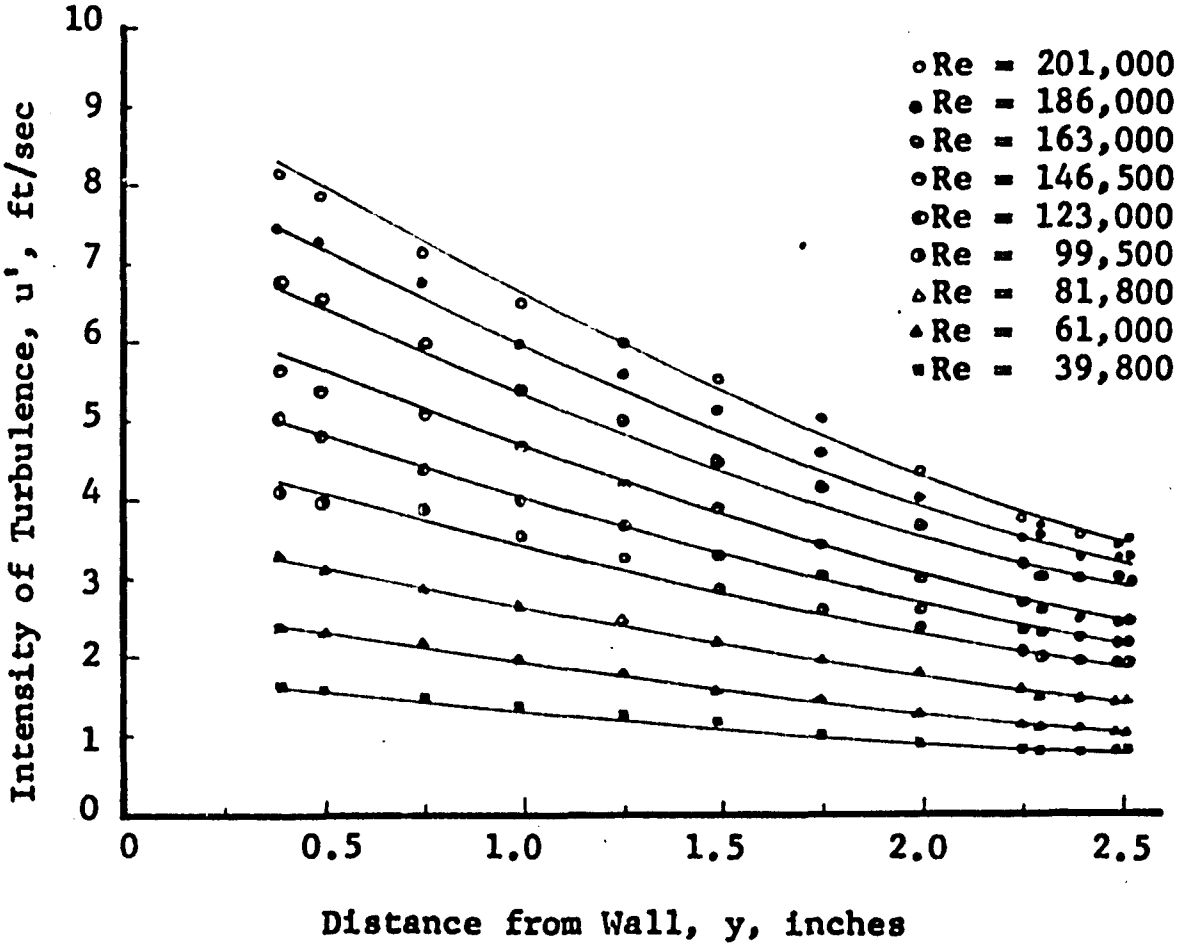

FIGURE (16)

INTENSITY OF TURBULENCE IN THE TURBULENT CORE
(LOW VELOCITY)

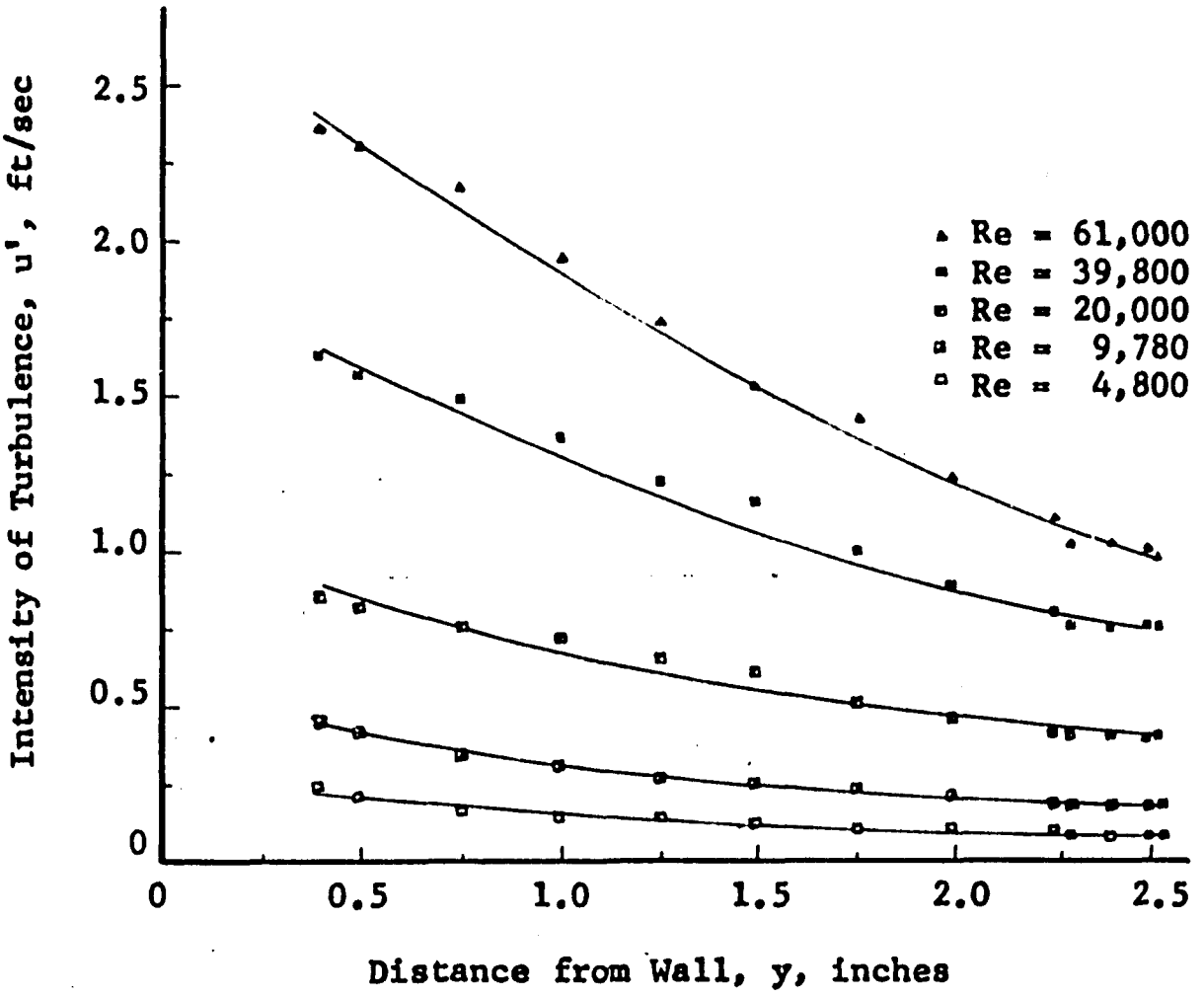

FIGURE (17)

INTENSITY OF TURBULENCE IN THE OUTER EDGE OF THE TRANSITION REGION
(HIGH VELOCITY)

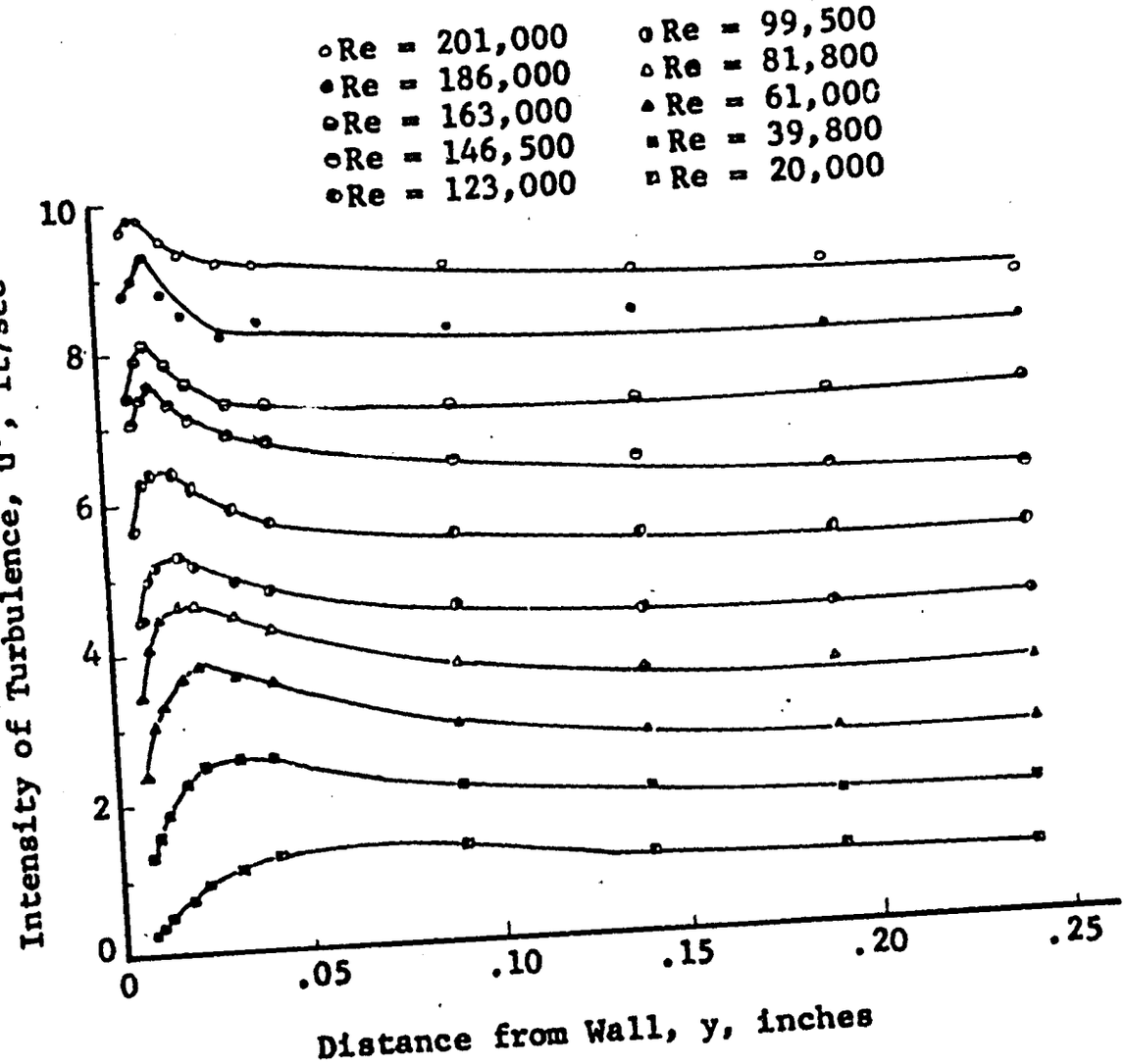

FIGURE (18)

INTENSITY OF TURBULENCE IN THE OUTER EDGE OF THE TRANSITION REGION
(LOW VELOCITY)

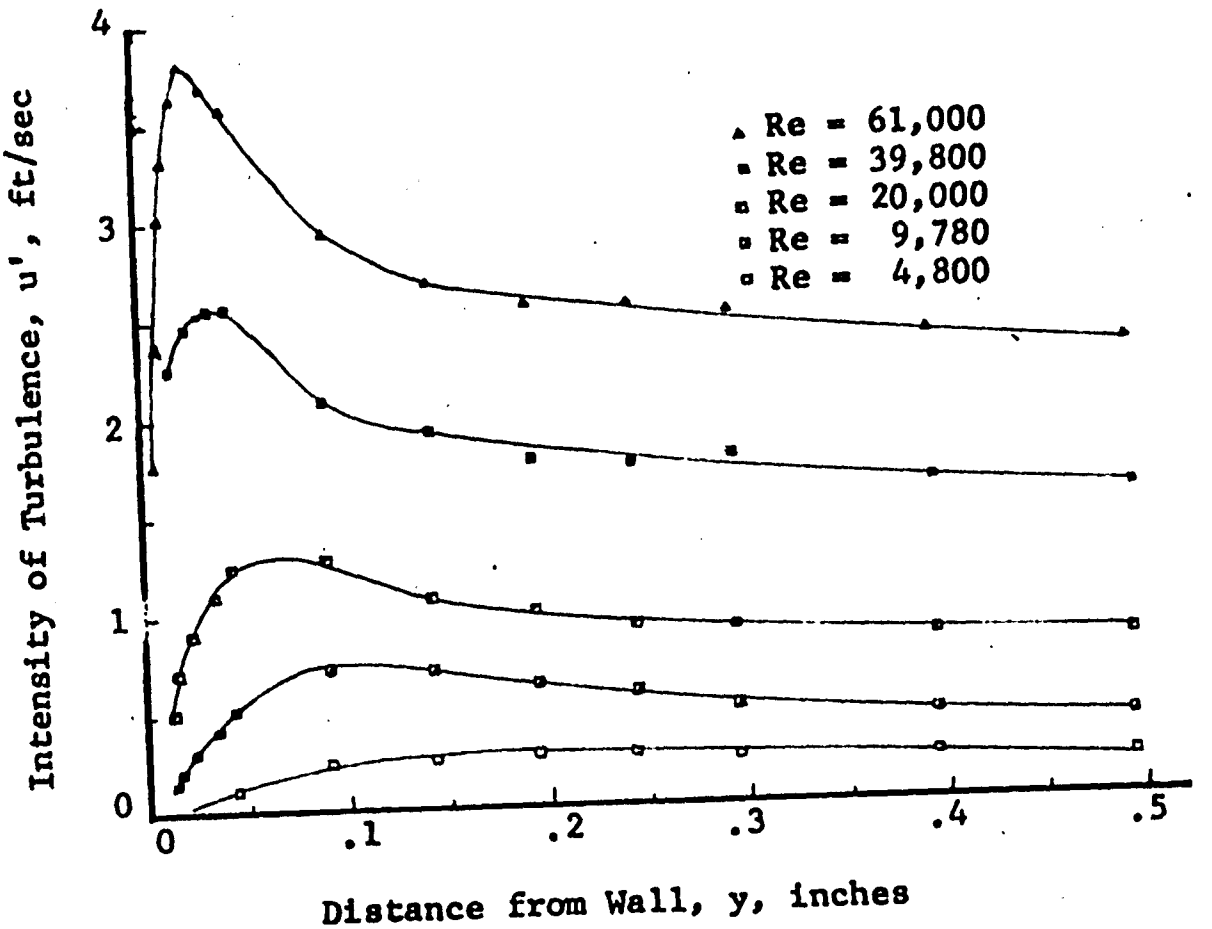

FIGURE (19)

INTENSITY OF TURBULENCE IN THE WALL REGION
(HIGH VELOCITY)

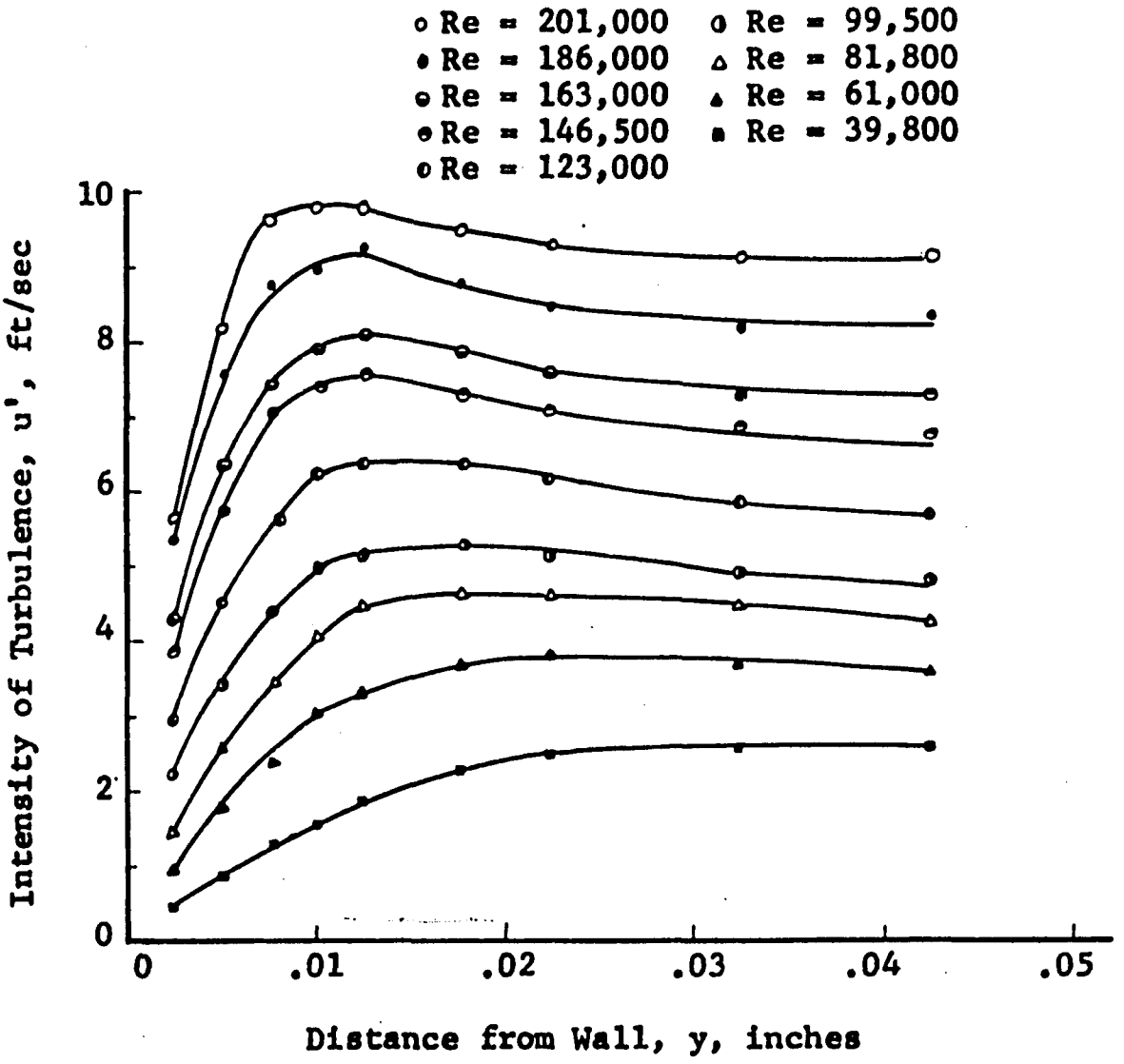

FIGURE (20)

INTENSITY OF TURBULENCE IN THE WALL REGION
(MODERATE VELOCITY)

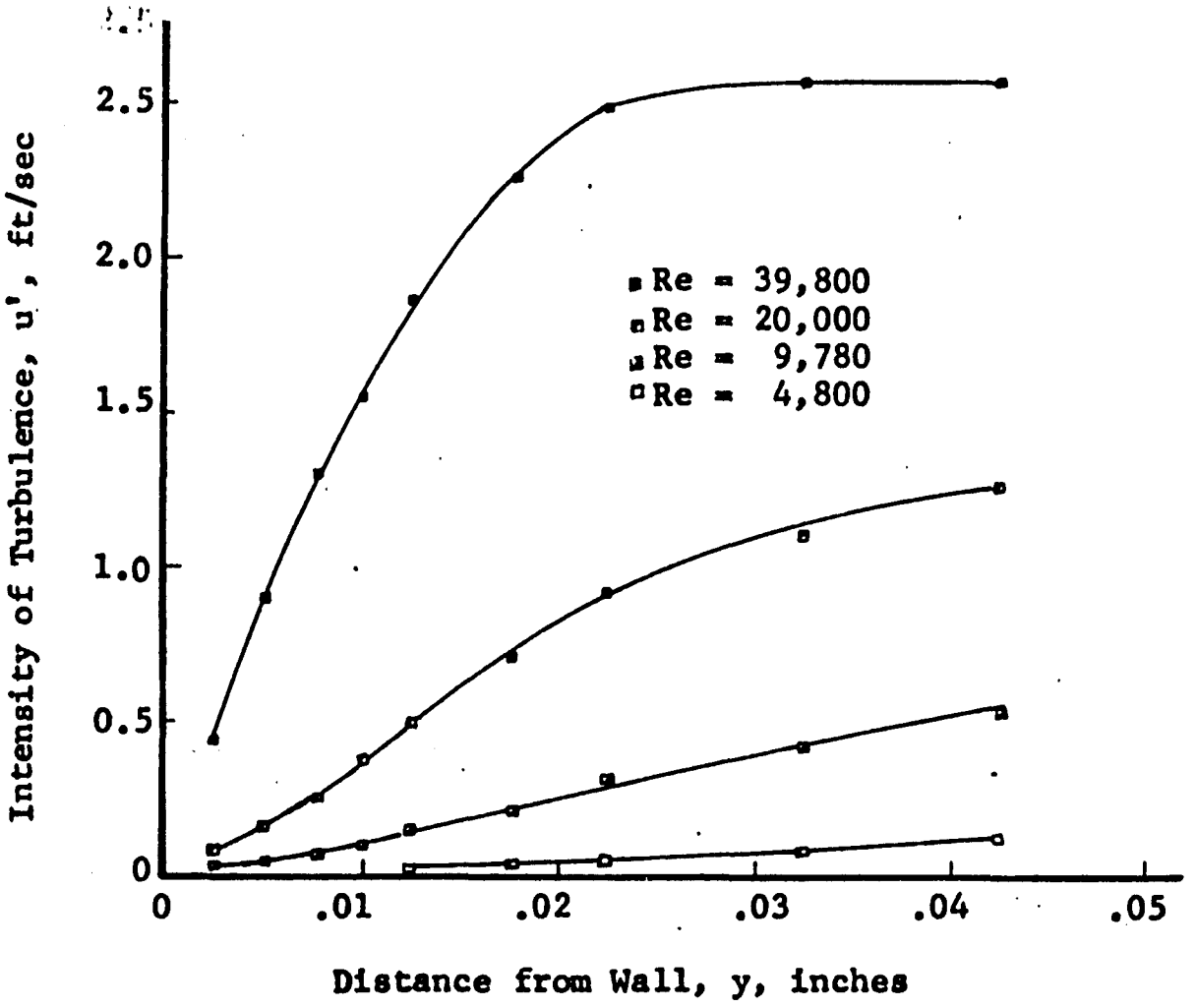

FIGURE (21)

INTENSITY OF TURBULENCE IN THE WALL REGION
(LOW VELOCITY)

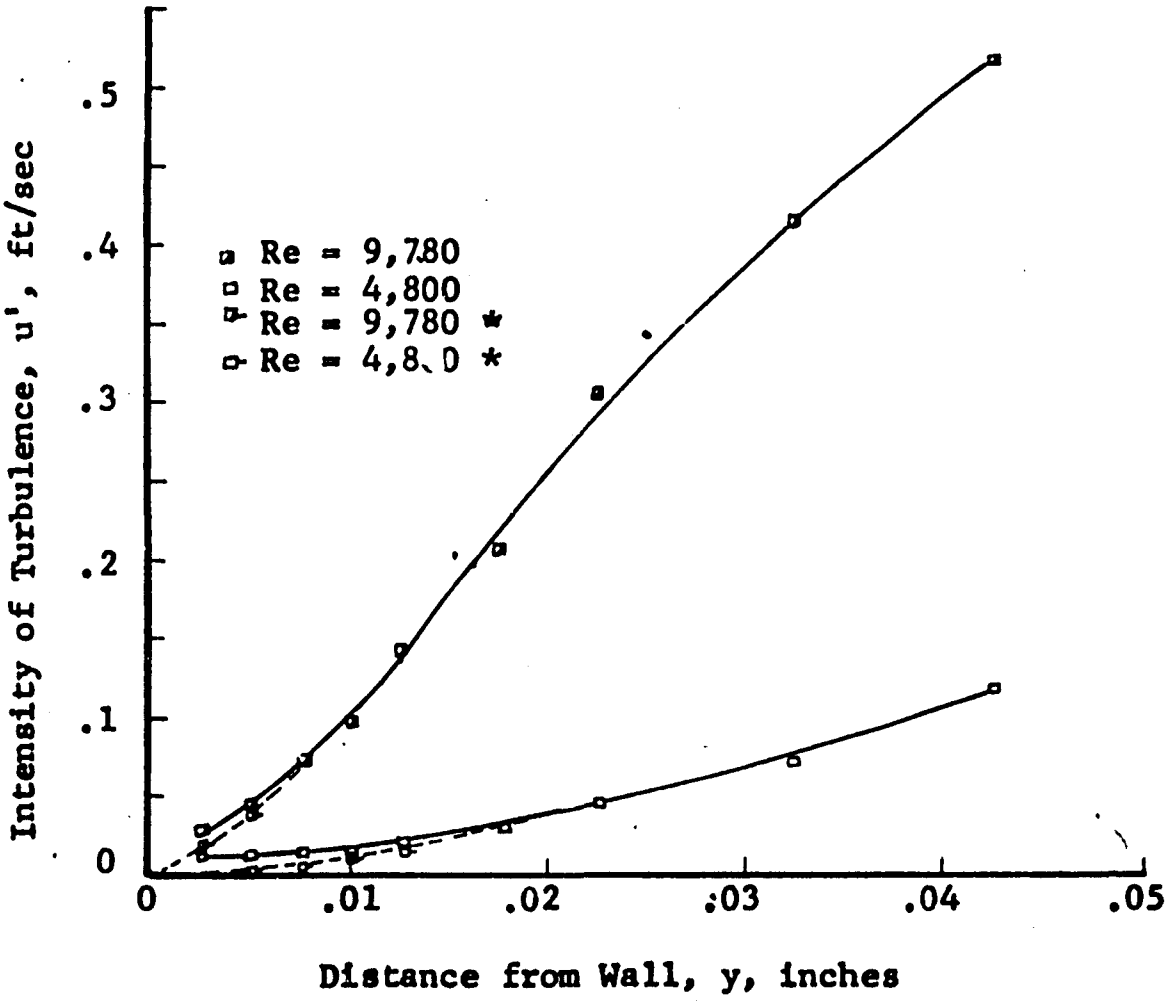

* Corrected for noise.

In the high velocity runs the intensity of turbulence was still fairly large as near to the wall as measurements could be made (y = 0.0025 inches). However, as the Reynolds number decreases, the intensity decreases, and at the lowest Reynolds number turbulence was not detectable at a distance of 0.0025 inches from the wall. Therefore, if this result is to be accepted, it must be concluded that a laminar sublayer exists in this turbulent flow.

The observation that the intensity of turbulence is zero at some finite distance from the wall merits some discussion, especially as to the validity of this result. Referring to Figure (21) notice that for the Reynolds number = 4,800 there are two curves in the region next to the wall. The dotted line (which gives $u' = 0$ at $y = 0.0025$) has been corrected for random noise probably caused by the wire being at an elevated temperature. This random noise causes a fluctuating signal which gives an indication on the I_T meter (u' indicating meter).

The procedure used to correct for this random noise was to measure it with zero velocity past the wire (which gave the same indication, namely $I_T = 1.00$, as the Re = 4,800 run with the probe 0.0025 inches from the wall) and to subtract this by a random noise correction procedure (see Appendix)[2].

It should also be pointed out that the vanishing of u' at this point could be attributed to (although this is not

believed to be the case) a dampening effect caused by the large amount of heat transfer to the wall.

4. Oscillogram Studies of the Fluctuating Velocity

In Figures (22), (23), and (24) are presented oscillograms of the fluctuating velocity for Reynolds numbers of 6,630, 39,800, and 186,000 respectively. Note that as the Reynolds number is increased the peaks become sharper and, of course, higher. The sensitivity in Figure (22c) is 1/875 of that in Figure (24e).

An interesting phenomenon occurs in the high velocity oscillograms near the wall Figure (22e) and to a lesser extent in Figure (23e); namely, the appearance of spikes. These spikes are the result of very sharp increases in velocity and are similar to those observed by von Rosenberg[25] in parallel flat jets.

von Rosenberg speculated that the spikes in the parallel flat jets were a consequence of the production of a series of vortexes as in the Karman vortex street and the resulting breaking away of the vortex from the region where it was formed. A similar analysis might apply to these results; i.e., it could be that vortexes are formed by the wall and the extreme velocity gradient in the region of the wall. When these vortexes break away from the wall and are picked up by the adjacent layer of fluid, which is at a much higher

FIGURE (22)

OSCILLOGRAMS OF THE AXIAL FLUCTUATING VELOCITY
Re = 186,000

(22a) y = 2.5000, Relative Amplification = 1/219

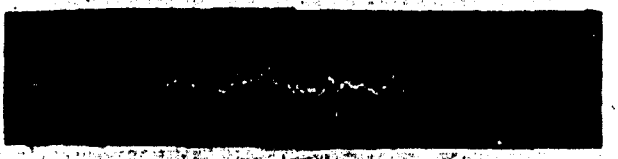

(22b) y = 1.0000, Relative Amplification = 1/438

(22c) y = 0.0400, Relative Amplification = 1/875

(22d) y = 0.0200, Relative Amplification = 1/875

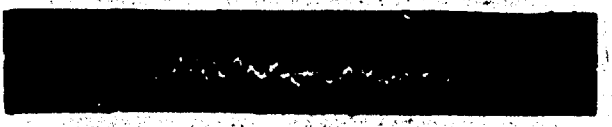

(22e) y = 0.0075, Relative Amplification = 1/438

FIGURE (23)

OSCILLOGRAM OF THE AXIAL FLUCTUATING VELOCITY
Re = 61,000

(23a) y = 2.5000, Relative Amplification = 1/80

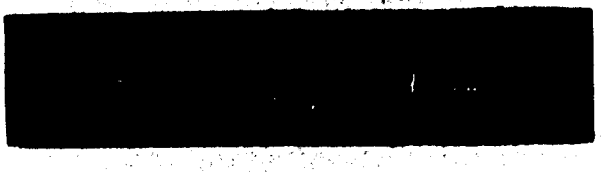

(23b) y = 1.0000, Relative Amplification = 1/160

(23c) y = 0.2500, Relative Amplification = 1/160

(23d) y = 0.0250, Relative Amplification = 1/320

(23e) y = 0.0075, Relative Amplification = 1/80

FIGURE (24)

OSCILLOGRAMS OF THE AXIAL FLUCTUATING VELOCITY
Re = 6,630

(24a) y = 2.5000, Relative Amplification = 1/10

(24b) y = 1,0000, Relative Amplification = 1/40

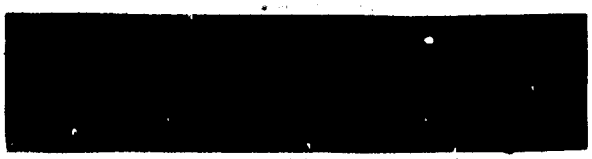

(24c) y = 0.4000, Relative Amplification = 1/20

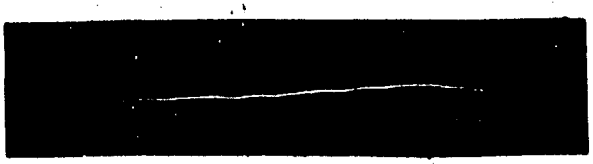

(24d) y = 0.2000, Relative Amplification = 1/5

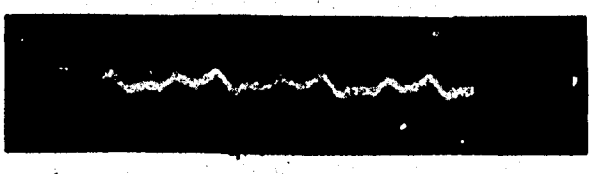

(24e) y = 0.0075, Relative Amplification = 1

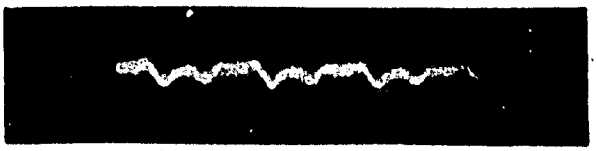

(24f) y = 0.0075, Relative Amplification = 1

velocity, there would be a sharp increase in velocity.

A second speculation as to the cause of the spikes is that high velocity eddies penetrate the layer next to the wall resulting in a sharp increase in velocity. Of course, it cannot be discounted that the spikes are not the result of some erratic behavior of the wire in the close proximity of the wall. However, the spikes are not believed to be due to erratic behavior of the wire and support is given this conclusion by the fact that von Rosenberg's measurements were not made near a wall.

5. Dissipation Length Measurements

Dissipation length measurements were made at center line velocities of 98.3, 90, 80, 70, 60, 50, and 40. At each velocity dissipation length measurements were made at the same pipe positions as mean velocity and intensity of turbulence. Dissipation length results are tabulated in Tables I through VII in the Appendix and are shown in Figures (25) and (26).

The dissipation length appears, for the range of Reynolds number investigated, to be relatively constant for a given distance from the wall. The dissipation length decreases gradually as the wall is approached. This is probably a result of the increase in turbulent action and in the velocity gradient.

In the turbulent core the dissipation length seems to be

FIGURE (25)

DISSIPATION LENGTH IN THE TURBULENT CORE

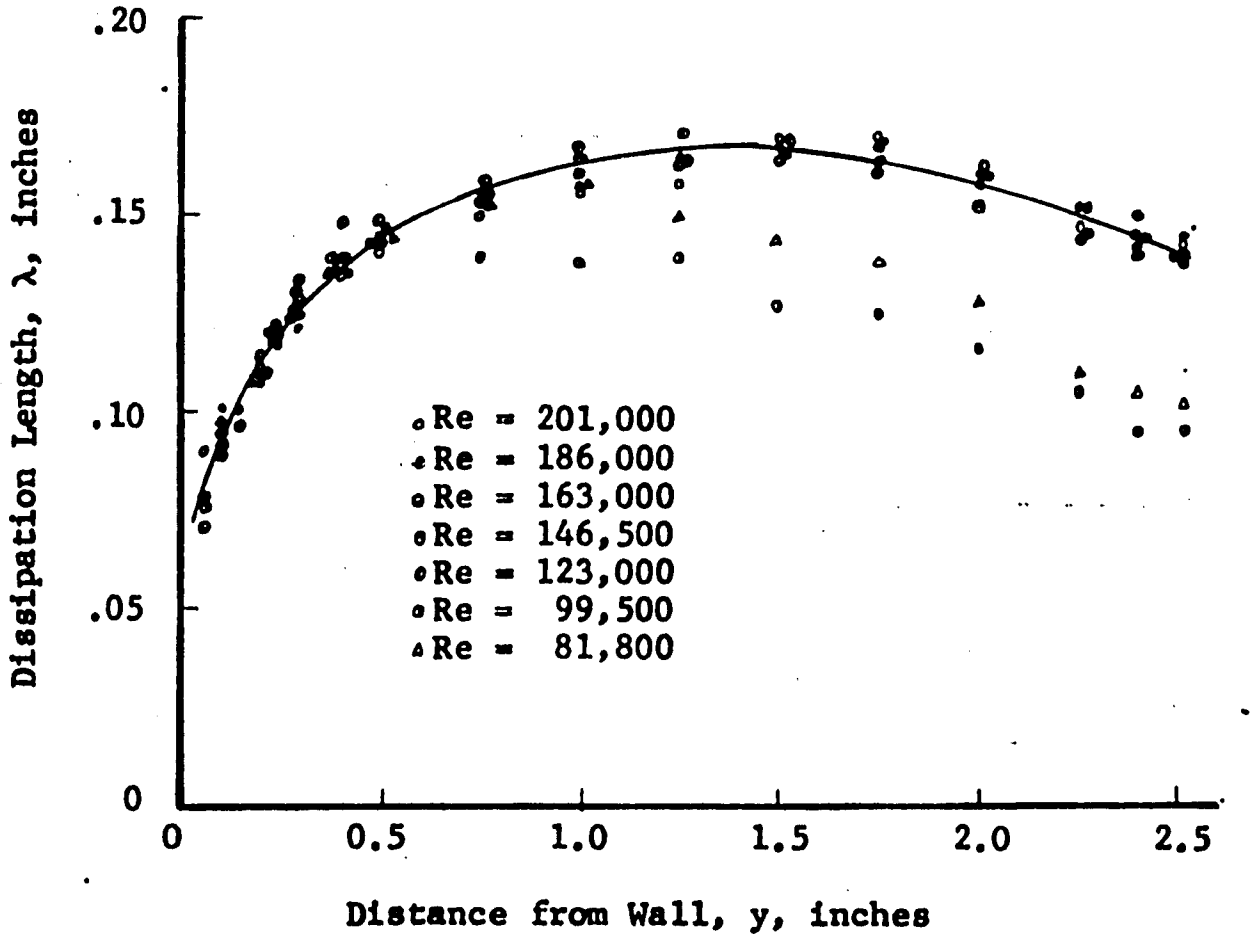

FIGURE (26)

DISSIPATION LENGTH IN THE WALL REGION

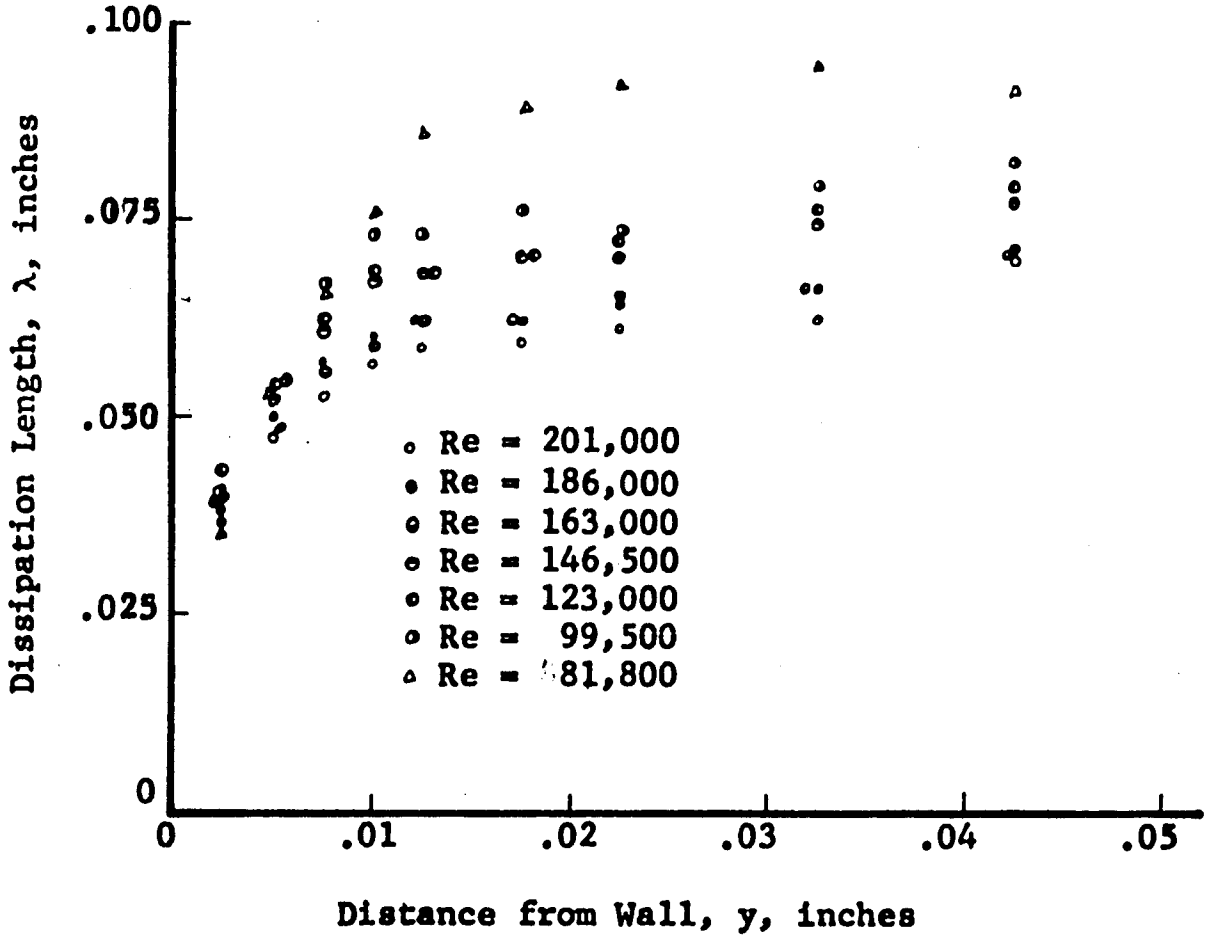

somewhat lower for the 50 ft/sec and 40 ft/sec runs. This finding is because the high noise level in the differentiating circuits gives a current reading (I_{T_D}) that is erroneous and high and causes the calculated dissipation length to be low (the dissipation length is inversely proportional to I_{T_D}, see Appendix).

There is a slight increase in the dissipation length in the wall region as Reynolds number is decreased. This is probably a result of a smaller percentage of the turbulent energy being produced there. However, it is not the slight changes in dissipation length that merit comment, but the fact that it is relatively constant for all the Reynolds numbers, that evades explanation. The only answer that comes forth is that the range of Reynolds numbers investigated was too small (81,800 to 201,000 or 2.5 fold variation) to show more than slight trends.

The reasons for not investigating a wider range of Reynolds numbers were:

(1) The upper limit was determined by blower capacity and thus, could not be exceeded.

(2) At Reynolds numbers below 81,800 the random noise, in the circuit used to determine the dissipation length (See Appendix), was of the same order of magnitude, and in some cases greater than, the signal from the wire.

6. Cross Wire Measurements

Cross wire measurements were taken at center line velocities

of 90, 80, 70, 60, and 50 ft/sec with the experimental points spaced 0.25 inches apart along the radius of the pipe. The results of the cross wire measurements are listed in Tables XIII and XIV. The w' measurements are presented in Figure (27) and the $\overline{uw}$ measurements in Figure (28).

These measurements are, in general, not very accurate as the procedure used to calibrate the wire was not the same as recommended in the manual by Hubbard[9]. Also, the $\overline{uw}$ measurements require taking the difference of two squares ($I_{T_1}^2 - I_{T_2}^2$) which, in this research, differed very little. This, too, caused discrepancies in the results. The method used to calibrate the crossed wires, along with some comments about the errors involved, is given in the Appendix.

In Figure (28) the $\overline{uw}$ measurements are not zero at the center of the pipe, as is required by the Reynolds equations. Both the $\overline{uw}$ and w' measurements are a minimum at the pipe center and both increase as the wall is approached. The w' measurements increase linearly as the wall is approached.

FIGURE (27)

AZIMUTHAL INTENSITY OF TURBULENCE
(TURBULENT CORE)

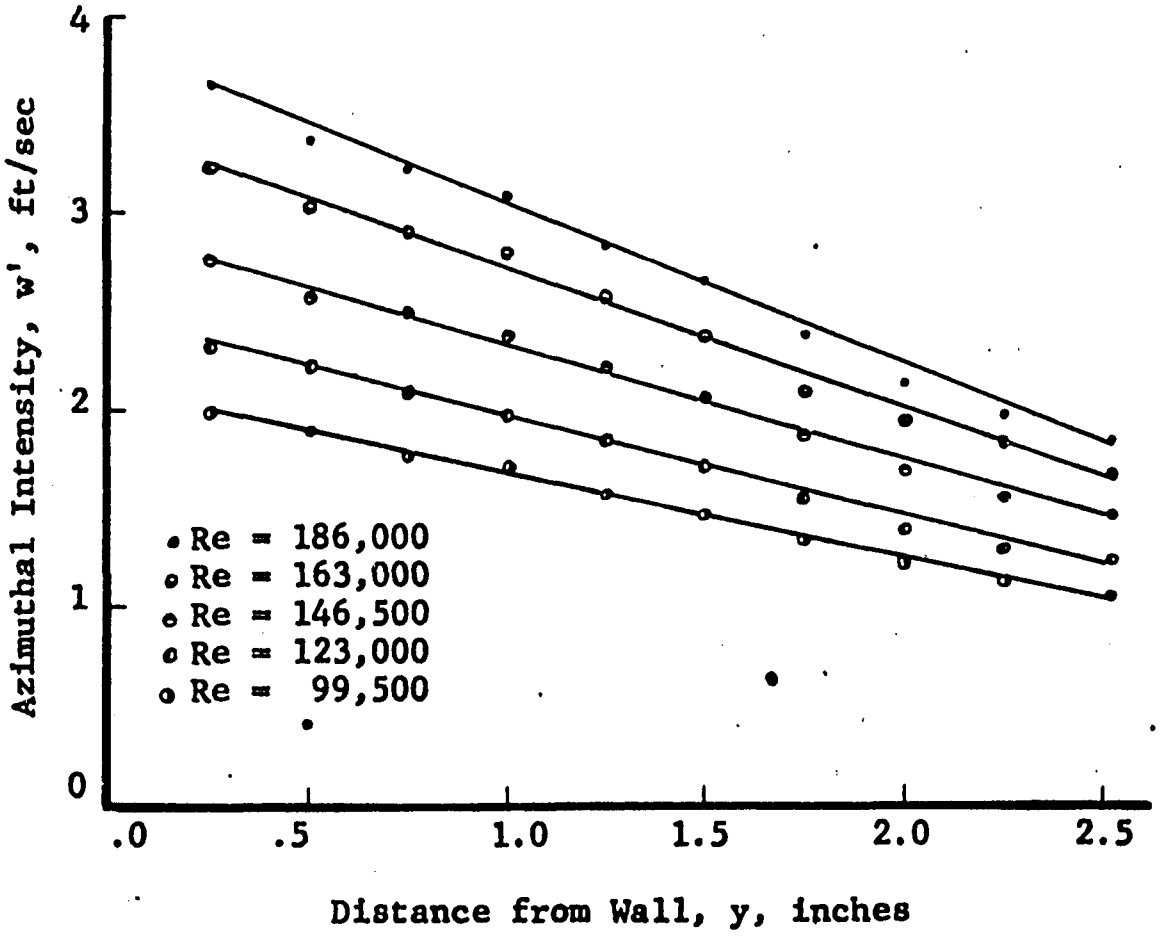

FIGURE (28)

CORRELATION BETWEEN AXIAL AND AZIMUTHAL
FLUCTUATING VELOCITIES
(TURBULENT CORE)

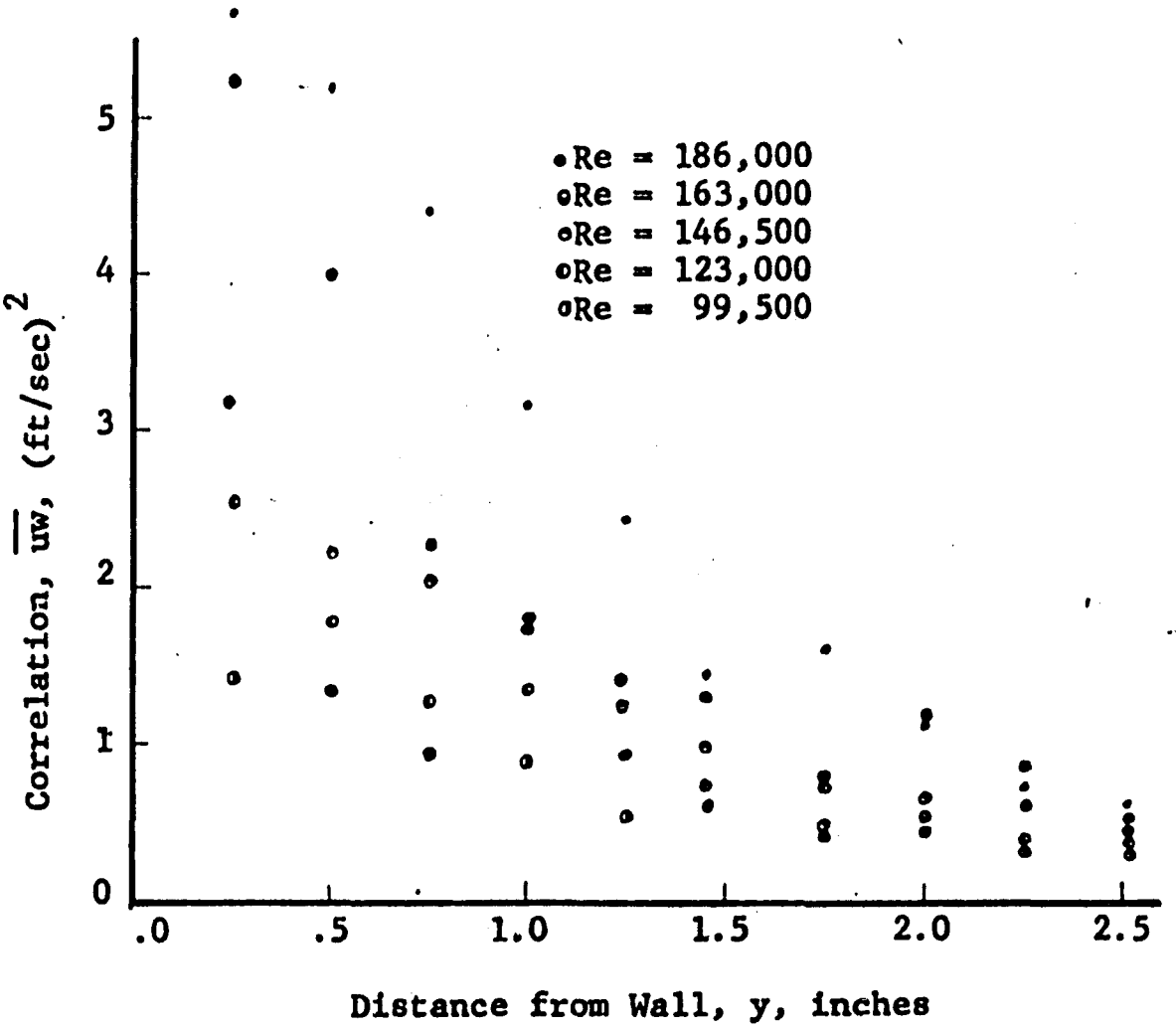

CHAPTER V

CORRELATION AND INTERPRETATION OF RESULTS

1. Mean Velocity

The mean velocity data, in dimensionless form ($\bar{U}/U^*$), are plotted versus a dimensionless distance from wall ($\frac{yU^*\rho}{\mu}$) in Figure (29). For $Y^+ \leqslant 5$ the data, with the exception of those taken extremely close to the wall, agree well with equation (II-44). The region of ($Y^+ < 5$) is considered to be the viscous sublayer and equation (II-44) is recommended for use in this region[12]. For $Y^+ > 20$ the data agree well with equation (II-47) when it is used with the constants recommended by Deissler[5]. For $5 < Y^+ < 20$ neither equation (II-44) nor equation (II-47) agree well with the data. It is in this region $Y^+ < 27$ that Deissler recommends the use of equation (II-48)[5]. However, equation (II-48) was not used in this research as it requires the evaluation of an iterated integral and an experimental constant, which would render it extremely cumbersome for general use.

The measurements for $Y^+ < 5$ that are above the $U^+ = Y^+$ curve are, in all probability, the result of the heat transfer to the wall. This fact was pointed out in section (2) of Chapter IV.

FIGURE (29)

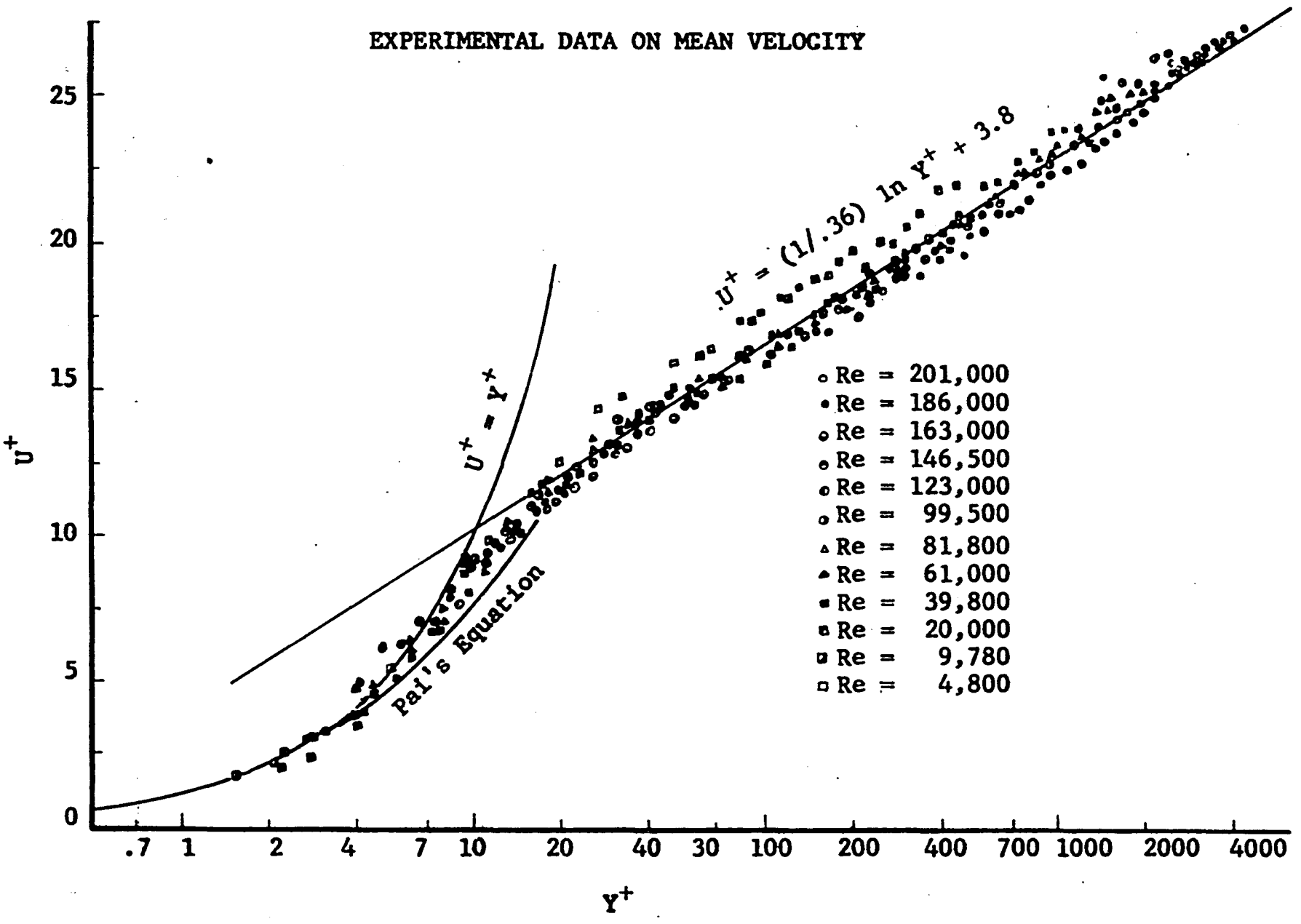
EXPERIMENTAL DATA ON MEAN VELOCITY
$U^+ = (1/.36) \ln Y^+ + 3.8$
$U^+ = Y^+$
Pai's Equation
Re = 201,000
Re = 186,000
Re = 163,000
Re = 146,500
Re = 123,000
Re = 99,500
Re = 81,800
Re = 61,000
Re = 39,800
Re = 20,000
Re = 9,780
Re = 4,800
U^+
Y^+
0
5
10
15
20
25
.7
1
2
4
7
10
20
40
30
100
200
400
700
1000
2000
4000

The use of two equations for the mean velocity profile in different regions of turbulent flow is not at all desirable, particularly when one of these will not satisfy the boundary of $\bar{U} = 0$ at the wall. This dilemma led the author to give consideration to the equation (II-33) recommended by Pai[18]. As pointed out previously this equation has the virtues of conforming to the boundary conditions, being a solution to the Reynolds Equations, and requires only one equation for the mean velocity profile across the entire pipe. However, as will be seen later, it too has its limitations and is not the ultimate answer to the problem.

Pai's equation

$$\frac{\bar{U}}{\bar{U}_{max}} = 1 + \frac{s - n}{n - 1}\eta^2 + \frac{1 - s}{n - 1}\eta^{2n} \qquad \text{(II-33)}$$

where

$$s = \frac{f}{32}\,Re\left(\frac{\bar{U}_A}{\bar{U}_{max}}\right) \qquad \text{(II-36)}$$

$$n = \frac{\frac{f}{64}\,Re - 1}{1 - \frac{\bar{U}_m}{\bar{U}_A}} \qquad \text{(II-41)}$$

allows the mean velocity profile to be evaluated from the readily available friction factor and $(\bar{U}_A/\bar{U}_m)$ plots. However, at the onset of this research equation (II-41) was yet to be derived and n had to be evaluated from the experimental data by the method of least squares.

Equation (II-33) contains the constant n both as a coefficient and an exponent to η. Therefore, by the conventional method of least squares, which sets

$$\frac{\partial \left(\frac{\overline{U}}{\overline{U}_{max}} \right)}{\partial n}$$

equal to zero, an equation explicit in n is not obtained. It was necessary to use a technique, known as Newton's method, which minimizes, by iteration,

$$\frac{\partial \left(\frac{\overline{U}}{\overline{U}_{max}} \right)}{\partial n}$$

This method requires a prohibitive number of calculations. Recourse was therefore made to a high speed computer, the IBM 650. The method used is outlined in the appendix.

It might be desirable to evaluate both n and s from the experimental data and therefore obtain optimum values of both constants. This would certainly be desirable from the curve fitting standpoing; however, the technique for optimizing equation (II-33) with respect to both n and s would be quite long. In fact, it is highly probable that it would be necessary to resort to a larger machine than the IBM 650.

After the work was completed on the calculation of n by the method of least squares, equation (II-41) was derived for evaluation of n from the friction factor and $(\overline{U}_A/\overline{U}_m)$ plots. The values of n calculated by both means are compared in

Table XV. A plot of equation (II-33), along with equations (II-44) and (II-47), is given in Figure (31) for Reynolds numbers of 201,000, 61,000, and 4,800. Velocities calculated by Pai's equation are compared to the experimental data in Tables I through XII. In Figure (30) Pai's equation, equation (II-44) and equation (II-47), are compared with the experimental data.

By comparing the mean velocities calculated by Pai's equation, to the measured velocities, it is seen that over approximately 90% of the pipe radius (turbulent core) the calculated and experimental values agree within about 5% and usually of the order of 1%. However, as the wall is approached, and the region of extreme curvature is entered, the calculated and experimental values deviate, in some cases, by as much as 20%.

In the tables in the appendix there are two velocities calculated by Pai's equation, one ($\overline{U}_{pt}$) using the n calculated from the friction factor and ($\overline{U}_A/\overline{U}_m$) plots, and the other, ($\overline{U}_{pe}$), using n calculated from the experimental data using the method of least squares. The ($\overline{U}_{pt}$) values agree better than the ($\overline{U}_{pe}$) over most of the pipe radius but disagree by much larger amounts near the wall. This is because the n used in calculating $\overline{U}_{pe}$ gives the smallest standard deviation for the points considered and a good fit in the turbulent core was sacrificed to improve on the very poor fit in the outer transition region.

FIGURE (30)

COMPARISON OF MEAN VELOCITY EQUATIONS
AND DATA FOR Re = 201,000

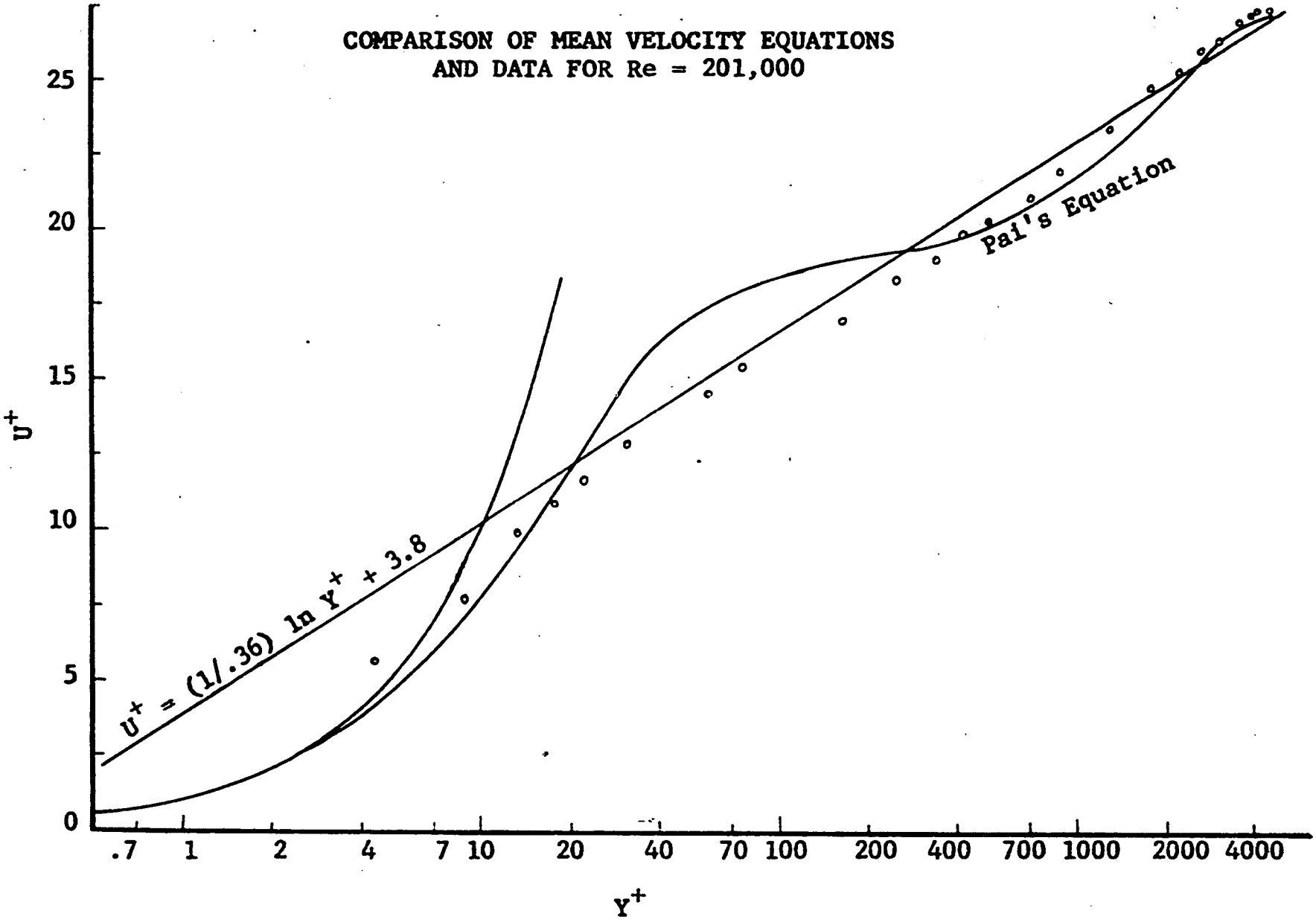

FIGURE (31)

COMPARISON OF MEAN VELOCITY EQUATIONS

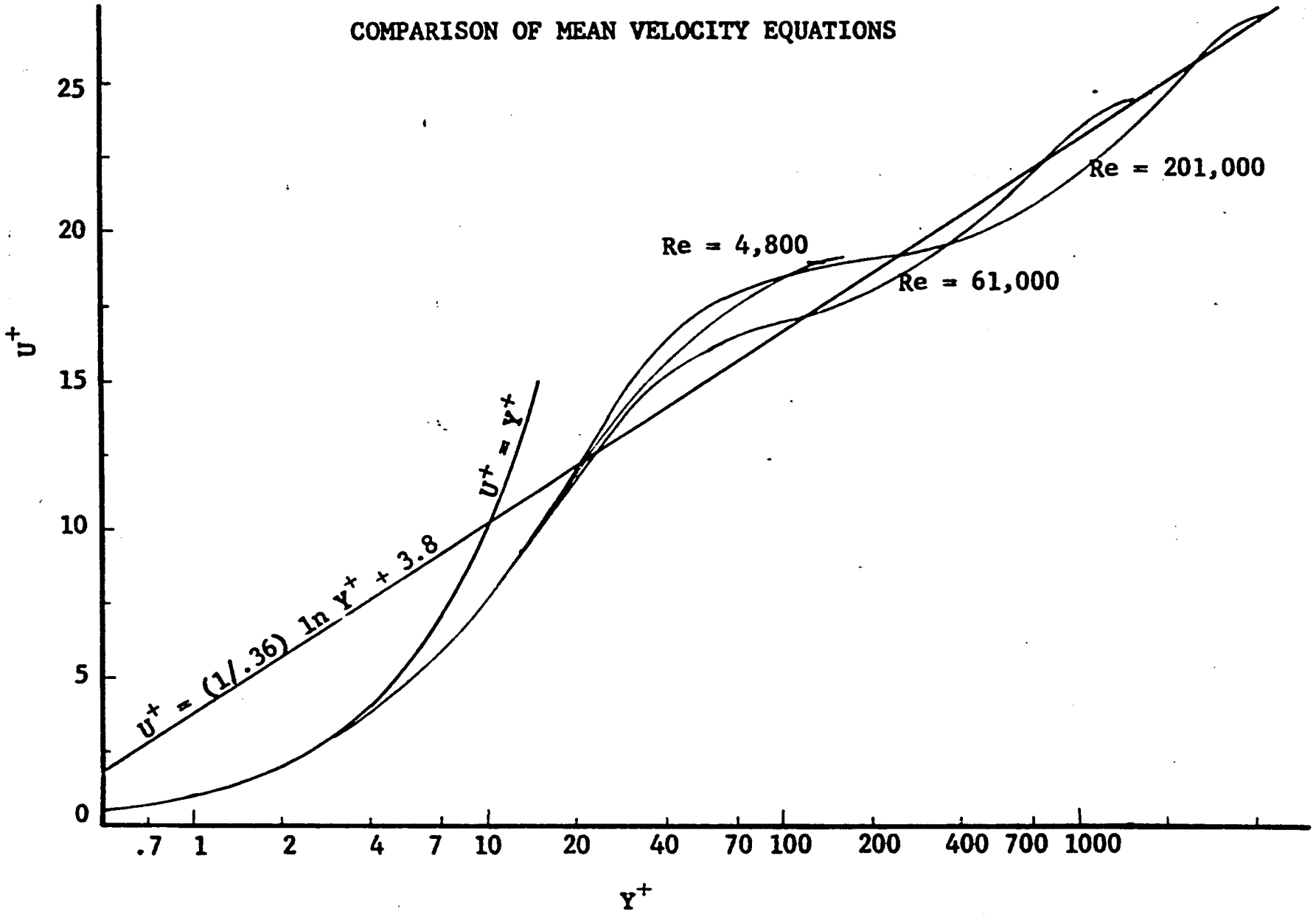

In this research s, in equation (II-33), was calculated from the Moody friction factor plot assuming that the pipe under consideration was smooth. It would have been desirable to calculate s from pressure drop measurements on the test section and therefore eliminate any errors that might be introduced by using the friction factor plot.

2. Intensity of Turbulence

In section (8) of Chapter II sufficient conditions, such that the following relationship might be expected to hold, were given.

$$\frac{u'}{U^*} = f\left(\frac{U^*\rho y}{\mu}\right) \qquad \text{(V-1)}$$

The conditions were that (1) the region near the wall is at energy equilibrium and (2) y is large enough to include substantially all the turbulent energy production but not so large as to be outside the constant stress region.

In Figure (32) u'/U^* is plotted versus $\frac{U^*\rho y}{\mu}$ and it is seen that the correlation is good out to $Y^+ \sim 7$, and for moderately high Reynolds numbers (say > 20,000) the correlation may be extended out to $Y^+ \sim 40$. The reason for the discrepancies at the low Reynolds numbers is that the conditions, set forth above, are not satisfied; i.e., the region of extreme velocity gradient extends a considerable distance from the

FIGURE (32)

INTENSITY CORRELATION NEAR WALL

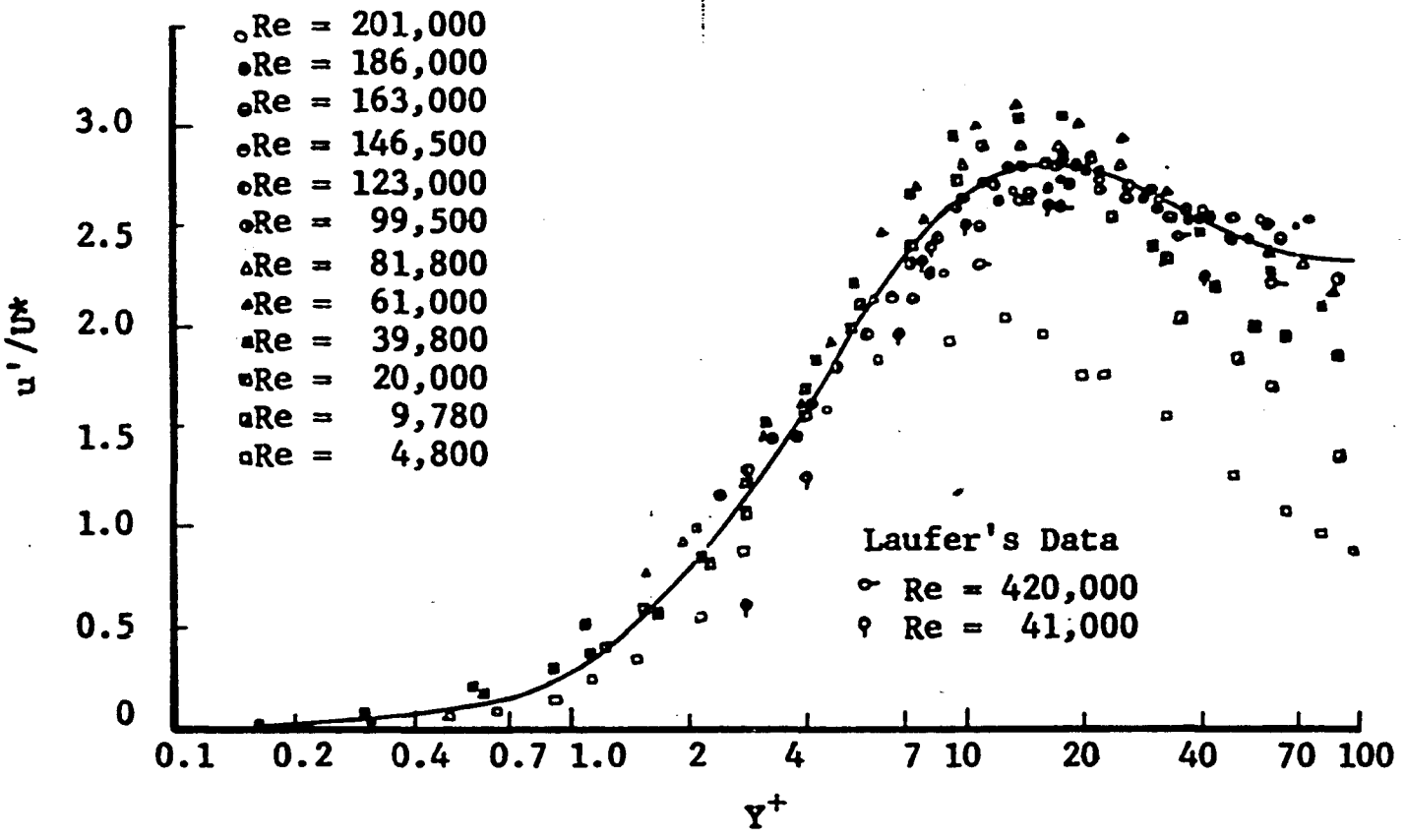

wall and $\overline{uv}$ reaches a maximum further from the wall. Since the turbulent energy production is proportional to $\overline{uv}\ (\partial\bar{U}/\partial r)$[24], a larger percentage of the turbulent energy production takes place outside the constant stress region at lower Reynolds numbers. If a large part of the turbulent energy production takes place outside this constant stress region then the constant stress region will probably be receiving turbulent energy from other sources and will not be in energy equilibrium. It should also be pointed out that, as the Reynolds number decreases, the value of Y^+ for a given distance from the wall and a given percentage variation in shear stress decreases. Therefore, on this basis alone, equation (V-1) could not be expected to hold for as large values of Y^+ as at the higher Reynolds numbers.

The data of Laufer are also presented in Figure (32) and agree well with the results obtained by the present author. This adds force to the above analysis as Laufer's results were taken in a larger pipe (10 inches) and at higher Reynolds number (up to 420,000).

From the same reasoning used to derive equation (II-45) Townsend[24] reasoned that in the turbulent core, where the influence of viscosity is negligible, the dimensionless turbulence quantities are a function only of (r/r_o). Figure (33) is a plot on this basis, and fair agreement is attained except for the two lower Reynolds numbers. This deviation is probably

FIGURE (33)

INTENSITY CORRELATION IN TURBULENT CORE

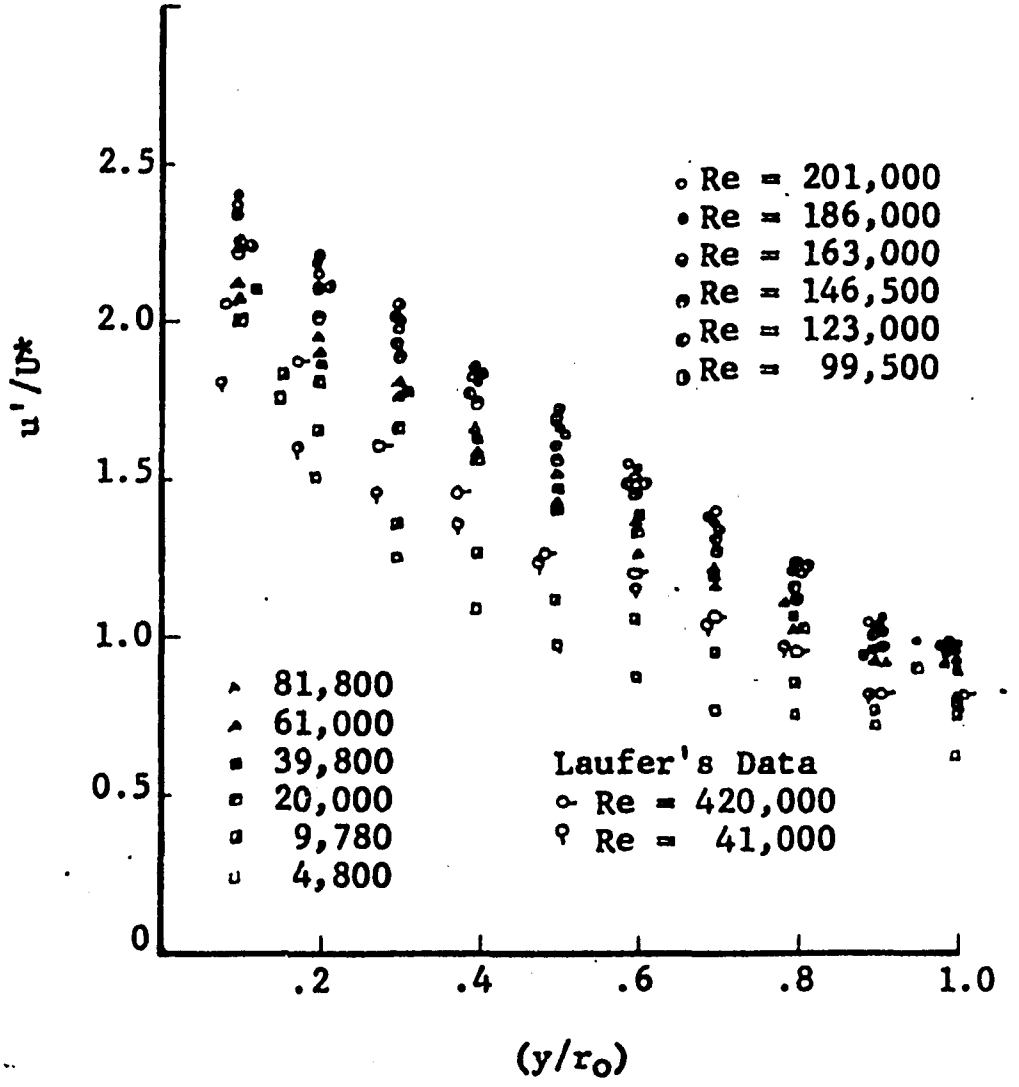

caused by the viscosity being important, at these low Reynolds numbers, and thus rendering his analysis invalid for low Reynolds numbers (say Re < 10,000).

Laufer's data are also plotted in Figure (33) and show the same general trend as the present author's data.

3. Dissipation Length

In Figures (25) and (26) dissipation length is plotted versus distance from the wall. In the range of Reynolds number investigated the dissipation length appears nearly constant for a given distance from the wall with the exception of the region near the wall where it decreases slightly with increasing Reynolds number. However, it should again be pointed out that in these measurements there was only a 2.5 fold variation in Reynolds number (81,800 to 201,000) and a much wider range should be investigated before concluding that dissipation length is independent of the Reynolds number.

4. $\overline{uw}$ Correlation

In Figure (34) the correlation between the axial and azimuthal fluctuating velocities, in dimensionless form, is plotted versus r/r_o. These data are appreciably less accurate than any of the other data in this paper. The reasons for the discrepancies were pointed out in section (6) of Chapter IV.

The lines that were drawn through the experimental data

FIGURE (34)

CORRELATION BETWEEN AXIAL AND AZIMUTHAL FLUCTUATING VELOCITIES IN THE TURBULENT CORE

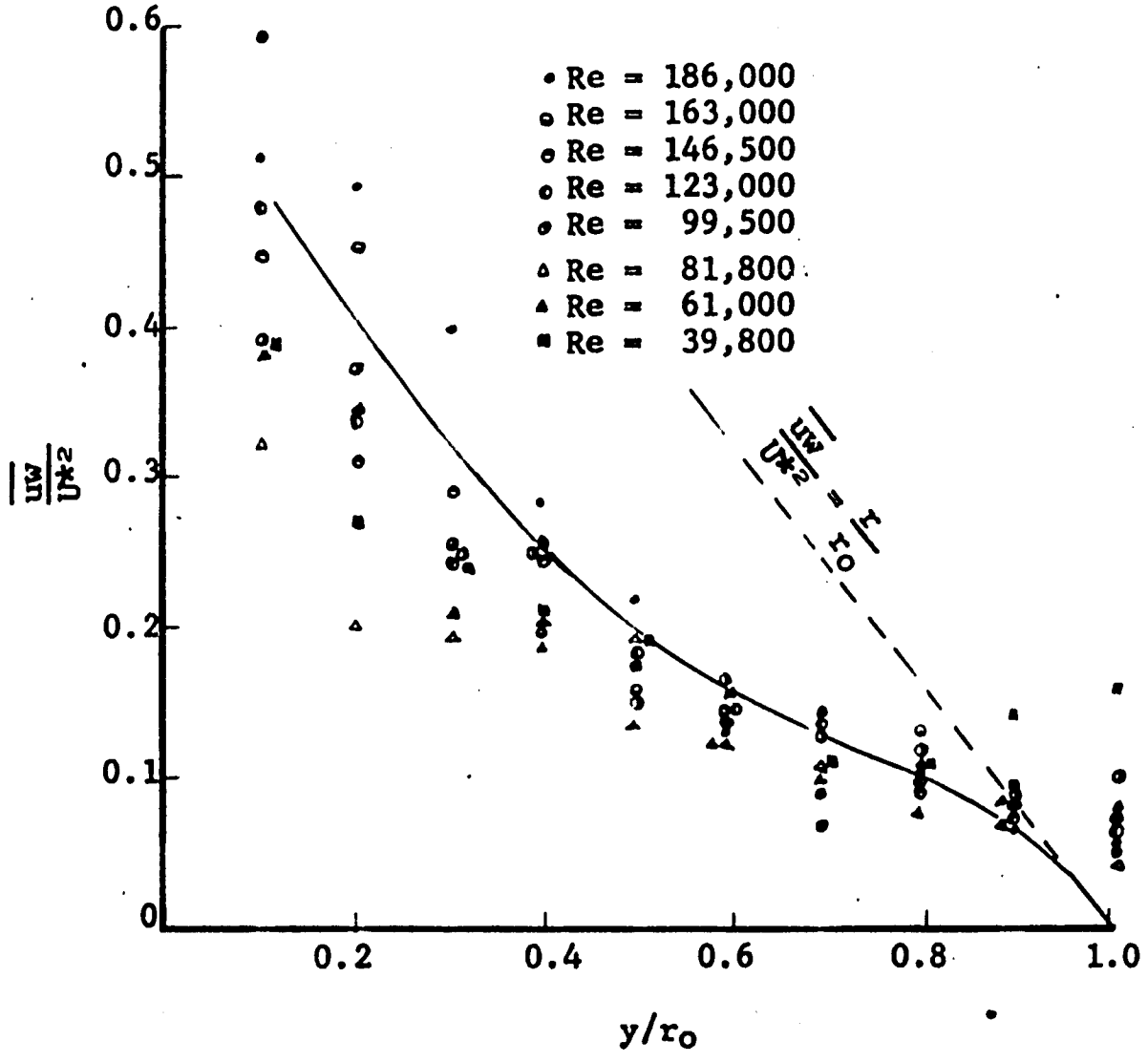

in Figure (34) merit some consideration as it appears that they do not agree with the experimental results. First, at the pipe center ($y/r_o = 1$), the curves pass through $\overline{uw}/U^{*2} = 0$. Then, as y/r_o decreases, the curves are drawn along the line $\overline{uw}/U^{*2} = y/r_o$. Although the experimental data do not exactly lie along this curve, the Reynolds equations would predict this type of behavior.

Actually the Reynolds equations predict the behavior for $\overline{uv}$. However, at the center of the pipe $\overline{uv} = \overline{uw}$, and $\overline{uv}$ is zero by equation (II-22). The fact that $\overline{uv} = \overline{uw}$ is brought about by the equality of the radial and azimuthal directions at the center of the pipe. In

$$\frac{\overline{uv}}{U^{*2}} = \frac{\mu}{\rho U^{*2}} \frac{d\bar{U}}{dr} + \frac{r}{r_o} \qquad \text{(II-22)}$$

For the central region of the pipe $\frac{\mu}{\rho U^{*2}} \frac{d\bar{U}}{dr}$ is negligible and equation (II-22) may be written

$$\frac{\overline{uv}}{U^{*2}} = \frac{r}{r_o} \qquad \text{(V-2)}$$

and very near the center where $\overline{uv} \sim \overline{uw}$

$$\frac{\overline{uw}}{U^{*2}} \sim \frac{r}{r_o} \qquad \text{(V-3)}$$

5. Azimuthal Intensity

The azimuthal intensity w' is plotted versus r/r_o in Figure (35) and is seen to give good correlation. When the results in Figure (35) are compared to Laufer's results in

FIGURE (35)

AZIMUTHAL INTENSITY CORRELATION IN THE TURBULENT CORE

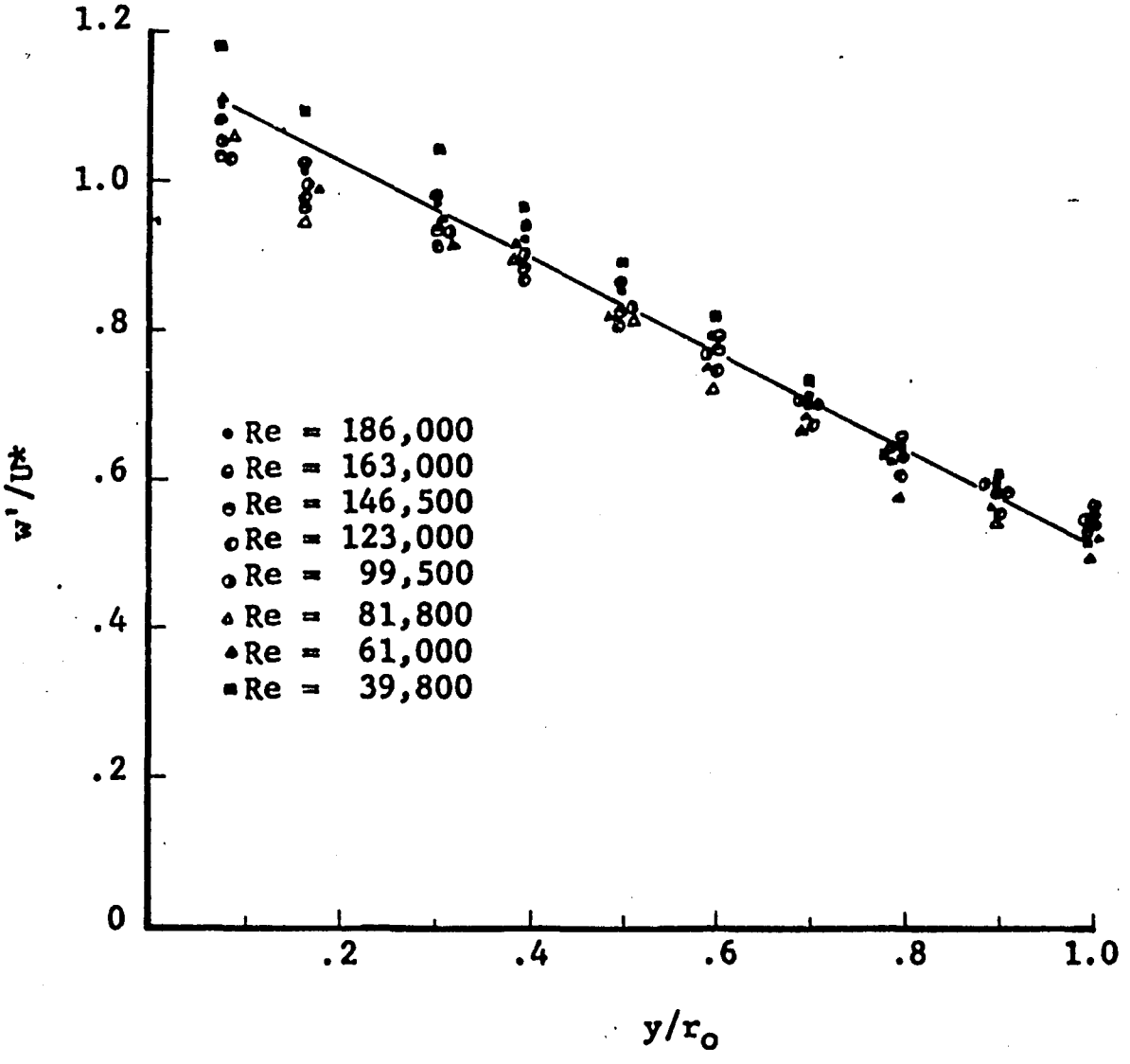

Table XVI it is seen that the present author's results are about 20% lower. Considering the approximations made in the experimental techniques and calculations this is remarkable agreement. However, the range of Reynolds number investigated was very small and these results should be used with caution outside this range.

6. Laminar Sublayer

In Figure (21) it is seen that at $Y^+ = 0.16$ the intensity of turbulence is zero. If it is assumed that the dimensionless thickness (Y^+) of the laminar sublayer is constant at (0.16), Figure (36) is obtained. This does not seem to be a bad assumption; as it appears, from the experimental data obtained in this research and in Laufer's research, that u' and $\bar{U}$ are functions only of Y^+ in the vicinity of the wall.

If the curves in Figure (36) are extrapolated to $Re \sim 8 \times 10^6$ then the thickness of the laminar sublayer is the same as the mean free path of nitrogen (3.66×10^{-6} inches) and, in principle, the laminar sublayer would no longer exist.

FIGURE (36)

THICKNESS OF LAMINAR SUBLAYER

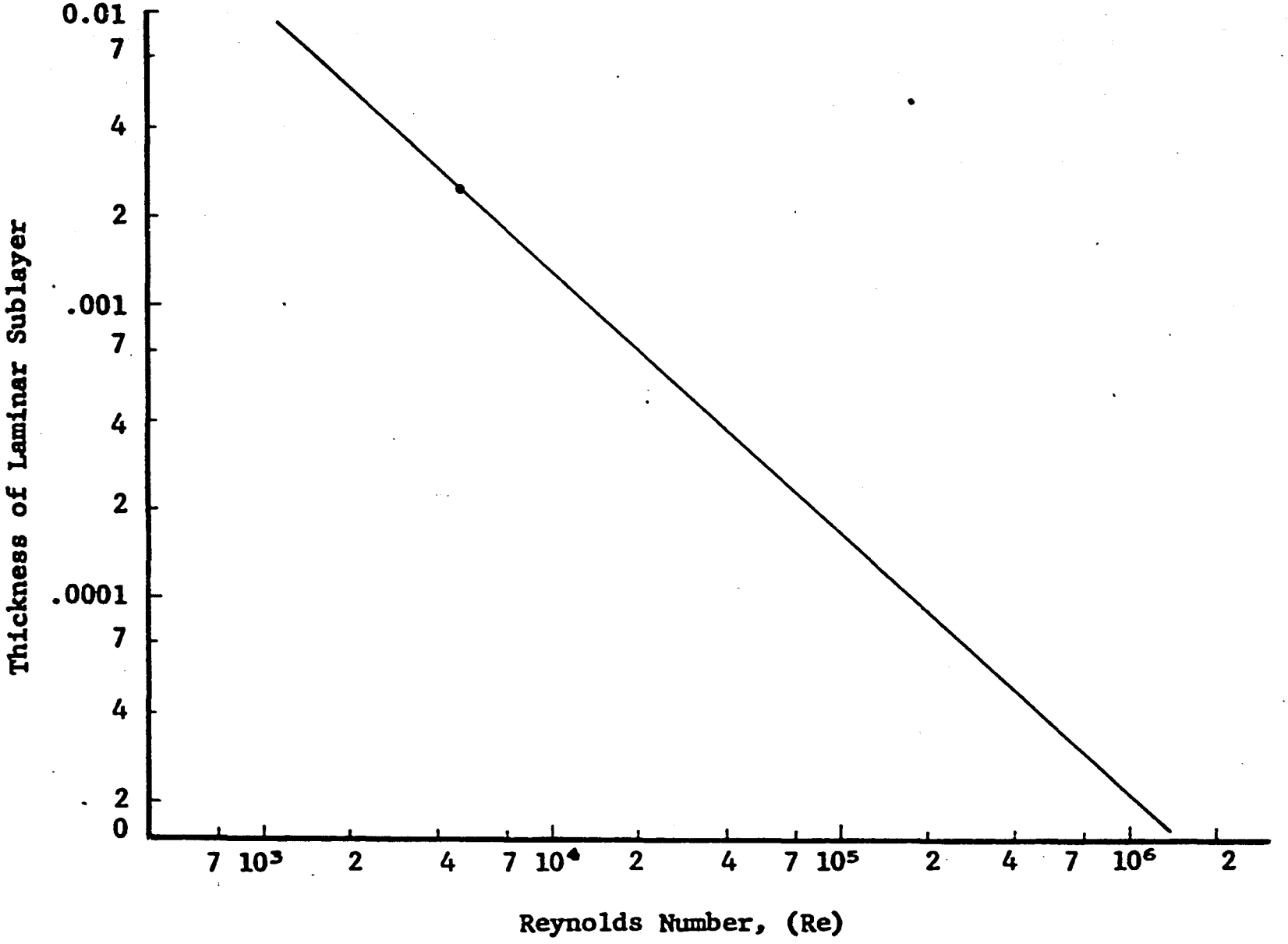

CHAPTER VI

CONCLUSIONS

1.) From the Figures in Chapter V it is obvious that a combination of the logarithmic velocity distribution and equation (II-43) gives, in general, a better fit than Pai's equation. This fact is particularly noticeable at high Reynolds numbers just outside the transition region where deviations up to 20% may be encountered. However, Pai's equation does give the best fit (within usually 1 or 2%) in the turbulent core which covers, for moderately high Reynolds, about 85% of the pipe radius. Pai's equation also reduces to, for $Y^+ < 4$, equation (II-43) and gives a good fit of the data in that region. Pai's equation has the virtues of satisfying the Reynolds equations, the boundary conditions and it is a single equation for the entire pipe. The constants in Pai's equation can be determined from data readily available in standard texts. The combination of the logarithmic and equation (II-43) have none of the before mentioned virtues.

From the foregoing conclusions it is obvious that the choice of which equation, or combination, to use will be dictated by their intended use. It is believed, however, that

the versatility and ease of use of Pai's equation should stimulate its extensive use in the future.

2.) The intensity results point out that for $U^+ < 7$ that u'/U^* is a function only of Y^+ and for $Re > 20,000$ this relation may be extended to Y^+ of approximately 40. The data also show that for $Re > 20,000$ the intensity reaches a maximum at about $Y^+ = 15$. However, at the lower Reynolds numbers it appears that the point of maximum intensity may be reached at a smaller value of Y^+.

In the turbulent core it appears that for moderately high Reynolds numbers ($> 20,000$) u'/U^* and w'/U^* vary only slightly with Reynolds number and are functions only of r/r_o. A tenfold variation in Reynolds number causes only about a 20% change in u'/U^*. However, at the lower Reynolds numbers u'/U^* seems to be very much a function of Reynolds number.

3.) In the range of Reynolds number investigated (81,800 to 201,000) dissipation length is independent of Reynolds number and dependent only on pipe position. The only exception to this finding is in the wall region ($y < 0.10$ inches) where the dissipation length appears to decrease slightly with increasing Reynolds number.

4.) The correlation between the axial and azimuthal fluctuating velocities ($\overline{uw}$) increases as the wall is approached, and

when expressed in dimensionless form ($\overline{uw}/U^{*2}$) much of the scatter is eliminated. However, the data are not reliable enough to draw firm conclusions as to the functional relationships that govern $\overline{uw}$.

5.) As the wall is approached the fluctuating velocities approach zero and at the lowest Reynolds number (Re = 4,800) turbulence was not detectable at $Y^+ = 0.16$. This is, to the knowledge of the author, the only experimental evidence of a true laminar sublayer in fully developed turbulent flow.

This finding is of cardinal importance in our understanding of the basis mechanism of heat and mass transfer in turbulent flow. The laminar film theory assumes that the laminar film controls the rate of transfer. However, the resistance of a laminar sublayer of thickness $Y^+ = 0.16$ is only about one tenth of the total resistance predicted by conventional heat transfer coefficient relations. See Table XV. Furthermore, as mentioned above, the laminar sublayer is of the dimensions of the mean free path at high Reynolds numbers.

6.) When the Reynolds equations are simplified for axially symmetrical pipe flow, it is seen that there is definitely a tendency towards isotropy at the pipe center. The conditions $\overline{uv} = \overline{uw} = \overline{vs} = 0$ and $v' = w'$ are satisfied with the only

conditions absent that $w' = u'$. In this research w' was about 30% lower than u', however, Laufer's data showed them to be equal. It is therefore necessary that more data, using refined methods, be taken on the azimuthal and radial intensities before it can be concluded that the turbulence is isotropic at the pipe center. It may, however, be asserted that there is a strong tendency toward isotropy at the center of the pipe.

CHAPTER VII

RECOMMENDATIONS

At the onset of this research it was obvious that the present study would not be the conclusion to the study of turbulent shear flow in pipes. In fact, no attempt was made in this research to measure space correlation coefficients, spectrum of turbulence, radial intensity, correlation between radial and axial fluctuating velocities, triple and quadruple correlations, or the terms in the turbulent energy equation. Certainly any study of turbulence would not be complete without measurements of many of those mentioned. The lack of measurements on the above variables shows that turbulent pipe flow is most certainly a field that needs much more extensive study. It is recommended that the present aurhor's research be extended so as to include measurements of the above mentioned variables.

In conducting this research certain less obvious shortcomings have arizen that concern the measurements and ideas set forth in this paper. Some of the more prominent ones are listed below.

(1) Further work - A more extensive study of the velocity

spikes, near the wall should be made. It is possible that quantitative conclusions as to the eddy structure and flow mechanisms might be accomplished from this study.

It would be desirable to extend the present results up to a Reynolds number of about 10^6. This would give more force to the conclusions and allow a 250 fold variation in Reynolds number.

(2) Equipment Improvements - A probe should be fabricated that would allow measurements closer to the wall than the 0.0025 inches attained in this research. A better method for determining the wall position would also be desirable.

In the mean velocity measurements close to the wall the heat transfer from the wire to the wall caused the mean velocity measurements to be high. An analysis of this situation should be made and corrections set forth that could be applied to the experimental results to correct for these effects.

The cross wire measurements left much to be desired. These could be improved on by fabrication of a traversing mechanism made especially for cross wire measurements.

High frequency filters, with a cut off at about 10,000 cycles per second, should be put between the amplifiers and the RMS Analyzer. This would eliminate the noise problem.

SELECTED BIBLIOGRAPHY

1. Bird, R. Byron, Stewart, Warren E., and Lightfoot, Edwin N. Transport Phenomena. New York: John Wiley and Sons, 1960.

2. Bryant, John Myron, Correll, James A., and Johnson, E. W. Alternating Current Circuits. New York: McGraw-Hill Book Company, Inc., 1939.

3. Coburn, Nathaniel. Vector and Tensor Analysis. New York: The Macmillan Company, 1955.

4. Corcoran, W. H., Opfell, J. B., and Sage, B. H. Momentum Transfer in Fluids. New York: Academic Press, Inc., 1956.

5. Deissler, Robert G. "Analysis of Turbulent Heat Transfer, Mass Transfer, and Friction in Smooth Tubes at High Prandtl and Schmidt Numbers," NACA Technical Report 1210, (1955).

6. Hanratty, Thomas J. "Turbulent Exchange of Mass and Momentum with a Boundary," A.I.Ch.E. Journal, 2, No. 3 (1956), 359-362.

7. Hinze, J. O. Turbulence. New York: McGraw-Hill Book Company, Inc., 1959.

8. Hodgman, Charles D., Editor in Chief, Handbook of Chemistry and Physics, 35th Edition, Cleveland, Ohio, Chemical Rubber Publishing Co., 1953.

9. Hubbard, Philip G. Operating Manual for the I I H R Hot-Wire and Hot-Film Anemometers. Iowa City, Iowa: State University of Iowa Press, 1957.

10. Hubbard, Philip G. Personal Correspondence, 1960.

11. Kern, Donald Q. Process Heat Transfer. New York: McGraw-Hill Book Company, Inc., 1950.

12. Knudsen, James G., and Katz, Donald L. Fluid Dynamics and Heat Transfer. New York: McGraw-Hill Book Company, Inc., 1958.

13. Laufer, J. "The Structure of Turbulence in Fully Developed Pipe Flow," NACA Technical Report 1174, (1954).

14. Laufer, J. "Investigation of Turbulent Flow in a Two-Dimensional Channel," NACA Technical Report 1053, (1951).

15. Lin, C. C. Turbulent Flows and Heat Transfer. Princeton, New Jersey: Princeton University Press, 1959.

16. McAdams, William H. Heat Transmission. Third Edition, New York: McGraw-Hill Book Company, Inc., 1954.

17. Michal, Aristotle D. Matrix and Tensor Calculus. New York: John Wiley and Sons, Inc., 1947.

18. Pai, S. I. "On Turbulent Flow in a Circular Pipe," Journal of the Franklin Institute, 256, No. 4 (1953), 337-352.

19. Pai, S. I. "On Turbulent Flow between Parallel Plates," Journal of Applied Mechanics, 20, No. 1 (1953), 109-114.

20. Pai, S. I. Viscous Flow Theory, Part II. New York: D. Van Nostrand Company, Inc., 1957.

21. Rouse, Hunter. Advanced Mechanics of Fluids. New York: John Wiley and Sons, Inc., 1959.

22. Schlichting, Herman. Boundary Layer Theory. New York: McGraw-Hill Book Company, Inc., 1954.

23. Streeter, Victor L. Fluid Mechanics. New York: McGraw-Hill Book Company, Inc., 1958.

24. Townsend, A. A. The Structure of Turbulent Shear Flow. London: Cambridge University Press, 1956.

25. von Rosenberg, Dale U. "Mixing of Gas Streams in Coaxial Circular Jets and Parallel Flat Jets," Sc.D. Thesis Massachusetts Institute of Technology, Cambridge, Massachusetts, 1953.

A P P E N D I X

APPENDIX A

TABLE I. RESULTS OF TURBULENCE MEASUREMENTS Re = 201,000

y (in)	η	Y^+	$\bar{U}_{exp}$ (Ft/sec)	U^+	U'_{exp} (Ft/sec)	U'/U^*	$(U'/\bar{U})\%$	$\bar{U}_{pe}$ (Ft/sec)	$\bar{U}_{pt}$ (Ft/sec)	$(\%E_r U_{pe})$	$(\%E_r U_{pt})$	λ (in)
2.5165	0.0030	4432	98.3	27.4	3.45	0.96	3.51	98.3	98.3	-0.0003	-0.0003	0.142
2.4925	0.0125	4390	98.3	27.4	3.38	0.94	3.44	98.3	98.3	-0.006	-0.005	0.139
2.3925	0.0521	4213	98.3	27.4	3.50	0.98	3.56	98.2	98.2	-0.10	-0.09	0.144
2.2925	0.0917	4037	97.3	27.2	3.62	1.01	3.72	98.0	98.0	0.70	0.75	0.146
2.2425	0.1115	3949	97.3	27.2	3.70	1.03	3.81	97.8	97.9	0.54	0.62	0.146
1.9925	0.2106	3509	96.3	26.9	4.30	1.20	4.47	96.6	96.9	0.31	0.59	0.157
1.7425	0.3096	3069	94.5	26.4	4.98	1.39	5.27	94.6	95.2	0.13	0.75	0.169
1.4925	0.4087	2628	93.0	26.0	5.48	1.53	5.89	91.9	92.9	-1.19	-0.10	0.168
1.2425	0.5077	2188	90.5	25.3	5.94	1.66	6.56	88.4	90.0	-2.30	-0.57	0.157
0.9925	0.6068	1748	87.5	24.4	6.48	1.81	7.40	84.1	86.4	-3.79	-1.24	0.155
0.7425	0.7058	1308	83.6	23.4	7.10	1.98	8.49	79.2	82.2	-5.27	-1.65	0.149
0.4925	0.8048	867	78.7	22.0	7.82	2.18	9.93	73.5	77.4	-6.67	-1.66	0.140
0.3925	0.8445	691	75.7	21.1	8.10	2.26	10.7	70.9	75.3	-6.28	-0.55	0.134
0.2925	0.8841	515	72.8	20.3	8.46	2.36	11.6	68.3	73.1	-6.16	0.37	0.124
0.2425	0.9039	427	70.8	19.8	8.46	2.36	11.9	67.0	71.9	-5.42	1.59	0.119
0.1925	0.9237	339	67.8	18.9	8.76	2.45	12.9	65.6	70.8	-3.29	4.36	0.111
0.1425	0.9435	251	65.8	18.4	8.76	2.45	13.3	64.2	69.6	-2.51	5.72	0.110
0.0925	0.9634	163	60.8	17.0	8.96	2.50	14.7	62.7	68.3	3.12	12.4	0.086
0.0425	0.9831	74.8	54.9	15.3	9.10	2.54	16.6	60.5	66.0	10.3	20.2	0.070
0.0325	0.9871	57.2	52.0	14.5	9.10	2.54	17.5	59.0	64.0	13.4	23.0	0.064
0.0225	0.9910	39.6	49.0	13.7	9.26	2.59	18.9	55.0	59.0	12.2	20.4	0.062
0.0175	0.9931	30.8	46.0	12.8	9.44	2.64	20.5	50.9	54.1	10.6	17.7	0.059
0.0125	0.9950	22.0	42.0	11.7	9.76	2.73	23.2	44.1	46.4	5.02	10.5	0.059
0.0100	0.9960	17.6	39.1	10.9	9.76	2.73	25.0	39.1	40.9	1.98	4.68	0.056
0.0075	0.9970	13.2	35.1	9.80	9.60	2.68	27.4	32.8	34.0	-6.53	-3.08	0.055
0.0050	0.9980	8.81	27.8	7.77	8.14	2.27	29.3	24.5	25.2	-11.7	-9.27	0.047
0.0025	0.9990	4.40	20.2	5.64	5.64	1.58	27.9	13.9	14.1	-31.4	-30.1	0.037

TABLE II. RESULTS OF TURBULENCE MEASUREMENTS Re = 186,000

y	η	Y^+	$\bar{U}_{exp}$	U^+	U'_{exp}	U'/U^*	$(U'/\bar{U})\%$	$\bar{U}_{pe}$	$\bar{U}_{pt}$	$(\%E_r U_{pe})$	$(\%E_r U_{pt})$	λ
2.5165	0.0030	4110	90.0	27.0	3.22	0.97	3.57	90.0	90.0	-0.0003	-0.0003	0.144
2.4925	0.0125	4071	90.0	27.0	3.22	0.97	3.57	90.0	90.0	-0.006	-0.005	0.142
2.3925	0.0521	3907	89.5	26.9	3.22	0.97	3.57	89.9	89.9	0.45	-0.47	0.141
2.2925	0.0917	3744	89.5	26.9	3.50	1.05	3.91	89.7	89.7	0.23	-0.28	0.153
2.2425	0.1115	3662	89.5	26.9	3.46	1.04	3.86	89.6	89.6	0.08	0.14	0.152
1.9925	0.2106	3254	88.0	26.4	3.99	1.20	4.53	88.5	88.7	0.53	0.77	0.159
1.7425	0.3096	2846	86.8	26.1	4.54	1.36	5.23	86.7	87.1	-0.13	0.38	0.168
1.4925	0.4087	2438	84.5	25.4	5.10	1.53	6.03	84.2	85.0	-0.31	0.60	0.167
1.2425	0.5077	2089	81.6	24.5	5.54	1.66	6.78	81.1	82.3	-0.61	0.84	0.164
0.9925	0.6068	1621	78.8	23.7	5.94	1.78	7.53	77.3	79.0	-1.91	0.24	0.157
0.7425	0.7058	1213	75.7	22.7	6.74	2.02	8.90	72.8	75.1	-3.83	-0.80	0.155
0.4925	0.8048	804	71.7	21.5	7.26	2.18	10.1	67.6	70.6	-5.67	-1.50	0.144
0.3925	0.8445	641	69.8	21.0	7.42	2.23	10.6	65.4	68.7	-6.33	-1.62	0.134
0.2925	0.8841	478	65.7	19.7	7.72	2.32	11.8	63.0	66.6	-4.09	1.40	0.121
0.2425	0.9039	396	64.8	19.5	7.84	2.35	12.1	61.8	65.6	-4.64	1.17	0.117
0.1925	0.9237	314	62.8	18.9	7.90	2.37	12.6	60.5	64.5	-3.60	2.67	0.111
0.1425	0.9435	233	59.8	18.0	8.24	2.47	13.8	59.3	63.4	-0.89	5.97	0.102
0.0925	0.9634	151	56.9	17.1	8.14	2.44	14.3	58.0	62.2	1.85	9.36	0.101
0.0425	0.9831	69.4	50.0	15.0	8.30	2.49	16.6	55.8	59.8	11.6	19.6	0.071
0.0325	0.9871	53.1	48.0	14.4	8.14	2.44	17.0	54.1	57.7	12.7	20.2	0.066
0.0225	0.9910	36.7	45.0	13.5	8.46	2.54	18.8	50.0	52.7	11.1	17.2	0.064
0.0175	0.9931	28.6	42.5	12.8	8.76	2.63	20.6	46.0	48.1	8.28	13.1	0.062
0.0125	0.9950	20.4	38.1	11.4	9.26	2.78	24.3	39.6	40.9	3.82	7.32	0.062
0.0100	0.9960	16.3	36.1	10.8	8.96	2.69	24.8	35.0	35.9	-3.17	-5.51	0.060
0.0075	0.9970	12.2	32.2	9.67	8.76	2.63	27.2	29.1	29.7	-9.61	-7.83	0.057
0.0050	0.9980	8.17	26.3	7.90	7.56	2.27	28.7	21.6	21.9	-17.7	-16.8	0.050
0.0025	0.9990	4.08	18.3	5.50	5.38	1.62	29.4	12.1	12.2	-33.9	-33.3	0.038

TABLE III. RESULTS OF TURBULENCE MEASUREMENTS Re = 163,000

y	η	Y^+	$\bar{U}_{exp}$	U^+	U'_{exp}	U'/U*	(U'/$\bar{U}$)%	$\bar{U}_{pe}$	$\bar{U}_{pt}$	(%$E_r U_{pe}$)	(%$E_r U_{pt}$)	λ
2.5165	0.0030	3701	80.0	26.9	2.88	0.97	3.60	80.0	80.0	-0.0003	-0.0003	0.140
2.4925	0.0125	3666	80.0	26.9	2.96	1.00	3.70	80.0	80.0	-0.006	-0.005	0.148
2.3925	0.0521	3519	79.7	26.8	2.96	1.00	3.71	79.9	79.9	0.27	0.29	0.149
2.2925	0.0917	3372	79.3	26.7	2.96	1.00	3.73	79.7	79.8	0.56	0.60	0.143
2.2425	0.1115	3298	78.7	26.5	3.12	1.05	3.96	79.6	79.7	1.17	1.23	0.148
1.9925	0.2106	2931	77.7	26.2	3.62	1.22	4.65	78.6	78.8	1.21	1.43	0.160
1.7425	0.3096	2563	76.9	25.9	4.14	1.39	5.38	77.1	77.4	0.20	0.69	0.169
1.4925	0.4087	2195	74.7	25.2	4.46	1.50	5.97	74.9	75.5	0.23	1.10	0.163
1.2425	0.5077	1828	71.8	24.2	4.98	1.68	6.93	72.1	73.1	0.39	1.79	0.163
0.9925	0.6068	1460	69.8	23.5	5.38	1.81	7.70	68.7	70.1	-1.59	0.47	0.160
0.7425	0.7058	1092	66.9	22.5	5.96	2.01	8.90	64.7	66.6	-3.29	-0.38	0.155
0.4925	0.8048	724	62.8	21.1	6.52	2.20	10.9	60.1	62.6	-4.30	-0.26	0.143
0.3925	0.8445	577	60.9	20.5	6.76	2.28	11.1	58.1	60.9	-4.61	-0.03	0.137
0.2925	0.8841	430	59.8	20.1	6.94	2.34	11.6	56.0	59.0	-6.37	-1.26	0.128
0.2425	0.9039	356	57.9	19.5	7.02	2.36	12.1	54.9	58.1	-5.18	0.34	0.119
0.1925	0.9237	283	55.9	18.8	7.02	2.36	12.6	53.8	57.1	-3.77	2.20	0.110
0.1425	0.9435	210	51.9	17.5	7.02	2.36	13.5	52.7	56.1	1.44	8.16	0.097
0.0925	0.9634	136	50.0	16.8	7.10	2.39	14.2	51.5	55.1	2.95	10.2	0.088
0.0425	0.9831	62.5	44.0	14.8	7.24	2.44	16.5	49.1	52.4	11.6	19.2	0.070
0.0325	0.9871	47.8	42.0	14.1	7.24	2.44	17.2	47.2	50.1	12.2	19.3	0.066
0.0225	0.9910	33.1	39.0	13.1	7.56	2.55	19.4	42.8	45.1	9.85	15.7	0.065
0.0175	0.9931	25.7	36.0	12.1	7.82	2.63	21.7	38.9	40.7	8.07	13.1	0.062
0.0125	0.9950	18.4	33.2	11.2	8.06	2.71	24.3	32.9	34.1	-0.90	2.83	0.062
0.0100	0.9960	14.7	30.2	10.2	7.90	2.66	26.2	28.8	29.7	-4.64	-1.52	0.059
0.0075	0.9970	11.0	27.2	9.16	7.40	2.49	27.2	23.7	24.4	-12.8	-10.4	0.056
0.0050	0.9980	7.35	21.3	7.17	6.36	2.14	29.8	17.4	17.8	-18.1	-16.4	0.047
0.0025	0.9990	3.68	15.3	5.15	4.30	1.45	28.1	9.65	9.80	-36.9	-35.9	0.038

TABLE IV. RESULTS OF TURBULENCE MEASUREMENTS Re = 146,000

y	η	Y^+	$\bar{U}_{exp}$	U^+	U'_{exp}	U'/U^*	$(U'/\bar{U})\%$	$\bar{U}_{pe}$	$\bar{U}_{pt}$	$(\%E_r U_{pe})$	$(\%E_r U_{pt})$	λ
2.5165	0.0030	3243	70.0	26.2	2.39	0.90	3.41	70.0	70.0	-0.0003	-0.0003	0.137
2.4925	0.0125	3212	70.0	26.2	2.39	0.90	3.41	70.0	70.0	-0.005	-0.005	0.137
2.3925	0.0521	3084	70.0	26.2	2.42	0.91	3.45	69.9	69.9	-0.09	-0.09	0.138
2.2925	0.0917	2955	70.0	26.2	2.53	0.95	3.61	69.8	69.8	-0.30	-0.28	0.142
2.2425	0.1115	2890	70.0	26.2	2.63	0.99	3.75	69.7	69.7	-0.44	-0.42	0.144
1.9925	0.2106	2568	69.3	25.9	2.94	1.10	4.24	68.9	69.0	-0.57	-0.50	0.151
1.7425	0.3096	2246	67.8	25.4	3.37	1.26	4.97	67.6	67.7	-0.24	-0.09	0.160
1.4925	0.4087	1924	66.2	24.8	3.85	1.44	5.81	65.9	66.1	-0.48	-0.20	0.164
1.2425	0.5077	1601	64.8	24.3	4.14	1.55	6.38	63.6	63.9	-1.79	-1.34	0.163
0.9925	0.6068	1279	62.8	23.5	4.61	1.73	7.36	60.9	61.3	-3.00	-2.34	0.164
0.7425	0.7058	957	59.9	22.4	5.03	1.88	8.39	57.7	58.3	-3.66	-2.72	0.156
0.4925	0.8048	635	57.0	21.3	5.38	2.01	9.43	54.0	54.7	-5.23	-3.96	0.143
0.3925	0.8445	506	54.9	20.6	5.62	2.10	10.2	52.4	53.2	-4.55	-3.09	0.136
0.2925	0.8841	377	52.6	19.7	5.82	2.18	11.1	50.7	51.6	-3.58	-1.92	0.124
0.2425	0.9039	313	51.2	19.2	5.91	2.21	11.5	49.8	50.8	-2.65	-0.87	0.118
0.1925	0.9237	248	49.0	18.4	6.02	2.25	12.3	48.9	49.9	-1.07	-1.84	0.110
0.1425	0.9435	184	47.5	17.8	6.29	2.36	13.2	48.0	49.0	1.13	3.28	0.108
0.0925	0.9634	119	45.4	17.0	6.36	2.38	14.0	47.1	48.1	3.68	5.93	0.090
0.0425	0.9831	54.8	40.2	15.1	6.72	2.52	16.7	44.5	45.3	10.7	12.6	0.077
0.0325	0.9871	41.9	38.3	14.3	6.86	2.57	14.2	42.3	42.9	10.5	11.9	0.074
0.0225	0.9910	29.0	35.2	13.2	7.08	2.65	20.1	37.8	38.1	7.50	8.23	0.070
0.0175	0.9931	22.6	33.0	12.4	7.30	2.73	22.1	34.0	34.1	2.97	3.20	0.070
0.0125	0.9950	16.1	29.4	11.0	7.55	2.83	25.7	28.3	28.2	-3.62	-3.91	0.068
0.0100	0.9960	12.9	27.2	10.2	7.42	2.78	27.3	24.6	24.5	-9.55	-10.1	0.067
0.0075	0.9970	9.67	23.6	8.84	7.08	2.65	30.0	20.1	19.9	-14.9	-15.7	0.061
0.0050	0.9980	6.44	19.2	7.19	5.75	2.15	29.9	14.6	14.4	-23.9	-24.8	0.052
0.0025	0.9990	3.22	13.4	5.02	3.85	1.44	28.7	8.02	7.88	-40.2	-41.2	0.038

TABLE V. RESULTS OF TURBULENCE MEASUREMENTS Re = 123,000

y	η	Y^+	$\bar{U}_{exp}$	U^+	U'_{exp}	U'/U^*	$(U'/\bar{U})\%$	$\bar{U}_{pe}$	$\bar{U}_{pt}$	$(\%E_r U_{pe})$	$(\%E_r U_{pt})$	λ
2.5165	0.0030	2823	60.0	26.2	2.12	0.93	3.53	60.0	60.0	-0.0003	-0.0003	0.139
2.4925	0.0125	2796	60.0	26.2	2.12	0.93	3.53	60.0	60.0	-0.006	-0.005	0.139
2.3925	0.0521	2683	60.0	26.2	2.18	0.95	3.63	60.0	60.0	-0.096	-0.092	0.143
2.2925	0.0917	2571	60.0	26.2	2.23	0.97	3.71	59.8	59.8	-0.30	-0.28	0.148
2.2425	0.1115	2515	60.0	26.2	2.29	1.00	3.81	59.7	59.7	-0.44	-0.42	0.151
1.9925	0.2106	2235	59.5	26.0	2.63	1.15	4.42	59.0	59.1	-0.74	-0.68	0.160
1.7425	0.3096	1954	58.4	25.5	3.00	1.31	5.13	58.0	58.0	-0.75	-0.60	0.172
1.4925	0.4087	1674	56.3	24.6	3.29	1.44	5.84	56.5	56.6	0.27	0.53	0.167
1.2425	0.5077	1394	55.0	24.0	3.66	1.60	6.65	55.5	54.8	-0.86	-0.45	0.170
0.9925	0.6068	1113	53.4	23.3	3.96	1.73	7.41	52.2	52.5	-2.28	-1.68	0.167
0.7425	0.7058	833	51.2	22.4	4.37	1.91	8.53	49.4	50.0	-3.47	-2.63	0.158
0.4925	0.8048	552	48.2	21.0	4.80	2.10	9.95	46.2	46.8	-4.06	-2.89	0.148
0.3925	0.8445	440	47.5	20.7	5.01	2.19	10.5	44.9	45.5	-5.56	-4.26	0.148
0.2925	0.8841	328	45.3	19.8	5.12	2.24	11.3	43.4	44.1	-4.19	-2.69	0.133
0.2425	0.9039	272	43.8	19.1	5.12	2.24	11.7	42.7	43.4	-2.62	-1.00	0.121
0.1925	0.9237	216	42.5	18.6	5.19	2.27	12.2	41.9	42.6	-1.45	0.29	0.113
0.1425	0.9435	160	40.2	17.6	5.27	2.30	13.1	41.1	41.9	2.22	4.14	0.103
0.0925	0.9634	104	37.3	16.3	5.40	2.36	14.5	40.2	41.0	7.82	9.93	0.091
0.0425	0.9831	47.7	33.8	14.8	5.69	2.48	16.8	37.1	37.8	9.93	11.8	0.079
0.0325	0.9871	36.5	31.6	13.8	5.85	2.55	18.5	34.8	35.3	10.1	11.7	0.076
0.0225	0.9910	25.3	28.6	12.5	6.14	2.68	21.5	30.4	30.7	6.17	7.30	0.072
0.0175	0.9931	19.6	26.5	11.6	6.36	2.78	24.0	26.8	27.1	1.26	2.11	0.070
0.0125	0.9950	14.0	23.6	10.3	6.36	2.78	26.9	22.0	22.1	-6.95	-6.42	0.068
0.0100	0.9960	11.2	21.6	9.43	6.24	2.72	29.2	18.9	18.9	-12.7	-12.3	0.068
0.0075	0.9970	8.41	18.4	8.03	5.60	2.45	30.4	15.2	15.3	-17.2	-17.0	0.062
0.0050	0.9980	5.60	14.7	6.42	4.50	1.97	30.6	10.9	11.0	-25.5	-25.5	0.054
0.0025	0.9990	2.80	11.0	4.80	2.95	1.29	26.8	5.93	5.92	-46.1	-46.2	0.043

TABLE VI. RESULTS OF TURBULENCE MEASUREMENTS Re = 99,500

y	η	Y^+	$\bar{U}_{exp}$	U^+	U'_{exp}	U'/U^*	$(U'/\bar{U})\%$	$\bar{U}_{pe}$	$\bar{U}_{pt}$	$(\%E_r U_{pe})$	$(\%E_r U_{pt})$	λ
2.5165	0.0030	2402	50.0	26.5	1.84	0.97	3.68	50.0	50.0	-0.0003	-0.0003	0.094
2.4925	0.0125	2379	50.0	26.5	1.84	0.97	3.68	50.0	50.0	-0.006	-0.005	0.094
2.3925	0.0521	2283	50.0	26.5	1.87	0.99	3.74	50.0	50.0	-0.10	-0.09	0.094
2.2925	0.0917	2188	49.7	26.3	1.93	1.02	3.88	49.8	49.9	0.29	0.31	0.100
2.2425	0.1115	2140	49.7	26.3	2.03	1.07	4.08	49.8	49.8	0.15	0.18	0.104
1.9925	0.2106	1902	49.0	25.9	2.34	1.24	4.77	49.2	49.2	0.39	0.49	0.115
1.7425	0.3096	1663	48.3	25.6	2.54	1.34	5.25	48.3	48.4	-0.10	0.12	0.124
1.4925	0.4087	1424	46.8	24.8	2.81	1.49	6.00	47.0	47.1	0.33	0.73	0.126
1.2425	0.5077	1186	45.3	24.0	3.24	1.71	7.15	45.3	45.6	0.005	0.63	0.138
0.9925	0.6068	947	43.2	22.9	3.50	1.85	8.10	43.3	43.7	0.21	1.15	0.137
0.7425	0.7058	709	41.8	22.1	3.85	2.04	9.21	40.9	41.5	-2.10	-0.79	0.138
0.4925	0.8048	470	39.6	21.0	3.96	2.10	10.0	38.2	38.9	-3.55	-1.75	0.145
0.3925	0.8445	375	38.2	20.2	4.08	2.16	10.7	37.0	37.8	-3.13	-1.08	0.138
0.2925	0.8841	279	36.6	19.4	4.27	2.26	11.7	35.8	36.6	-2.30	0.04	0.130
0.2425	0.9039	231	36.0	19.0	4.21	2.23	11.8	35.1	36.0	-2.47	0.02	0.121
0.1925	0.9237	184	34.5	18.2	4.21	2.23	12.2	34.5	35.4	-0.14	2.57	0.110
0.1425	0.9435	136	32.2	17.0	4.27	2.26	13.3	33.8	34.7	4.87	7.89	0.096
0.0925	0.9634	88.3	30.8	16.3	4.43	2.34	14.4	32.9	33.9	6.83	10.1	0.088
0.0425	0.9831	40.6	27.2	14.4	4.79	2.53	17.6	29.3	30.2	7.86	11.2	0.077
0.0325	0.9871	31.0	26.5	14.0	4.90	2.59	18.5	26.9	27.7	1.64	4.70	0.079
0.0225	0.9910	21.5	22.8	12.1	5.12	2.71	22.5	22.9	23.5	0.30	3.24	0.073
0.0175	0.9931	16.7	21.4	11.3	5.27	2.79	24.6	19.9	20.4	-7.16	-4.49	0.076
0.0125	0.9950	11.9	18.4	9.74	5.12	2.71	27.82	15.9	16.4	-13.4	-10.9	0.073
0.0100	0.9960	9.54	17.0	8.99	4.98	2.63	29.29	13.6	13.9	-20.3	-18.1	0.073
0.0075	0.9970	7.16	14.6	7.72	4.38	2.32	30.00	10.8	11.1	-25.9	-23.9	0.067
0.0050	0.9980	4.77	11.5	6.08	3.41	1.80	29.65	7.68	7.89	-33.2	-31.4	0.054
0.0025	0.9990	2.39	8.20	4.34	2.21	1.17	26.95	4.10	4.21	-49.9	-48.6	0.040

TABLE VII. RESULTS OF TURBULENCE MEASUREMENTS Re = 81,800

y	η	Y^+	$\bar{U}_{exp}$	U^+	U'_{exp}	U'/U^*	$(U'/\bar{U})\%$	$\bar{U}_{pe}$	$\bar{U}_{pt}$	$(\%E_r U_{pe})$	$(\%E_r U_{pt})$	λ
2.5165	0.0030	1956	40.0	25.2	1.36	0.86	3.40	40.0	40.0	-0.0003	-0.0003	0.101
2.4925	0.0125	1937	40.0	25.2	1.36	0.86	3.40	40.0	40.0	-0.005	-0.003	0.101
2.3925	0.0521	1859	40.0	25.2	1.40	0.88	3.50	40.0	40.0	-0.10	-0.09	0.104
2.2925	0.0917	1782	40.0	25.2	1.43	0.90	3.57	39.9	39.9	-0.30	-0.29	0.107
2.2425	0.1115	1743	40.0	25.2	1.46	0.92	3.65	39.8	39.8	-0.45	-0.42	0.109
1.9925	0.2106	1549	39.7	25.0	1.75	1.10	4.40	39.4	39.4	-0.85	-0.77	0.127
1.7425	0.3096	1354	39.0	24.5	1.92	1.21	4.92	38.6	38.7	-0.97	-0.79	0.137
1.4925	0.4087	1160	38.1	24.0	2.16	1.36	5.66	37.6	37.7	-1.32	-1.00	0.143
1.2425	0.5077	966	36.7	23.1	2.40	1.51	6.53	36.3	36.5	-1.11	-0.61	0.149
0.9925	0.6068	771	35.8	22.5	2.63	1.65	7.34	34.7	35.0	-3.06	-2.32	0.157
0.7425	0.7058	577	33.8	21.3	2.84	1.79	8.40	32.8	33.2	-2.85	-1.80	0.152
0.4925	0.8048	383	31.6	19.9	3.09	1.94	9.77	30.7	31.1	-2.90	-1.43	0.143
0.3925	0.8445	305	30.3	19.1	3.24	2.04	11.0	29.7	30.3	-1.84	-0.15	0.136
0.2925	0.8841	227	28.8	18.1	3.30	2.08	11.5	28.8	29.3	-0.15	1.80	0.126
0.2425	0.9039	188	28.4	17.9	3.27	2.12	11.9	28.2	28.8	-0.53	1.53	0.121
0.1925	0.9237	150	27.2	17.1	3.49	2.19	12.8	27.7	28.3	1.94	4.18	0.110
0.1425	0.9435	111	26.2	16.5	3.51	2.21	13.4	27.2	27.8	3.72	6.13	0.101
0.0925	0.9634	71.9	24.5	15.4	3.69	2.32	15.0	26.4	27.0	7.66	10.2	0.095
0.0425	0.9831	33.0	22.0	13.8	4.26	2.68	19.4	22.8	23.2	3.77	5.59	0.091
0.0325	0.9871	25.3	20.7	13.0	4.46	2.81	21.5	20.7	21.0	-0.17	1.28	0.094
0.0225	0.9910	17.5	18.1	11.4	4.60	2.89	25.4	17.2	17.4	-4.84	-3.83	0.092
0.0175	0.9931	13.6	16.4	10.3	4.60	2.89	28.0	14.8	14.9	-9.76	-9.01	0.089
0.0125	0.9950	9.72	13.8	8.68	4.46	2.81	32.3	11.7	11.8	-15.0	-14.5	0.086
0.0100	0.9960	7.77	11.7	7.36	4.04	2.54	34.5	9.90	9.94	-15.4	-15.0	0.076
0.0075	0.9970	5.83	10.0	6.29	3.42	2.15	34.2	7.85	7.87	-21.5	-21.3	0.067
0.0050	0.9980	3.89	7.80	4.90	2.56	1.61	32.8	5.53	5.54	-29.1	-29.0	0.053
0.0025	0.9990	1.94	5.90	3.71	1.46	0.92	24.7	2.93	2.93	-50.3	-50.3	0.035

TABLE VIII. RESULTS OF TURBULENCE MEASUREMENTS Re = 61,000

y	η	Y^+	$\bar{U}_{exp}$	U^+	U'_{exp}	U'/U^*	$(U'/\bar{U})\%$	$\bar{U}_{pe}$	$\bar{U}_{pt}$	$(\%E_r U_{pe})$	$(\%E_r U_{pt})$
2.5165	0.0030	1523	30.0	24.6	0.97	0.80	3.23	30.0	30.0	-0.0003	-0.0003
2.4925	0.0125	1508	30.0	24.6	1.00	0.82	3.33	30.0	30.0	-0.005	-0.005
2.3925	0.0521	1448	30.0	24.6	1.03	0.84	3.43	30.0	30.0	-0.10	-0.09
2.2925	0.0917	1387	30.0	24.6	1.03	0.84	3.43	29.9	29.9	-0.30	-0.29
2.2425	0.1115	1357	29.7	24.3	1.09	0.89	3.67	29.9	29.9	0.57	0.58
1.9925	0.2106	1206	29.0	23.8	1.23	1.01	4.24	29.5	29.5	1.83	1.87
1.7425	0.3096	1054	28.5	23.4	1.42	1.16	4.98	29.0	29.0	1.70	1.78
1.4925	0.4087	903	28.0	23.0	1.52	1.25	5.42	28.2	28.3	0.83	0.97
1.2425	0.5077	752	27.3	22.4	1.73	1.42	6.33	27.3	27.3	-0.11	0.12
0.9925	0.6068	601	26.2	21.5	1.93	1.58	7.36	26.1	26.2	-0.39	-0.04
0.7425	0.7058	449	25.2	20.7	2.16	1.77	8.57	24.7	24.8	-1.90	-1.42
0.4925	0.8048	298	23.3	19.1	2.30	1.89	9.87	23.1	23.3	-0.70	-0.02
0.3925	0.8445	237	22.7	18.6	2.36	1.93	10.4	22.4	22.6	-1.13	-0.36
0.2925	0.8841	177	21.7	17.8	2.49	2.04	11.5	21.7	21.9	0.08	0.96
0.2425	0.9039	147	21.3	17.5	2.53	2.07	11.9	21.3	21.5	0.19	1.13
0.1925	0.9237	116	20.6	16.9	2.53	2.07	12.3	20.9	21.2	1.69	2.69
0.1425	0.9435	86.2	19.8	16.2	2.67	2.19	13.5	20.5	20.7	3.46	4.52
0.0925	0.9634	60.0	18.8	15.4	2.90	2.38	15.4	19.6	20.0	4.19	5.18
0.0425	0.9831	25.7	16.3	13.4	3.57	2.93	21.9	15.8	16.0	-2.87	-2.35
0.0325	0.9871	19.7	14.6	12.0	3.68	3.02	25.2	14.0	14.0	-4.50	-4.13
0.0225	0.9910	13.6	12.5	10.2	3.80	3.11	30.4	11.2	11.3	-10.1	-9.94
0.0175	0.9931	10.6	10.8	8.85	3.63	2.98	33.6	9.47	9.48	-12.3	-12.3
0.0125	0.9950	7.56	8.80	7.21	3.29	2.70	37.4	7.35	7.34	-16.5	-16.5
0.0100	0.9960	6.05	7.40	6.07	3.02	2.48	40.8	6.13	6.13	-17.1	-17.2
0.0075	0.9970	4.54	6.10	5.00	2.36	1.93	38.7	4.80	4.80	-22.3	-21.4
0.0050	0.9980	3.03	4.80	3.93	1.77	1.45	36.9	3.34	3.34	-30.3	-30.5
0.0025	0.9990	1.51	3.80	3.11	0.94	0.77	24.7	1.75	1.75	-53.9	-54.1

TABLE IX. RESULTS OF TURBULENCE MEASUREMENTS Re = 39,800

y	η	Y^+	$\bar{U}_{exp}$	U^+	U'_{exp}	U'/U*	(U'/$\bar{U}$)%	$\bar{U}_{pe}$	$\bar{U}_{pt}$	(%$E_r U_{pe}$)	(%$E_r U_{pt}$)
2.5165	0.0030	1051	20.0	23.9	0.75	0.90	3.75	20.0	20.0	-0.0003	-0.0003
2.4925	0.0125	1041	20.0	23.9	0.75	0.90	3.75	20.0	20.0	-0.006	-0.005
2.3925	0.0521	999	20.0	23.9	0.75	0.90	3.75	20.0	20.0	-0.10	-0.09
2.2925	0.0917	957	20.0	23.9	0.76	0.91	3.80	19.9	19.9	-0.33	-0.28
2.2425	0.1115	937	19.8	23.7	0.79	0.94	3.98	19.9	19.9	0.52	0.58
1.9925	0.2106	832	19.5	23.3	0.87	1.04	4.46	19.7	19.7	0.80	1.02
1.7425	0.3096	728	19.2	22.9	0.99	1.18	5.15	19.3	19.4	0.29	0.78
1.4925	0.4087	623	18.5	22.1	1.15	1.37	6.21	18.7	18.9	1.10	1.99
1.2425	0.5077	520	17.8	21.3	1.22	1.46	6.85	18.0	18.3	1.12	2.54
0.9925	0.6068	415	17.1	20.4	1.36	1.62	7.95	17.1	17.5	0.25	2.36
0.7425	0.7058	310	16.3	19.5	1.48	1.77	9.07	16.1	16.6	-1.02	1.98
0.4925	0.8048	206	15.3	18.3	1.56	1.86	10.2	15.0	15.6	-2.14	2.01
0.3925	0.8445	164	15.0	17.9	1.62	1.94	10.8	14.5	15.2	-3.56	1.10
0.2925	0.8841	122	13.8	16.5	1.76	2.10	12.8	13.9	14.7	0.96	6.50
0.2425	0.9039	101	13.3	15.9	1.73	2.07	13.0	13.6	14.4	2.62	8.59
0.1925	0.9237	80.4	12.8	15.3	1.76	2.10	13.8	13.3	14.1	4.14	10.5
0.1425	0.9435	59.5	12.5	14.9	1.91	2.28	15.3	12.9	13.7	3.01	9.38
0.0925	0.9634	38.6	11.8	14.1	2.07	2.47	17.5	11.9	12.6	0.72	6.49
0.0425	0.9831	17.8	9.40	11.2	2.55	3.05	27.1	8.74	9.11	-7.04	-3.12
0.0325	0.9871	13.6	8.40	10.0	2.55	3.05	30.4	7.45	7.74	-11.1	-7.80
0.0225	0.9910	9.40	6.70	8.00	2.47	2.95	36.9	5.81	5.99	-13.3	-10.5
0.0175	0.9931	7.31	5.70	6.81	2.25	2.69	39.5	4.80	4.94	-15.8	-13.4
0.0125	0.9950	5.22	4.20	5.02	1.85	2.21	44.0	3.65	3.74	-13.2	-10.9
0.0100	0.9960	4.18	3.20	3.82	1.54	1.84	48.1	3.01	3.08	-5.88	-3.61
0.0075	0.9970	3.13	2.80	3.35	1.29	1.54	46.0	2.33	2.39	-16.7	-14.8
0.0050	0.9980	2.09	2.40	2.87	0.83	0.99	34.6	1.61	1.64	-33.1	-31.7
0.0025	0.9990	1.04	--	--	0.43	0.51	--	0.83	0.85	--	--

TABLE X. RESULTS OF TURBULENCE MEASUREMENTS Re = 20,000

y	η	Y^+	$\bar{U}_{exp}$	U^+	U'_{exp}	U'/U^*	$(U'/\bar{U})\%$	$\bar{U}_{pe}$	$\bar{U}_{pt}$	$(\%E_r U_{pe})$	$(\%E_r U_{pt})$
2.5165	0.0030	562	10.0	22.0	0.40	0.89	4.00	10.0	10.0	-0.0003	-0.0003
2.4925	0.0125	557	10.0	22.0	0.39	0.86	3.90	10.0	10.0	-0.005	-0.005
2.3925	0.0521	534	10.0	22.0	0.40	0.89	4.00	9.99	9.99	-0.10	-0.09
2.2925	0.0917	512	10.0	22.0	0.41	0.90	4.10	9.97	9.97	-0.30	-0.28
2.2425	0.1115	501	10.0	22.0	0.41	0.90	4.10	9.96	9.96	-0.45	-0.42
1.9925	0.2106	445	10.0	22.0	0.46	1.01	4.60	9.84	9.85	-1.60	-1.49
1.7425	0.3096	389	9.90	21.8	0.51	1.12	5.15	9.65	9.68	-2.48	-2.24
1.4925	0.4087	333	9.60	21.1	0.60	1.32	6.25	9.40	9.44	-2.10	-1.66
1.2425	0.5077	277	9.10	20.0	0.64	1.41	7.08	9.07	9.14	-0.32	0.39
0.9925	0.6068	222	8.70	19.1	0.71	1.56	8.16	8.67	8.77	-0.31	0.76
0.7425	0.7058	166	8.20	18.0	0.75	1.65	9.14	8.20	8.33	0.05	1.59
0.4925	0.8048	110	7.70	16.9	0.81	1.78	10.5	7.66	7.83	-0.47	1.65
0.3925	0.8445	87.7	7.40	16.3	0.84	1.85	11.4	7.42	7.60	0.29	2.68
0.2925	0.8841	65.3	7.05	15.5	0.89	1.96	12.6	7.13	7.32	1.17	3.78
0.2425	0.9039	54.2	6.60	14.5	0.91	2.00	13.8	6.94	7.12	5.08	7.80
0.1925	0.9237	43.0	6.60	14.5	1.00	2.20	15.2	6.64	6.81	0.66	3.16
0.1425	0.9435	31.8	6.15	13.5	1.07	2.35	17.4	6.14	6.28	-0.11	2.06
0.0925	0.9634	20.7	5.40	11.9	1.28	2.81	23.7	5.19	5.27	-3.96	2.44
0.0425	0.9831	9.49	4.04	8.88	1.24	2.73	30.7	3.24	3.26	-19.8	-19.3
0.0325	0.9871	7.26	3.05	6.70	1.09	2.40	35.7	2.65	2.66	-13.1	-12.8
0.0225	0.9910	5.03	2.35	6.15	0.90	1.98	38.3	1.97	1.97	-16.4	-16.3
0.0175	0.9931	3.91	1.75	3.85	0.70	1.54	40.0	1.58	1.58	- 9.5	- 9.5
0.0125	0.9950	2.79	1.46	3.20	0.49	1.08	35.0	1.17	1.17	-19.7	-19.8
0.0100	0.9960	2.23	1.15	2.52	0.37	0.81	32.2	0.95	0.95	-17.0	-17.1
0.0075	0.9970	1.67	1.10	2.41	0.25	0.55	22.7	0.73	0.73	-33.7	-33.9
0.0050	0.9980	1.11	--	--	0.16	0.35	--	0.49	0.49	--	--
0.0025	0.9990	0.56	--	--	0.089	0.20	--	0.25	0.25	--	--

TABLE XI. RESULTS OF TURBULENCE MEASUREMENTS Re = 9,780

y	η	Y^+	$\bar{U}_{exp}$	U^+	U'_{exp}	U'/U^*	$(U'/\bar{U})\%$	$\bar{U}_{pe}$	$\bar{U}_{pt}$	$(\%E_r U_{pe})$	$(\%E_r U_{pt})$
2.5165	0.0030	305	5.03	20.6	0.178	0.73	3.53	5.03	5.03	-0.0003	-0.0003
2.4925	0.0125	302	5.03	20.6	0.178	0.73	3.53	5.03	5.03	-0.005	-0.006
2.3925	0.0521	290	5.03	20.6	0.178	0.73	3.53	5.03	5.03	-0.09	-0.08
2.2925	0.0917	277	5.03	20.6	0.178	0.73	3.53	5.02	5.02	-0.27	-0.25
2.2425	0.1115	271	5.03	20.6	0.186	0.76	3.69	5.01	5.01	-0.40	-0.37
1.9925	0.2106	241	4.94	20.2	0.206	0.84	4.17	4.96	4.96	0.36	0.49
1.7425	0.3096	211	4.83	19.8	0.230	0.94	4.76	4.87	4.89	0.90	1.20
1.4925	0.4087	181	4.73	19.4	0.254	1.04	5.36	4.76	4.78	0.59	1.11
1.2425	0.5077	150	4.62	18.9	0.270	1.11	5.84	4.61	4.65	-0.22	0.61
0.9925	0.6068	120	4.42	18.1	0.308	1.26	6.96	4.43	4.48	-0.22	1.46
0.7425	0.7058	89.9	4.22	17.3	0.330	1.35	7.81	4.21	4.29	-0.11	1.63
0.4925	0.8048	59.6	3.92	16.1	0.414	1.66	10.6	3.94	4.03	0.43	2.71
0.3925	0.8445	47.5	3.62	14.8	0.446	1.83	12.3	3.77	3.86	4.05	6.54
0.2925	0.8841	35.4	3.42	14.0	0.496	2.03	14.5	3.49	3.58	2.16	4.60
0.2425	0.9039	29.3	3.21	13.2	0.580	2.38	18.0	3.28	3.36	2.27	4.62
0.1925	0.9237	23.3	3.01	12.3	0.620	2.54	20.6	2.99	3.05	-0.76	1.37
0.1425	0.9435	17.2	2.91	11.9	0.700	2.87	24.0	2.56	2.61	-11.9	10.2
0.0925	0.9634	11.2	2.40	9.84	0.708	2.90	29.5	1.95	1.99	-18.6	7.3
0.0425	0.9831	5.14	1.23	5.04	0.514	2.11	41.8	1.07	1.08	-13.3	-12.2
0.0325	0.9871	3.93	0.85	3.48	0.414	1.70	48.7	0.85	0.86	-0.50	0.63
0.0225	0.9910	2.72	0.55	2.25	0.304	1.25	55.3	0.61	0.61	10.4	11.5
0.0175	0.9931	2.12	0.48	1.97	0.206	0.84	42.9	0.48	0.49	0.22	1.21
0.0125	0.9950	1.51	0.42	1.72	0.142	0.58	33.8	0.35	0.35	-16.7	-15.9
0.0100	0.9960	1.21	--	--	0.097	0.40	--	0.28	0.29	--	--
0.0075	0.9970	0.91	--	--	0.070	0.29	--	0.21	0.22	--	--
0.0050	0.9980	0.61	--	--	0.040	0.16	--	0.14	0.15	--	--
0.0025	0.9990	0.30	--	--	0.017	0.07	--	0.073	0.073	--	--

TABLE XII. RESULTS OF TURBULENCE MEASUREMENTS Re = 4,800

y	η	Y^+	$\bar{U}_{exp}$	U^+	U'_{exp}	U'/U^*	$(U'/\bar{U})\%$	$\bar{U}_{pe}$	$\bar{U}_{pt}$	$(\%E_r U_{pe})$	$(\%E_r U_{pt})$
2.5165	0.0030	163	2.53	19.0	0.081	0.61	3.20	2.53	2.53	-0.0002	-0.0002
2.4925	0.0125	162	2.53	19.0	0.081	0.61	3.20	2.53	2.53	-0.003	-0.004
2.3925	0.0521	155	2.53	19.0	0.081	0.61	3.20	2.53	2.53	-0.05	-0.07
2.2925	0.0917	149	2.53	19.0	0.081	0.61	3.20	2.53	2.52	-0.17	-0.22
2.2425	0.1115	146	2.53	19.0	0.093	0.70	3.67	2.52	2.52	-0.26	-0.33
1.9925	0.2106	129	2.47	18.6	0.097	0.73	3.92	2.51	2.50	1.49	1.22
1.7425	0.3096	113	2.42	18.2	0.101	0.76	4.17	2.48	2.47	2.47	1.88
1.4925	0.4087	96.9	2.36	17.7	0.116	0.87	4.91	2.44	2.42	3.49	2.43
1.2425	0.5077	80.7	2.31	17.4	0.129	0.97	5.58	2.40	2.36	3.61	1.97
0.9925	0.6068	64.4	2.20	16.5	0.143	1.08	6.56	2.33	2.27	5.73	3.39
0.7425	0.7058	48.2	2.13	16.0	0.166	1.25	7.79	2.22	2.15	4.00	1.16
0.4925	0.8048	32.0	1.97	14.8	0.204	1.54	10.4	1.98	1.92	0.49	-2.33
0.3925	0.8445	25.5	1.92	14.4	0.233	1.76	12.1	1.81	1.76	-5.78	-8.25
0.2925	0.8841	19.0	1.68	12.6	0.233	1.76	13.9	1.56	1.53	-7.05	-9.17
0.2425	0.9039	15.7	1.52	11.4	0.261	1.96	17.2	1.40	1.37	-7.99	-9.87
0.1925	0.9237	12.5	1.35	10.2	0.270	2.03	20.0	1.20	1.18	-11.0	-12.5
0.1425	0.9435	9.25	1.23	9.25	0.255	1.92	20.7	0.97	0.95	-21.5	-22.6
0.0925	0.9634	6.01	0.78	5.86	0.242	1.82	31.0	0.68	0.67	-12.6	-13.5
0.0425	0.9831	2.76	0.40	3.00	0.116	0.87	29.0	0.34	0.34	-14.6	-15.2
0.0325	0.9871	2.11	0.28	2.10	0.070	0.53	25.0	0.27	0.26	-5.07	-5.58
0.0225	0.9910	1.46	--	--	0.043	0.32	--	0.19	0.19	--	--
0.0175	0.9931	1.14	--	--	0.029	0.22	--	0.15	0.15	--	--
0.0125	0.9950	0.81	--	--	0.0163	0.12	--	0.11	0.11	--	--
0.0100	0.9960	0.65	--	--	0.0101	0.07	--	0.085	0.085	--	--
0.0075	0.9970	0.49	--	--	0.0048	0.04	--	0.064	0.064	--	--
0.0050	0.9980	0.32	--	--	0.0023	0.02	--	0.043	0.043	--	--
0.0025	0.9990	0.16	--	--	0.0	0.0	--	0.022	0.022	--	--

TABLE XIII. CROSS WIRE RESULTS

Re →		186,000				163,000			
x	x/r_o	$\overline{uw}$	w'	$\overline{uw}/U^{*2}$	w'/U^*	$\overline{uw}$	w'	$\overline{uw}/U^{*2}$	w'/U^*
2.524	1.0000	0.61	1.83	0.055	0.55	0.44	1.65	0.050	0.56
2.250	0.8914	0.70	1.96	0.063	0.59	0.83	1.72	0.094	0.58
2.000	0.7924	1.11	2.42	0.10	0.64	1.13	1.93	0.128	0.65
1.750	0.6933	1.58	2.36	0.14	0.71	0.77	2.08	0.087	0.70
1.500	0.5943	1.42	2.64	0.13	0.79	1.27	2.36	0.14	0.79
1.250	0.4952	2.42	2.83	0.22	0.85	1.38	2.55	0.16	0.86
1.000	0.3962	3.13	3.07	0.28	0.92	1.72	2.79	0.20	0.94
0.750	0.2971	4.39	3.22	0.40	0.97	2.25	2.90	0.26	0.98
0.500	0.1981	5.35	3.36	0.48	1.01	3.98	3.02	0.45	1.02
0.250	0,0990	5.66	3.67	0.51	1.10	5.21	3.22	0.59	1.08

Re →		146,000				123,000			
x	x/r_o	$\overline{uw}$	w'	$\overline{uw}/U^{*2}$	w'/U^*	$\overline{uw}$	w'	$\overline{uw}/U^{*2}$	w'/U^*
2.524	1.0000	0.49	1.45	0.069	0.54	0.35	1.21	0.067	0.53
2.250	0.8914	0.57	1.54	0.080	0.58	0.37	1.27	0.071	0.55
2.000	0.7924	0.63	1.67	0.088	0.63	0.52	1.37	0.099	0.60
1.750	0.6933	0.47	1.86	0.066	0.70	0.72	1.54	0.14	0.67
1.500	0.5943	0.96	2.06	0.14	0.77	0.72	1.70	0.14	0.74
1.250	0.4952	1.22	2.20	0.17	0.82	0.92	1.84	0.18	0.80
1.000	0.3962	1.73	2.36	0.24	0.88	1.33	1.96	0.25	0.86
0.750	0.2971	2.05	2.48	0.29	0.93	1.25	2.08	0.24	0.91
0.500	0.1981	2.20	2.55	0.31	0.96	1.76	2.21	0.34	0.97
0.250	0.0990	3.17	2.75	0.45	1.03	2.51	2.37	0.48	1.03

TABLE XIX. CROSS WIRE RESULTS

Re →		99,500				81,800			
x	x/r_o	$\overline{uw}$	w'	$\overline{uw}/U^{*2}$	w'/U^*	$\overline{uw}$	w'	$\overline{uw}/U^{*2}$	w'/U^*
2.524	1.000	0.35	1.03	0.098	0.54	0.10	0.78	0.040	0.49
2.250	0.8914	0.31	1.11	0.087	0.59	0.16	0.86	0.063	0.54
2.000	0.7924	0.41	1.21	0.12	0.64	0.19	0.91	0.075	0.57
1.750	0.6933	0.45	1.33	0.13	0.70	0.26	1.05	0.10	0.66
1.500	0.5943	0.58	1.45	0.16	0.77	0.30	1.15	0.12	0.72
1.250	0.4952	0.52	1.56	0.15	0.83	0.47	1.28	0.19	0.81
1.000	0.3962	0.86	1.70	0.24	0.90	0.51	1.42	0.20	0.89
0.750	0.2971	0.91	1.76	0.25	0.93	0.47	1.46	0.19	0.92
0.500	0.1981	1.32	1.88	0.37	0.99	0.51	1.50	0.20	0.94
0.250	0.0990	1.38	1.98	0.39	1.05	0.80	1.69	0.32	1.06

Re →		61,000				39,800			
x	x/r_o	$\overline{uw}$	w'	$\overline{uw}/U^{*2}$	w'/U^*	$\overline{uw}$	w'	$\overline{uw}/U^{*2}$	w'/U^*
2.524	1.000	0.11	0.64	0.074	0.52	0.11	0.48	0.16	0.57
2.250	0.8914	0.12	0.68	0.081	0.56	0.10	0.50	0.14	0.60
2.000	0.7924	0.16	0.77	0.11	0.63	0.08	0.55	0.11	0.65
1.750	0.6933	0.15	0.83	0.10	0.68	0.08	0.61	0.11	0.73
1.500	0.5943	0.18	0.91	0.12	0.75	0.11	0.69	0.16	0.82
1.250	0.4952	0.20	0.99	0.13	0.81	0.13	0.75	0.19	0.89
1.000	0.3962	0.28	1.11	0.19	0.91	0.15	0.81	0.21	0.96
0.750	0.2971	0.31	1.15	0.21	0.94	0.17	0.87	0.24	1.04
0.500	0.1981	0.50	1.21	0.34	0.99	0.19	0.92	0.27	1.09
0.250	0.0990	0.57	1.35	0.38	1.11	0.27	0.99	0.39	1.18

TABLE XV. LAMINAR SUBLAYER

Re	$y^{\neq}_{ese}$	h_{ese} Btu/Hr-Ft^2-°F
201,000	0.000091	2,060
186,000	0.000098	1,900
103,000	0.000110	1,690
146,000	0.000124	1,500
123,000	0.000143	1,300
99,500	0.000168	1,110
81,800	0.000206	902
61,000	0.000265	702
39,800	0.000383	486
20,000	0.000717	259
9,780	0.00132	141
4,800	0.0025	74.3

$\neq$ y_{ese} and h_{ese} are based on the laminar sublayer having a thickness of $Y^+ = 0.161$.

TABLE XVI. LAUFER'S DATA*

Re →	420,000		41,000	
y/r_o	U'/U^*	w'/U^*	U'/U^*	w'/U^*
1.00	0.80	0.75	0.78	0.73
0.90	0.81	0.77	0.80	0.75
0.80	0.94	0.82	0.94	0.79
0.69	1.05	0.90	1.03	0.89
0.59	1.19	0.96	1.14	0.95
0.48	1.26	1.09	1.25	1.02
0.37	1.45	1.19	1.35	1.17
0.27	1.60	1.27	1.45	1.22
0.17	1.87	1.34	1.60	1.25
0.08	2.05	1.52	1.80	1.28

Re →	420,000				41,000			
y/r_o	y	Y^+	U'/U^*	y/r_o	y	Y^+	U'/U^*
0.0013	0.0063	11.0	2.30	0.0028	0.0136	2.82	0.60
0.0017	0.0085	14.5	2.63	0.0040	0.0194	4.03	1.25
0.0020	0.0098	17.2	2.60	0.0068	0.0330	6.86	1.96
0.0040	0.0195	34.2	2.45	0.0078	0.0378	7.85	2.32
0.0070	0.0340	59.7	2.25	0.0080	0.0388	8.06	2.40
0.0140	0.0680	119.0	2.25	0.0100	0.0486	10.1	2.50
0.0250	0.1210	212.0	2.20	0.0165	0.0800	16.6	2.60
				0.0410	0.1990	41.3	2.20

* These data were read from the graphs in reference 13 and are subject to the errors that occur therefrom.

TABLE XVII. PARAMETERS FOR THE DESCRIPTION OF TURBULENT PIPE FLOW

Re	$\bar{U}_{max}$ (Ft/sec)	$\bar{U}_A/\bar{U}_{max}$	S	n_{pe}	n_{pt}	U*
201,000	98.3	0.824	80.7	131.7	120.6	3.58
186,000	90.0	0.832	76.6	123.6	113.4	3.33
163,000	80.0	0.820	67.7	109.1	102.0	2.97
146,000	70.0	0.841	63.4	97.4	93.1	2.67
123,000	60.0	0.825	53.9	82.9	80.9	2.29
99.500	50.0	0.800	44.2	69.0	68.5	1.89
81,800	40.0	0.823	39.2	60.6	58.9	1.59
61,000	30.0	0.818	30.8	47.0	46.3	1.22
39,800	20.0	0.800	21.7	34.7	32.8	0.837
20,000	10.0	0.803	13.0	19.7	18.9	0.455
9,780	5.03	0.781	7.36	10.4	10.1	0.244
4,800	2.53	0.762	4.32	5.19	5.51	0.133

TABLE XVIII. OSCILLOGRAM DATA

Fig. #	Re	y (in)	Relative Amplification	U' (Ft/Sec)	$\bar{U}$ (Ft/Sec)	(U'/$\bar{U}$)%	Millisec cm
22a	186,000	2.5000	1/219	3.14	90.0	3.49	5
22b	186,000	1.0000	1/438	5.44	80.0	6.80	5
22c	186,000	0.04000	1/875	8.13	50.0	16.3	5
22d	186,000	0.02000	1/875	8.57	41.6	20.6	5
22e	186,000	0.0075	1/438	4.29	22.4	19.2	5
23a	61,000	2.5000	1/80	0.89	30.0	2.96	5
23b	61,000	1.0000	1/160	1.68	26.8	6.27	5
23c	61,000	0.2500	1/160	2.28	22.4	10.2	5
23d	61,000	0.0250	1/320	3.58	13.4	26.7	5
23e	61,000	0.0075	1/80	1.1	4.3	25.5	5
24a	6,630	2.5000	1/10	0.14	3.5	4.0	5
24b	6,630	1.0000	1/40	0.27	3.15	8.57	5
24c	6,630	0.4000	1/20	--	--	--	5
24d	6,630	0.2000	1/5	0.037	--	--	5
24e	6,630	0.0075	1	--	--	--	5
24f	6,630	0.0075	1	--	--	--	5

APPENDIX B

THE DETERMINATION OF n (PAI'S EQUATION) BY THE METHOD OF LEAST SQUARES

Pai's equation (II-33) contains two constants, s and n, both of which can be calculated from friction factor and $\overline{U}_A/\overline{U}_m$ plots. However, before equation (II-41) was derived, to calculate n from the generalized plots, it was necessary to predict n from the experimental data. To calculate n from experimental data, the method of least squares, with slight modifications, was used.

Pai's equation (II-33) may be written as

$$Y = \frac{\overline{U}}{\overline{U}_m} - 1 = \frac{s - n}{n - 1}\eta^2 + \frac{1 - s}{n - 1}\eta^{2n} \qquad \text{(B-1)}$$

The method of least squares minimizes $(Y_o - Y)^2$ by taking the first derivative of $(Y_o - Y)^2$ with respect to n and setting it equal to zero. However, when this is done as equation explicit in n cannot be obtained. It is therefore necessary to resort to a numerical method for the determination of n. The method used in this research was that of Newton.

Newton's method consists of assuming a value of n (n_i) and calculating $\frac{\partial (Y_o - Y)^2}{\partial n}$ and $\frac{\partial^2 (Y_o - Y)^2}{\partial^2 n}$ using the assumed value

of n. The second (i + 1) trial value of n is calculated by

$$n_{i+1} = n_i - \left(\frac{\partial (Y_o - Y)^2}{\partial n} \frac{\partial^2 (Y_o - Y)^2}{\partial^2 n} \right)_i \qquad \text{(B-2)}$$

This operation is repeated until $\frac{\partial (Y_o - Y)^2}{\partial n}$ is sufficiently close to zero.

For Pai's equation

$$(Y_o - Y)^2 = Y_o^2 - 2\left(\frac{s-n}{n-1}\right) Y_o \eta^2 - 2\left(\frac{1-s}{n-1}\right) Y_o \eta^{2n} + \left(\frac{s-n}{n-1}\right)^2 \eta^4 + 2\left(\frac{1-s}{n-1}\right)\left(\frac{s-n}{n-1}\right) \eta^2 \eta^{2n} + \left(\frac{1-s}{n-1}\right)^2 \eta^{4n} \qquad \text{(B-3)}$$

$$\frac{\partial (Y_o - Y)^2}{\partial n} = -2\frac{(1-s)}{(n-1)^2} \sum Y_o \eta^2 - 4\frac{(1-s)}{(n-1)} \sum Y_o \eta^{2n} \operatorname{Ln} \eta + 2\frac{(1-s)}{(n-1)^2} \sum Y_o \eta^{2n} + \frac{2(s-n)(1-s)}{(n-1)^3} \sum \eta^4 + \frac{4(1-s)(s-n)}{(n-1)^2} \sum \eta^2 \eta^{2n} \operatorname{Ln} \eta - \frac{2(1-s)(2s-n-1)}{(n-1)^3} \sum \eta^2 \eta^{2n} + \frac{4(1-s)^2}{(n-1)^2} \sum \eta^{4n} \operatorname{Ln} \eta - \frac{2(1-s)^2}{(n-1)^3} \sum \eta^{4n} \qquad \text{(B-4)}$$

$$\frac{\partial (Y_o - Y)^2}{\partial n} = -\frac{2(1-s)}{(n-1)^2} \sum Y_o \eta^2 - \frac{4(1-s)}{(n-1)} \sum Y_o \eta^{2n} \operatorname{Ln} \eta + \frac{2(1-s)}{(n-1)^2} \sum Y_o \eta^{2n} + \frac{2(s-n)(1-s)}{(n-1)^3} \sum \eta^4 + \frac{4(1-s)(s-n)}{(n-1)^3} \sum \eta^2 \eta^{2n} \operatorname{Ln} \eta - \frac{2(1-s)(2s-n-1)}{(n-1)^3} \sum \eta^2 \eta^{2n} + \frac{4(1-s)^2}{(n-1)^2} \sum \eta^{4n} \operatorname{Ln} \eta - \frac{2(1-s)^2}{(n-1)^3} \sum \eta^{4n} \qquad \text{(B-5)}$$

The calculation of these equations, by hand, would require a prohibitive amount of time; therefore, the IBM 650 was used for the calculations. The 650 programs were written in FOR TRANSIT.

APPENDIX C

DERIVATION OF EQUATIONS FOR CROSS WIRE MEASUREMENTS

In Section 11 of Chapter III a qualitative analysis was made of the cross wire operation. It is now desirable to put the before analysis into quantitative form.

Considering wire 1, in Figure (1b), the component of the velocity in the plane of the paper perpendicular to the wire is

$$(\overline{U} + u) \text{ Sin } \phi_1 + w \text{ Cos } \phi_1$$

and that perpendicular to the plane of the paper is v. Thus the value of the vector $\vec{U}_e$ is

$$\vec{U}_e = \left[(\overline{U} + u)^2 \text{ Sin}^2 \phi_1 + w \text{ Cos } \phi_1 \right]^2 + v^2 \quad ^{\frac{1}{2}} \qquad \text{(II-67)}$$

or

$$\vec{U}_e = (\overline{U} + u)^2 \text{ Sin}^2 \phi_1 + 2(\overline{U} + u)(w) \text{ Sin } \phi_1 \text{ Cos } \phi_1 + w^2 \text{ Cos}^2 \phi_1 + v^2 \quad ^{\frac{1}{2}} \qquad \text{(II-68)}$$

but $\overline{U^2} \gg \overline{Uu} \sim \overline{Uw} \gg v^2$ or, neglecting v^2,

$$\vec{U}_e = (\overline{U} + u) \text{ Sin } \phi_1 + w \text{ Cos } \phi_1 \qquad \text{(II-69)}$$

Taking the average

$$\overline{\vec{U}_e} = \overline{U} \text{ Sin } \phi_1 \qquad \text{(II-70)}$$

where

$\vec{\bar{U}}_e$ = average value of the effective velocity

and subtracting $\vec{\bar{U}}_e$ from $\vec{U}_e$

$$\vec{U}_e - \vec{\bar{U}}_e = u \text{ Sin } \phi_1 + w \text{ Cos } \phi_1 \qquad \text{(II-71)}$$

In equation (II-64) it is seen that the square root of the velocity, however, the Type 3A Hot Wire Anemometer (the one used in this paper) has a linearizing tube in which the relationship between the signal current and control voltage (across the wire) is the inverse of the bridge characteristic for a wire of the recommended size if operated at the recommended temperature.[9] Thus, the current in the metering circuits is proportional to the instantaneous velocity; i.e., the instantaneous value of the effective velocity perpendicular to the wire. For the instantaneous velocity we may write

$$I_1 = \frac{1}{A_1} \vec{U}_e = \frac{1}{A_1} \left[(\bar{U} + u) \text{ Sin } \phi_1 + w \text{ Cos } \phi_1 \right] \qquad \text{(II-72)}$$

where

I_1 = instantaneous current in the metering circuit

A_1 = calibration constant for wire 1

similarly for the average velocity $\vec{\bar{U}}_e$

$$\bar{I}_1 = \frac{1}{A_1} \vec{\bar{U}}_e = \frac{1}{A_1} \bar{U} \text{ Sin } \phi_1 \qquad \text{(II-73)}$$

where

$\bar{I}_1$ = average current in the metering circuit and the reading of the D.C. panel meter

If the current in the metering circuit (I_1) (which is proportional to $\vec{U}_e$) is passed through a blocking capacitor, and the resultant current ($I_1 - \bar{I}_1$) is measured on a root mean square indicating meter, the meter indication, I_{T_1}, will be proportional to the root mean square of ($I_1 - \bar{I}_1$) and also ($\vec{U}_e - \bar{\vec{U}}_e$), or

$$I_{T_1} \alpha \left[(I_1 - \bar{I}_1)^2\right]^{\frac{1}{2}} = \frac{1}{A_1}\left[(\vec{U}_e - \bar{\vec{U}}_e)^2\right]^{\frac{1}{2}} \qquad \text{(II-74)}$$

where

I_{T_1} = root mean square meter indication for position 1

further

$$I_{T_1} \alpha \frac{1}{A_1}\left[\overline{u^2}\,\mathrm{Sin}^2\,\phi_1 + w^2\,\mathrm{Cos}^2\,\phi_1 + 2\overline{uw}\,\mathrm{Sin}\,\phi_1\,\mathrm{Cos}\,\phi_1\right]^{\frac{1}{2}} \qquad \text{(II-75)}$$

The constants of proportionality are supplied by the electronic equipment, thus (II-75) becomes

$$I_{T_1} = \frac{1}{A_1F_1B}\left[\overline{u^2}\,\mathrm{Sin}^2\,\phi_1 + \overline{w^2}\,\mathrm{Cos}^2\,\phi_1 + 2\overline{uw}\,\mathrm{Sin}\,\phi_1\,\mathrm{Cos}\,\phi_1\right]^{\frac{1}{2}} \qquad \text{(II-76)}$$

where

B = basic calibration constant of RMS Analyzer

F_1 = multiplying factor for RMS Analyzer position 1

By a similar analysis it can be shown that I_{T_2} may be represented by

$$I_{T_2} \alpha \left[\overline{(I_2 - \bar{I}_2)^2}\right]^{\frac{1}{2}} = \frac{1}{A_2}\left[(\vec{U}_e - \bar{\vec{U}}_e)\right]^{\frac{1}{2}} \qquad \text{(II-77)}$$

where

I_{T_2} = root mean square meter reading position 2

or

$$I_{T_2} = \frac{1}{A_2 F_2 B}\left[\overline{u^2}\,\mathrm{Sin}^2\,\phi_2 + \overline{w^2}\,\mathrm{Cos}^2\,\phi_2 - 2\overline{uw}\,\mathrm{Sin}\,\phi_2\,\mathrm{Cos}\,\phi_2\right]^{\frac{1}{2}} \qquad \text{(II-78)}$$

where

F_2 = multiplying factor for RMS Analyzer position 2

If $A_1 = A_2 = A$ and $\phi_1 = \phi_2 = \phi$ (which are the conditions assumed in experiment) subtracting $I_{T_2}^2$ from $I_{T_1}^2$ yields

$$F_1^2 I_{T_2}^2 - F_2^2 I_2^2 = \frac{1}{A^2 B^2}\, 4\,\overline{uw}\,\mathrm{Sin}\,\phi\,\mathrm{Cos}\,\phi \qquad \text{(II-79)}$$

or

$$\overline{uw} = \frac{A^2 B^2}{\mathrm{Sin}\,\phi\,\mathrm{Cos}\,\phi}\left(F_1^2\, I_{T_1}^2 - F^2\text{-}I_{T_2}^2\right) \qquad \text{(II-80)}$$

which is the correlation between the axial and the azimuthal fluctuating velocities.

Consider now if $(I_1 - \bar{I}_1)$ and $(I_2 - \bar{I}_2)$ are added and metered by the RMS meter. The meter indication I_{T_a} would be

$$I_{T_a} = \frac{1}{ABF}\left[\overline{(I_1 - \bar{I}_1) + (I_2 - \bar{I}_2)^{\,2}}\right]^{\frac{1}{2}} \qquad \text{(II-81)}$$

where

I_{T_a} = RMS meter indication when the fluctuating currents from wire 1 and 2 are added

F_a = multiplying factor for RMS Analyzer position A

$$I_{T_a} = \frac{1}{ABF_a}\, 2(\overline{U^2})^{\frac{1}{2}}\,\mathrm{Sin}\,\phi \qquad \text{(II-82)}$$

further

$$(\overline{u^2})^{\frac{1}{2}} = \frac{ABF_a I_{T_a}}{2 \sin \phi} \qquad \text{(II-83)}$$

which is the intensity of turbulence. A similar procedure applied to $(I_1 - \bar{I}_1) - (I_2 - \bar{I}_2)$ yields

$$I_{T_b} = \frac{1}{ABF_b} \left[\overline{(I_1 - \bar{I}_1) - (I_2 - \bar{I}_2)^2} \right]^{\frac{1}{2}} \qquad \text{(II-84)}$$

or

$$(\overline{w^2})^{\frac{1}{2}} = \frac{ABF_b I_{T_b}}{2 \sin \phi} \qquad \text{(II-85)}$$

where

I_{T_b} = RMS meter indication when the fluctuating current from wire 2 is subtracted from the fluctuating current in wire 1

F_b = multiplying factor for RMS Analyzer position B

From the foregoing analysis it is thus possible to calculate u', w' and $\overline{uw}$ and, it should be obvious, that by rotating the wires 90° it will be possible to similarly calculate v^2 and $\overline{uv}$.

The wire orientations considered above are certainly not the only ones that can be used nor are the turbulence components, given above, the only ones that can be measured; however, they are the ones that were considered in this research.

APPENDIX D

ERROR ANALYSIS

When measuring turbulent flows with a hot wire anemometer many factors influence the accuracy of the results. Some of the more prominent ones are:

1. The electronic equipment used to measure turbulence has built in errors due to the inherent inaccuracy of the meters, resistors, capacitors, etc., used in the circuits. Hubbard[10] estimates that because of the high quality components used in the Type 3A Anemometer these errors will be less than 5%. The 5% has probably been improved on since the multiplier resistors in the RMS Analyzer were calibrated by the author.

2. The accuracy of the results depends on the slope of D.C. panel meter current vs mean velocity curve (A). This curve can usually be made linear by varying the overheating ratio of the hot wire. However, in some cases complete linearity was not achieved. It is estimated that the slope of the before curve did not deviate more than 5%.

3. Low frequency turbulence causes the meters to fluctuate considerably. This is particularly aggravating at low velocities and is almost nonexistent at the higher velocities.

This could cause errors up to about 20% in the low velocity runs (less than 5 ft/sec) when the turbulence was of high relative intensity and low frequency.

4. In the calculations of the cross wire measurements it is assumed that the wires are at 45° angles to the flow and that the calibration constant, A, is the same for both wires. In this research the angles of the wires were set by a very approximate method. Further, the angle that the wires made with the flow changed as the probe position changed. With these facts in mind it is doubtful that the cross wire results could be better than 30%.

With the above analysis as a guide it is estimated that the accuracy of the results is as follows:

1. Mean Velocity--5%, except in low velocity, low frequency, high relative intensity turbulence where errors as high as 10% might be expected.

2. Intensity of Turbulence--10%, except in low velocity, low frequency, high intensity turbulence where errors as high as 20% might be expected.

3. Dissipation length--10%, except at the Reynolds numbers below 100,000 where the random noise signal is of the same order of magnitude as the turbulence signal.

4. Azimuthal intensity of turbulence--30%.

5. Correlation between the axial and azimuthal fluctuating velocities--100%. The reason for the unreasonably

high error in these results is that it is necessary to take the difference of the square of two numbers that differ by very little and both of the numbers are subject to considerable error.

APPENDIX E

CALIBRATION OF MULTIPLIER ON THE RMS ANALYZER

The calibration curves for Channel 1 of the RMS Analyzer are shown in Figures (37) and (38). The data for these curves were obtained by feeding a known voltage, of variable frequency, into the plug jack on the front of the RMS Analyzer, and recording the reading on the turbulence indicating milliammeter (I_T). The frequency was varied between 10 and 40,000 cycles per second; however, the average reading for a given input voltage was determined by assuming that most of the turbulence lies at frequencies below 4,000 cycles per second.

The Channel 2 calibration is essentially the same as Channel 1 and is therefore not displayed.

FIGURE (37)

CALIBRATION OF RMS ANALYZER CHANNEL 1

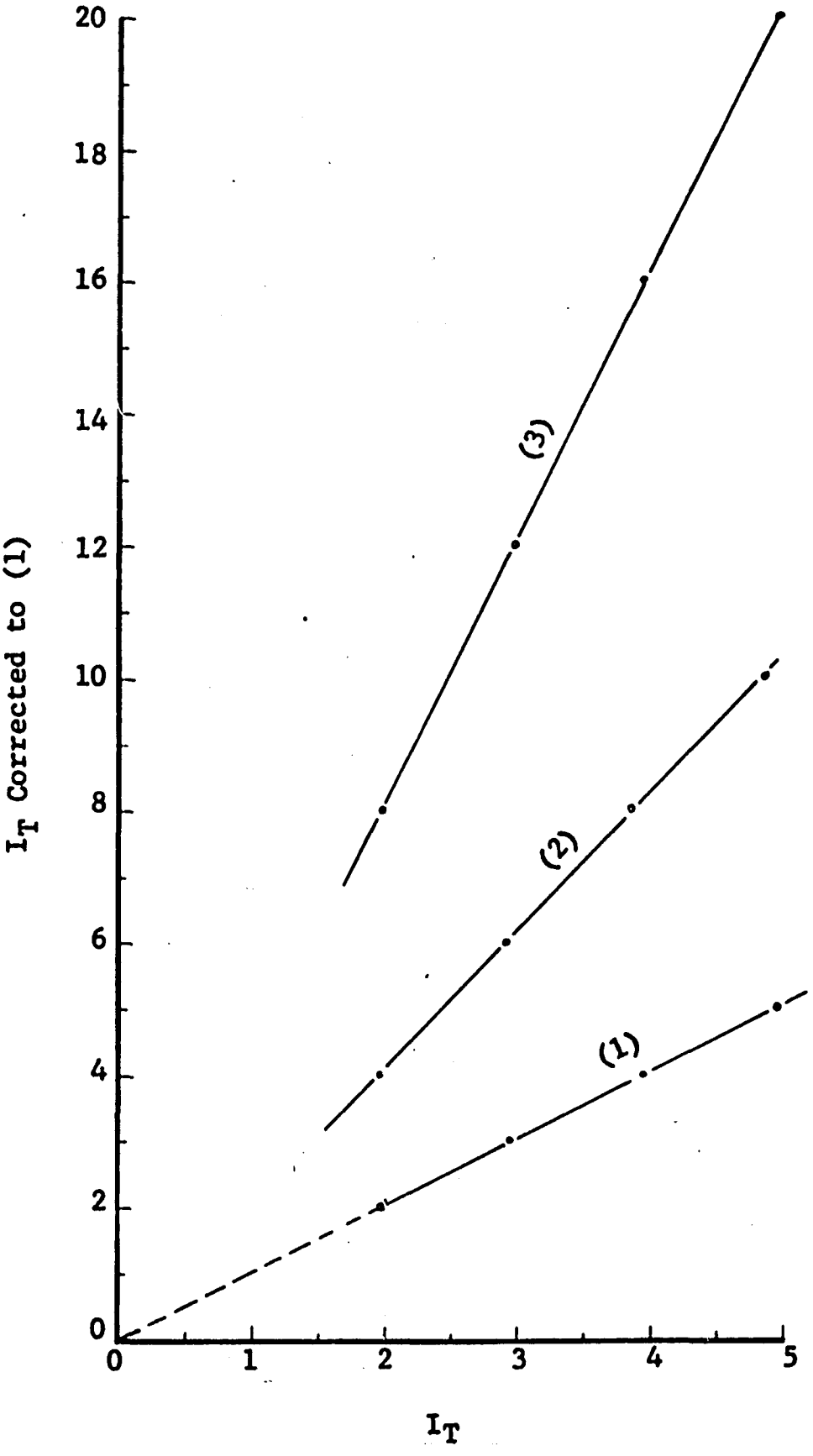

FIGURE (38)

CALIBRATION OF RMS ANALYZER CHANNEL 1

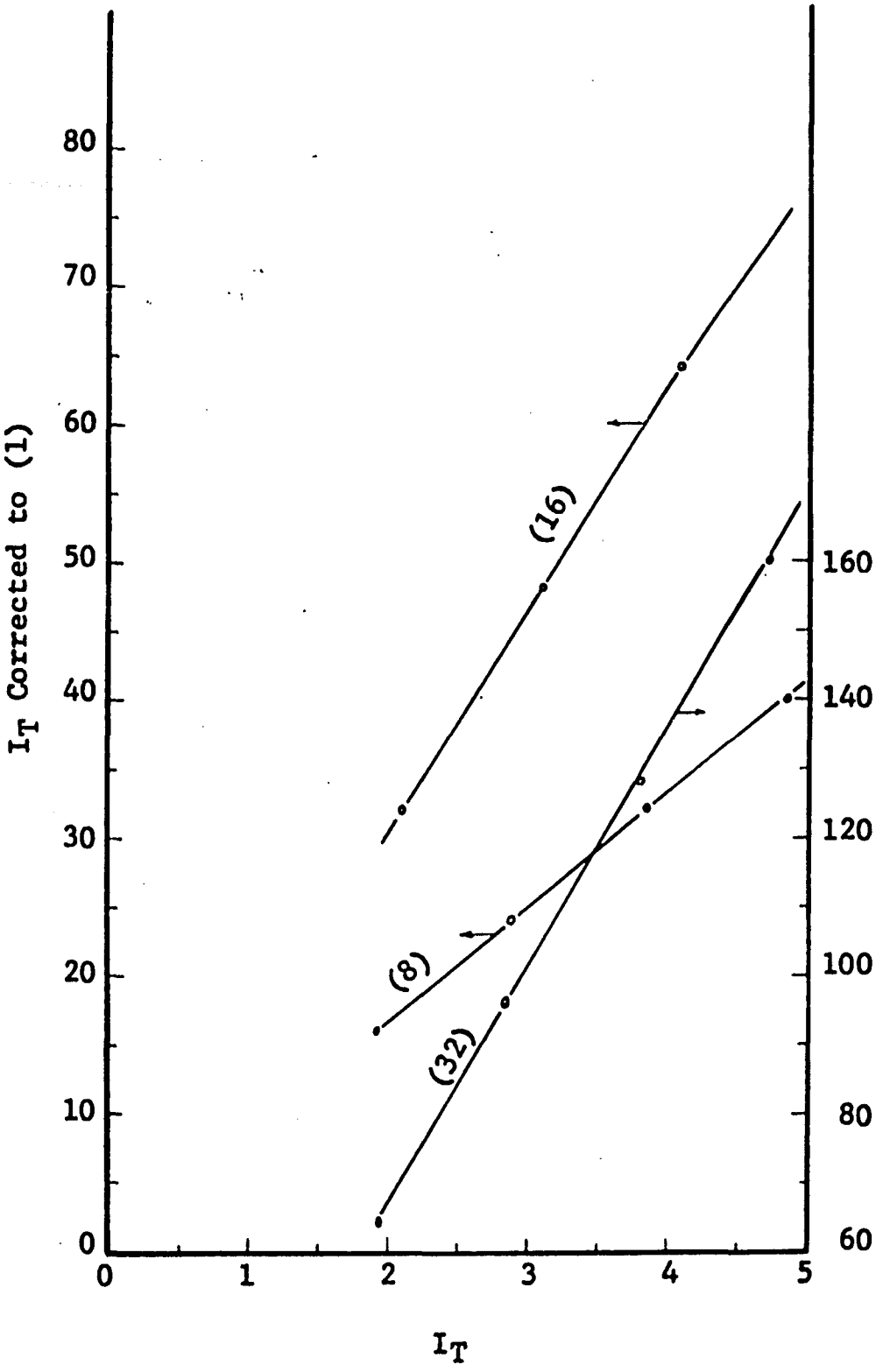

APPENDIX F

CALIBRATION OF THE HOT WIRE

A typical hot wire calibration is shown in Figure (39). The hot wire is calibrated by placing the hot wire, in a constant velocity gas stream, along side a pitot tube. The velocity of the gas stream is determined from the manometer connected to the pitot tube and for each velocity the D.C. panel meter reading ($\bar{I}$) is recorded. The slope of a plot of $\bar{U}$ vs $\bar{I}$ gives the calibration constant, A, used in the calculation of the turbulence quantities.

The calibration constant for the cross wires is obtained in a similar way (i.e., $\bar{U}$ Sin ϕ is plotted vs $\bar{I}$) and the slope of this curve gives the calibration constant, A.

FIGURE (39)

CALIBRATION OF THE HOT WIRE

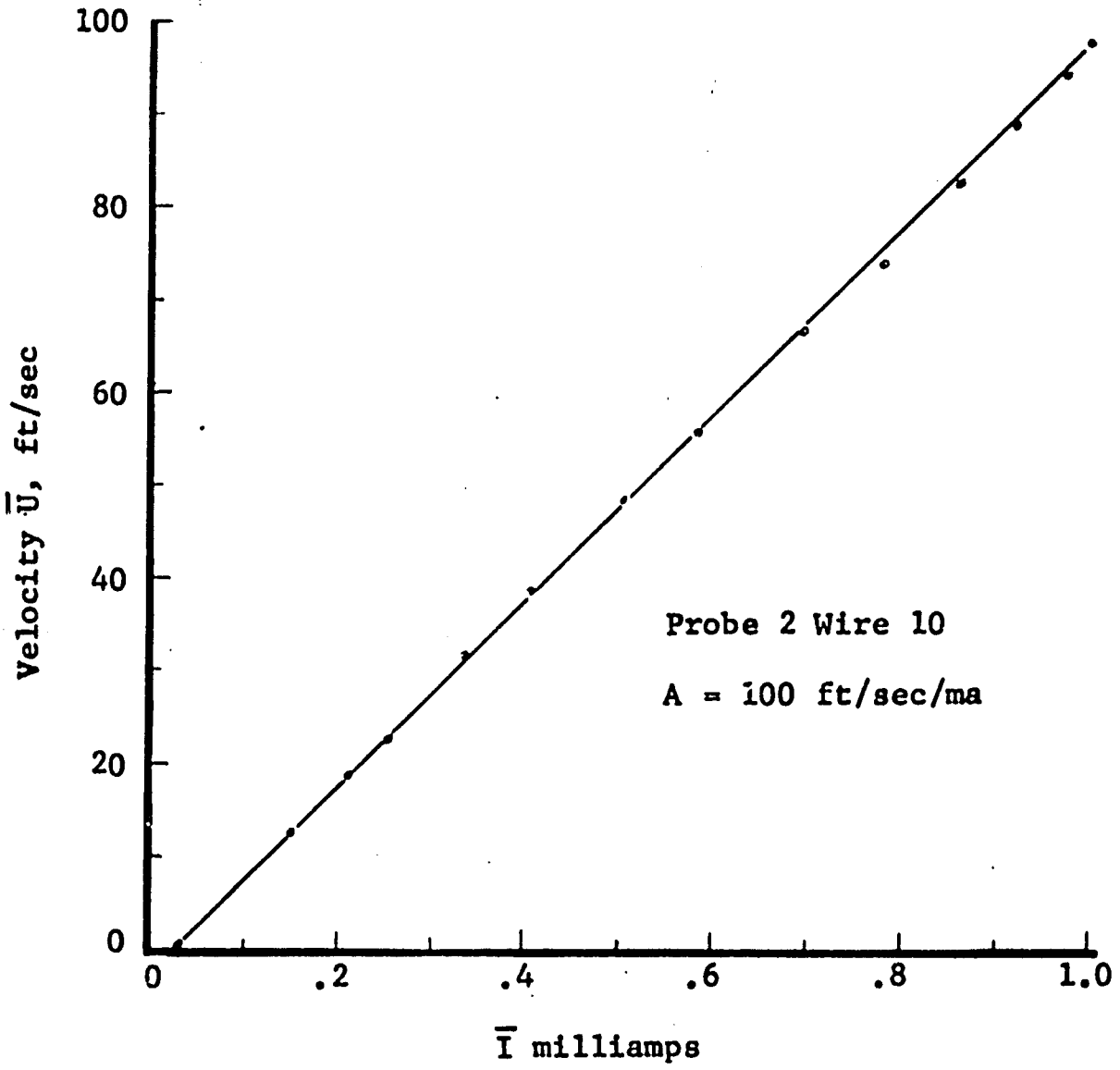

APPENDIX G

SAMPLE CALCULATIONS

1. Intensity of Turbulence

$$u' = ABF\ I_T$$

For Probe 2 Wire 12, 0-100 Ft/sec calibration

$A = 99.8$ Ft/sec/ma

$B = 0.002$

At $r = 0$, $Re = 201{,}000$

$FI_T = 17.25$

$u' = (99.8)(0.002)(17.25) = 3.45$ Ft/sec

2. Dissipation Length

$$\lambda = \frac{\overline{U}B\ F_T\ I_T}{D\ F_{T_d}\ I_{T_d}}$$

For Probe 2, Wire 12, 0-100 Ft/sec calibration

$B = 0.002$

$D = 37.7$

For $r = 0$, $Re = 201{,}000$

$\overline{U} = 98.3$

$F_T I_T = 17.25$

$F_{T_d} = 2$

$I_{T_d} = 3.70$

$$\lambda = \frac{(98.3)(0.002)(17.25)}{(37.7)(2)(3.70)} = 0.0118 \text{ Ft}$$

3. Axial Intensity of Turbulence

$$w' = \frac{ABF}{2 \cos \phi} I_{TB}$$

For Probe 3 Wires 1a and 1b, 0-100 Ft/sec calibration

$A = 67.3$ Ft/sec/ma

$B = 0.002$

$\phi = 45°$

At r = 0, Re = 186,000

$FI_{TB} = 19.3$

$$w' = \frac{(67.3)(0.002)(19.3)}{2(0.707)} = 1.83 \text{ Ft/sec}$$

4. Correlation Between the Axial and Azimuthal Fluctuating Velocities

$$\overline{uv} = \frac{A^2B^2}{4 \sin \phi \cos \phi} \left[(F_{T_1} I_{T_1})^2 - (F_{T_2} I_{T_2})^2 \right]$$

For Probe 3 Wires 1a and 1b, 0-100 Ft/sec calibration

$A = 67.3$

$B = 0.002$

$\phi = 45°$

At r = 0, Re = 186,000

$F_{T_1} I_{T_1} = 18.9$

$F_{T_2} I_{T_2} = 17.0$

$$\overline{uv} = \frac{(67.3)^2(0.002)^2}{4(0.707)(0.707)} \left[18.9^2 - 17.0^2 \right] = 0.61 \text{ (Ft/sec)}^2$$

APPENDIX H

NOMENCLATURE

A - constant in logarithmetic velocity distribution or calibration constant for hot wire

A_1 - calibration constant for wire 1

A_2 - calibration constant for wire 2

B - constant in logarithmic velocity distribution or basic calibration constant for RMS Analyzer

C_p - heat capacity

d - diameter of hot wire or thickness of the layer, near the wall where most of the turbulent energy production takes place

F_1 - multiplying factor for RMS Analyzer Position 1

F_2 - multiplying factor for RMS Analyzer Position 2

F_A - multiplying factor for RMS Analyzer Position A

F_B - multiplying factor for RMS Analyzer Position B

f - Moody friction factor

$f(\psi)$ - longitudinal correlation coefficient

$(Gr)_w$ - Grashof number for hot wire

h - heat transfer coefficient

h_{ese} - heat transfer coefficient based on thickness of laminar sublayer

I - instantaneous current in the metering circuit

i - instantaneous current through the wire

I_1 - instantaneous current in the metering circuit from wire 1

I_2 - instantaneous current in the metering circuit from wire 2

$\bar{I}_1$ - average current in the metering circuit from wire 1, and also the reading of the D.C. Panel meter in Channel 1

$\bar{I}_2$ - average current in the metering circuit from wire 2, and also the reading of the D.C. Panel meter in Channel 2

I_T - RMS Analyzer reading

I_{T_1} - RMS Analyzer reading Position 1

I_{T_2} - RMS Analyzer reading Position 2

I_{T_A} - RMS Analyzer reading Position A

I_{T_B} - RMS Analyzer reading Position B

I_{T_d} - RMS Analyzer reading with differentiator on

K_1 - constant in King's equation

K_2 - constant in King's equation

k - thermal conductivity

m - constant in Deissler's mean velocity distribution

$(Nu)_w$ - Nusselt number for hot wire

n - constant in Pai's mean velocity distribution

Pr - Prandtl number

$\bar{P}$ - average pressure

$\bar{P}_{rx}$ - average pressure at (r,x)

p - fluctuating pressure

R - electrical resistance

$(Re)_w$ - Reynolds number of hot wire

Re^* - friction Reynolds number

R_w - resistance of hot wire

R_o - resistance of hot wire at an arbitrary reference temperature

R_g - resistance the hot wire would have at T_g

Re - pipe Reynolds number $\frac{2r_o U_A \rho}{\mu}$

$(R_{ij})_{AB}$ - correlation coefficient between the fluctuating velocities i and j at points A and B respectively

r - radial coordinate

r_o - pipe radius

S - length of hot wire

s - constant in Pai's equation for mean velocity distribution

T - temperature

Tg - temperature of gas stream

Tw - temperature of hot wire

t - time

U - instantaneous velocity in axial direction

$\bar{U}$ - average velocity in axial direction

u - fluctuating velocity in axial direction

u' - intensity of turbulence in axial direction

U^* - friction velocity

U^+ - a dimensionless velocity

U^o - a velocity characteristic of the flow

U_t - an arbitrary velocity of the flow

$(u_i)_A$ - fluctuating velocity in direction i at point A

$(u_j)_B$ - fluctuating velocity in direction j at point B

$(u_i')_A$ - intensity of turbulence in direction i at point A

$(u_j')_B$ - intensity of turbulence in direction j at point B

$\vec{U}_e$ - effective vector velocity perpendicular to the wire

$\overline{\vec{U}}$ - average of the effective vector velocity perpendicular to wire

$\vec{U}$ - vector velocity

$\overline{U}_{exp}$ - experimental value of mean velocity

$\overline{U}_{pe}$ - average velocity calculated from Pai's equation using n determined from experimental data

$\overline{U}_{pt}$ - average velocity calculated from Pai's equation using n determined from friction and $(\overline{U}_A/\overline{U}_{max})$ plots

V - instantaneous velocity in radial direction

$\overline{V}$ - average velocity in radial direction

v - fluctuating velocity in radial direction

v' - intensity of turbulence in radial direction

W - instantaneous velocity in azimuthal direction

$\overline{W}$ - average velocity in azimuthal direction

w - fluctuating velocity in azimuthal direction

w' - intensity of turbulence in azimuthal direction

x - axial coordinate

Y - $\left(\frac{\overline{U}}{\overline{U}_m} - 1\right)$

Y^+ - dimensionless distance from pipe wall

Y_o - experimental value of $\left(\frac{\bar{U}}{U_m} - 1 \right)$

y - distance from pipe wall

y_{ese} - thickness of laminar sublayer

θ - azimuthal coordinate

τ - shear stress

τ_o - shear stress at the pipe wall

η - (r/r_o) a normalized radial distance from the center of the pipe

ψ - axial distance between the points where the fluctuating velocities are measured in the relationship for the longitudinal correlation coefficient $f(\psi)$

λ - dissipation length

ϕ_1 - angle between x axis and wire 1

ϕ_2 - angle between x axis and wire 2

β - coefficient of expansion of the gas

ρ - density

AUTOBIOGRAPHY

The author was born August 6, 1935, in Shreveport, Louisiana. He attended the public schools of Lufkin, Texas, and was graduated from Lufkin High School in May, 1952. He attended Kilgore College in 1952-53. He entered the University of Houston in September, 1953, and received the B.S. in Chemical Engineering from there in 1957. The attendance at the University of Houston was concurrent with employment at the Houston Research Laboratories of the Shell Development Company. On September 1, 1957, he was married to the former Cynthia Ann Gaida. In the same month he entered the Graduate School of Louisiana State University from which he was awarded a Master of Science in Chemical Engineering in February, 1959. He is at present a Candidate for the degree of Doctor of Philosophy in Chemical Engineering. When the requirements for this final degree are met the author and his wife will move to Baytown, Texas, where he will be employed by the Humble Division of Humble Oil and Refining Company.

EXAMINATION AND THESIS REPORT

Candidate: William A. Brookshire

Major Field: Chemical Engineering

Title of Thesis: A Study of the Structure of Turbulent Shear Flow in Pipes

Approved:

Dale U. von Rosenberg
Major Professor and Chairman

Richard J. Russell
Dean of the Graduate School

EXAMINING COMMITTEE:

J. R. Groves Jr.

James B Gardiner

Edwin C. Johnson

Leonard Lassiter

Jesse Coates

D. R. Schaaly

Date of Examination:

December 12, 1960